Fall 2011

Circulation of the Western Antarctic Peninsula: Implications for Biological Production

Maria Andrea Piñones Valenzuela
Old Dominion University

CIRCULATION ON THE WESTERN ANTARCTIC PENINSULA: IMPLICATIONS FOR BIOLOGICAL PRODUCTION

by

Maria Andrea Piñones Valenzuela
B.S. December 2003, Catholic University of Valparaiso, Chile
M.S. December 2006, Old Dominion University

A Dissertation Submitted to the Faculty of
Old Dominion University in Partial Fulfillment of the
Requirements for the Degree of

DOCTOR OF PHILOSOPHY

OCEANOGRAPHY

OLD DOMINION UNIVERSITY
December 2011

Approved by:

Eileen E. Hofmann (Director)

Kendra L. Daly (Member)

Gail E. Dodge (Member)

Chester E. Grosch (Member)

John M. Klinck (Member)

ABSTRACT

CIRCULATION ON THE WESTERN ANTARCTIC PENINSULA: IMPLICATIONS FOR BIOLOGICAL PRODUCTION

Maria Andrea Piñones Valenzuela
Old Dominion University, 2011
Director: Dr. Eileen E. Hofmann

The western Antarctic Peninsula (wAP) continental shelf is characterized by large persistent populations of Antarctic krill (*Euphausia superba*) and by regions of enhanced concentrations of marine mammals and other predators (hot spots). This study focused on understanding the role of ocean circulation in providing retention/connectivity of wAP Antarctic krill populations and in maintaining biological hot spot regions. Numerical Lagrangian particle tracking simulations obtained from the Regional Ocean Modeling System (ROMS) configured for the wAP region provided quantitative estimates of retention, immigration and emigration from the wAP continental shelf. Additional simulations with a one-dimensional temperature-dependent growth model for krill embryos and early larval stages allowed mapping of the Lagrangian trajectories into krill developmental stages. The simulated particle trajectories showed preferred sites for across-shelf transport, with Marguerite Trough being a primary pathway for movement into Marguerite Bay, Crystal Sound, and the inner shelf regions. Residence times for the biological hot spots were 18 to 27 days for Alexander Island and Crystal Sound and almost 35 days for Laubeuf Fjord (biological hot spot regions). Particles released in the Bellingshausen Sea (remote source) were transported to the wAP shelf with a time scale consistent with the time required for Antarctic krill embryos to develop into larvae (120 days). The trajectories of floats released along the wAP shelf inside the 500-m isobath (local source) showed retention times on the order of 3 months and low connectivity among different release sites on

the mid to inner shelf, suggesting that local reproduction and development can be important contributors to wAP Antarctic krill populations. Successful completion of the descent-ascent cycle of Antarctic krill embryo-larvae occurred along the outer shelf and in shelf regions where bottom depths were greater than 500 m. Estimated residence times in these areas were 20-30 days, which suggests that krill spawned in the mid and inner shelf are retained in these regions through development to the first feeding stage (calyptopis I). These results suggest that wAP Antarctic krill populations along the outer and mid shelf may be dependent on inputs from upstream sources. Maintenance of populations confined to the inner shelf regions may be dependent on local processes. Simulated trajectories obtained for projected future environmental conditions suggested that the circulation would enhance advection of krill larvae to the shelf but that recruitment and reproduction may be altered, thereby impeding survival of Antarctic krill.

To my beloved family, Diego and Luna

ACKNOWLEDGEMENTS

I would like to give my gratitude to my advisor Dr. Eileen Hofmann for always encouraging and kindly sharing her knowledge during all these years. I am deeply grateful for all the wonderful opportunities that she has given me, supporting me, and mentoring me during my Ph.D. research, presenting my research at national and international meetings, and also supporting me during my journey to Antarctica. I also want to thank Dr. John Klinck, Dr. Chester Grosch and Dr. Kendra Daly for their helpful and constructive comments on the early state of this research. Especially, I would like to thank Mike Dinniman for patiently helping me with all my ROMS questions. You are the best. I am also grateful to Julie Morgan for her kind words and always so helpful when paperwork was overwhelming.

To all the friends I have made during my stay in the United States, it surely would not be the same wonderful experience without you. Jose Luis and Ivonne you welcomed me, Diego and Luna in your home and made us feel like it was ours. We miss you very much. To my friends Alexandra and Jose, special thanks for taking care of me while Diego was away. To those that are still here and to those who have started a new journey to you....Jose Luis, Ivonne, Karelys, Alexandra, Jose, Tosca, Tian, Heber, Roberto, Teresa, Olga, Elkin, Kata, Stacy, Ruben, Billur, Rodrigo, Angie, Diego.co and more, thanks for sharing all those great conversations, laughs, outdoor-adventures, dances and culture exchanges.

Finally I would like to acknowledge the National Science Foundation Grant ANT-0523172, that funded this research. This study was part of the U.S. Southern Ocean GLOBEC Program synthesis and integration phase. Thanks to Dr. Robert Beardsley, Woods Hole Oceanographic Institution, for providing the data sets from the four drifters deployed on the western Antarctic Peninsula continental shelf in January 2005 that were used for the simulated drifter evaluations.

TABLE OF CONTENTS

Page

LIST OF TABLES

Table Page

LIST OF FIGURES

Figure Page

Figure Page

Figure Page

Figure Page

CHAPTER 1

INTRODUCTION AND RESEARCH QUESTIONS

The western Antarctic Peninsula (wAP) (Fig. 1) has been the focus of several multidisciplinary oceanographic research programs because of the large stocks of marine living resources that are supported in this region. The first of these programs, the Biological Investigations of Marine Antarctic Systems and Stocks (BIOMASS), was designed to provide understanding of the marine ecosystem that could be used as a basis for management of living marine resources (e.g. El-Sayed, 1977, 1987, 1994). The research undertaken during BIOMASS, The First International BIOMASS Experiment (FIBEX, 1980-1981) and the Second International BIOMASS Experiment (SIBEX 1983-1985), provided descriptions of the distribution and ecology of zooplankton, especially Antarctic krill (*Euphausia superba*), in relation to the environment (Siegel, 1986; Quetin et al., 1994; Schnack-Schiel and Mujica, 1994; Siegel and Kalinowski, 1994). Subsequent multidisciplinary programs, the Antarctic Marine Living Resources (AMLR) Program (Holt et al., 1991), the Antarctic Marine Ecosystem Research at the Ice-Edge Zone (AMERIEZ) Program (Sullivan and Ainley, 1987) and the Antarctic Coastal Ecosystem Rates (RACER) Program (Huntley et al., 1987, 1991), extended the understanding of physical and biological interactions in the wAP region, and provided valuable multidisciplenary data sets for this area.

Most recently, the wAP was the focus of the Southern Ocean Global Ocean Ecosystem Dynamics (SO GLOBEC) Program, which has a primary scientific goal of understanding the physical and biological factors that contribute to enhanced growth, reproduction, recruitment and survivorship through the year of Antarctic krill (Hofmann et al., 2002). The U.S. SO GLOBEC field studies took place in the Marguerite Bay region of the wAP (Fig. 1) during April-June 2001 and 2002 and July-September

This dissertation follows the style of *Deep-Sea Research II*

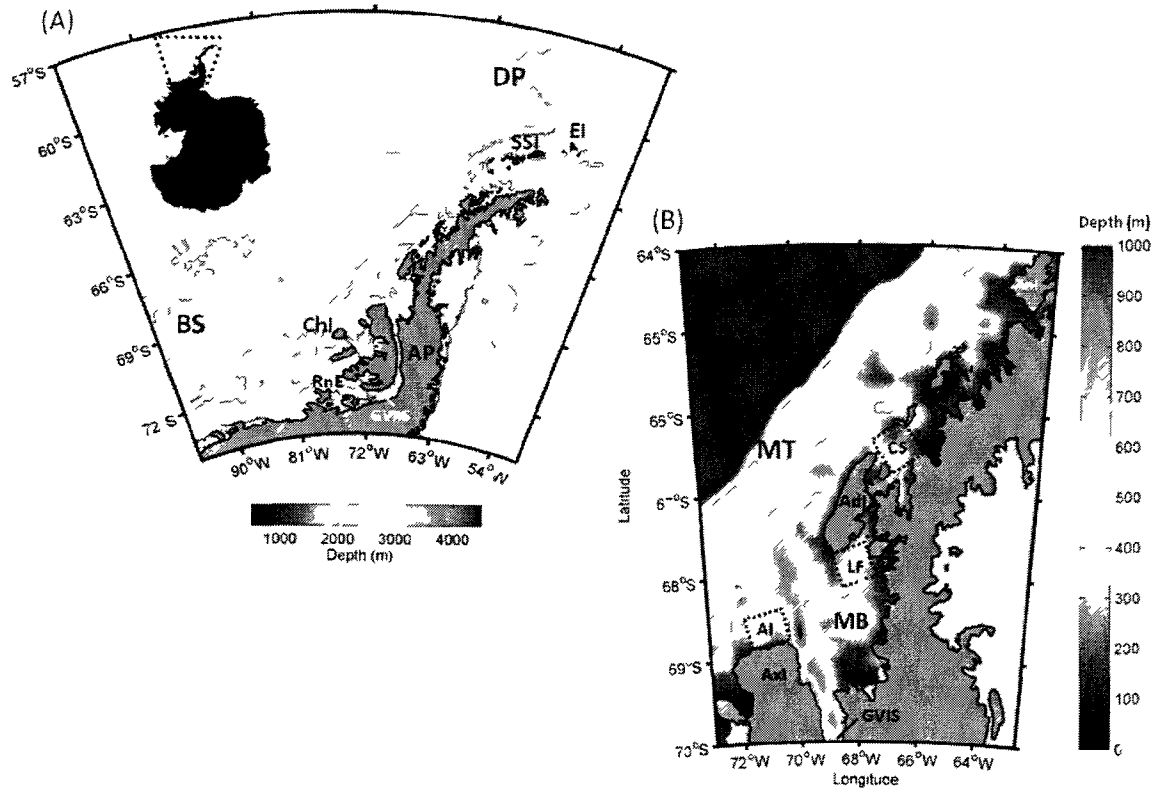

Fig. 1. (A) Map of the study area showing the western Antarctic Peninsula (wAP) region and bottom bathymetry (m). Geographic names are abreviated as: AP = Antarctic Peninsula, BS = Bellingshausen Sea, DP = Drake Passage, GVIIS = George VI Ice Shelf, LIS = Larsen Ice Shelf, WIS = Wilkins Ice Shlef, ChI = Charcot Island, EI = Elephant Island, SSI = South Shetland Islands, RnE = Ronne Entrance. (B) Marguerite Bay (MB) region of the wAP with biological hot spot regions indicated (dotted line box). Geographic names are abbreviated as: MT = Marguerite Trough, AI = Alexander Island hot spot, CS = Crystal Sound hot spot, LF = Laubeuf Fjord hot spot, AxI = Alexander Island, AdI = Adelaide Island, LvI = Lavoisier Island, RI = Renaud Island, AnI = Anvers Island.

2001 and 2002 (Hofmann et al., 2004). This program provided extensive hydrographic and circulation measurements (Beardsley et al., 2004; Howard et al., 2004; Klinck et al., 2004; Costa et al., 2008) that were coincident with measurements of biological distributions that included zooplankton (Daly, 2004; Lawson et al., 2004; Ashjian et al., 2008) and top predator (e.g. penguins and seals) distributions (Burns et al., 2004; Chapman et al., 2004; Ribic et al., 2008). A primary result from analyses of the environmental and biological data sets was the identification of localized areas in and around Marguerite Bay that are characterized by sustained higher biomass that is in excess of average conditions (biological hot spots) (Costa et al., 2007; Fig. 1B). Associated with these regions are enhanced abundances of top predators (Burns et al., 2004; Chapman et al., 2004; Ribic et al., 2008).

The areas of the wAP where top predators congregate (Fig. 1B) tend to be associated with areas of above-average sea ice concentration and shallow, but irregular, bathymetry (Burns et al., 2004), or coastal areas that have marginal sea ice (Trathan et al., 1996; Chapman et al., 2004; Thiele et al., 2004) and where large zooplankton and adult krill are abundant (Lawson et al., 2004; Ashjian et al., 2008). Predator distributions have been used as indices of resource availability to describe regions with localized productivity (Costa, 1991; Trathan et al., 1996) and as indicators of special oceanographic features such as polynyas or recirculation areas (Trathan et al., 1993).

An additional feature that contributes to enhanced biological production is the presence of Circumpolar Deep Water (CDW) below about 120 m on the wAP continental shelf (Prézelin et al., 2004; Daly, 2004). Intrusions of CDW onto the wAP shelf are persistent and seasonally independent (Klinck, 1998; Smith and Klinck, 2002; Dinniman and Klinck, 2004). Intrusions of CDW have an important effect on the water mass structure of the wAP continental shelf (Klinck, 1998; Prézelin et al., 2000) but the magnitude and extent of the across-shelf exchange, retention dynamics and transport mechanisms associated with these events remains to be determined.

Areas where these events occur are characterized by enhanced primary production (Prézelin et al., 2000, 2004). The presence of CDW affects distributions of Antarctic krill (Lascara et al., 1999) and potentially affects all trophic levels (Burns et al., 2004; Chapman et al., 2004; Širović et al., 2004; Thiele et al., 2004). The contribution of this water mass to the creation and maintenance of biological hot spots remains to be quantified.

The overall goal of this research is to identify the role of ocean circulation in producing the observed biological distributions on the wAP shelf. To address this goal, research questions that focus on the variability and extent of the across-shelf exchange and the linkages between the circulation and hot spots were posed as:

Research Question 1: What are the transport pathways, preferred sites for across-shelf exchange and residence time for localized areas of the wAP continental shelf?.

Research Question 2: What is the role of the circulation in developing and maintaining localized areas of enhanced production and in structuring the distributions of Antarctic krill larvae on the wAP continental shelf?.

Research Question 3: What is the contribution of local retention versus inputs from remote sources to maintenance of Antarctic krill populations on the wAP continental shelf?

Research Question 4: How are Antarctic krill reproduction success and larval krill distribution modified by environmental conditions that may potentially occur as the result of global warming?

To address these questions a high-resolution numerical circulation model was implemented for the wAP continental shelf. The simulated circulation fields obtained with the model were used to track Lagrangian particles along and over the continental shelf on the wAP for different seasons and depths. Particles were released at several sites along the wAP shelf break, in regions upstream of the wAP and over the continental shelf. The Lagrangian particle simulations were used to determine residence

times and to link circulation pathways with areas of high predator abundances. The simulated transport pathways were compared with measured development times for krill larvae to determine the link between circulation and observed distributions of krill larvae and juvenile stages. A one-dimensional temperature dependent growth model for the embryos and early larval stages of Antarctic krill was implemented for the wAP shelf to determine which regions of the shelf support a successful reproduction of Antarctic krill.

Background information on the circulation and biological distributions of the wAP continental shelf is provided in the next chapter. This is followed by a description of the Lagrangian tracking experiments done to determine transport pathways, residence times and across-shelf exchanges along the wAP. This also provides insights into the role of circulation in maintaining biological hot spots. A modeling study designed to determine the role of circulation in providing remote versus local connectivity for the Antarctic krill populations along the wAP is described in Chapter IV. The one-dimensional temperature-dependent krill model and results are given in Chapter V. This chapter also provides insights into how reproduction of Antarctic krill in the wAP region may be affected by modified environmental conditions such as may occur as result of global warming. The final chapter provides a summary of the results within the context of the research questions and gives insights into the extent to which the biological distributions on this shelf are influenced by present and future environmental conditions.

CHAPTER 2

BACKGROUND

2.1 PHYSICAL ENVIRONMENT

2.1.1 Study Region Characteristics

The bathymetry of the wAP continental shelf is rugged and variable. The continental shelf depths range from 200 to 500 m and deepen onshore as a consequence of glaciological processes (Anderson, 1999). The coastline along the wAP is irregular, composed of numerous islands, fjords and embayments that are connected through deep and narrow channels. The largest embayment is Marguerite Bay located at the southern end of the Antarctic Peninsula (Fig. 1). The Bay is connected to the shelf break through a deep trough, Marguerite Trough, which has a maximum depth of 1600 m and is oriented to the northwest off of Adelaide Island (Beardsley et al., 2004; Bolmer, 2008). Located at the southern end of Marguerite Bay is George VI Ice Shelf, which extends between the Antarctic continent and the eastern side of Alexander Island (Fig. 1). This ice shelf is the largest on the western side of the Antarctic Peninsula and extends for over 500 km, connecting Marguerite Bay in the north with the Ronne Entrance in the Bellingshausen Sea to the south (Potter and Paren, 1984, Fig. 1). George VI ice shelf is an important component of the circulation and freshwater budget for the wAP shelf region (Lennon et al., 1982; Potter and Paren, 1985; Dorland and Zhou, 2008).

2.1.2 General Circulation and hydrography

The water mass structure and circulation of the wAP continental shelf is influenced by the Antarctic Circumpolar Current (ACC), which flows to the northeast along the outer shelf (Orsi et al., 1995). The ACC transports CDW, a relatively warm

(1.8-2.0°C), high salinity (34.72), low oxygen, and nutrient-rich water mass, that is found below 200 m (Sievers and Nowlin, 1984; Hofmann et al., 1996). This water mass is divided into Upper Circumpolar Deep Water (UCDW), which is characterized by a temperature maximum at a potential density of 27.72, low oxygen, and high nutrient concentrations (Orsi et al., 1995; Klinck, 1998; Klinck et al., 2004) and Lower Circumpolar Deep Water (LCDW), which is characterized by a salinity maximum of 34.74 at a potential density of 27.8 (Stein, 1986; Hofmann et al., 1996).

The water mass structure of the wAP continental shelf is composed of Antarctic Surface Water (AASW, -1.8-1.0 °C, 33.0-33.7), Winter Water (WW, -1.5 °C, 33.8-34.0) and UCDW (Toole, 1981; Sievers and Nowlin, 1984; Hofmann et al., 1996). The water masses above the permanent pycnocline (about 150-200 m) undergo seasonal modifications. Surface cooling during the winter produces WW and AASW is formed during the summer by surface heating and inputs of freshwater due to ice melting. The WW is the portion of AASW that retains the temperature and salinity structure from the winter. By austral summer the signature of WW is eroded due to mixing and seasonal heating within the upper water column (Smith et al., 1999).

Below the permanent pycnocline, onshelf flow of UCDW is maintained by the ACC through a combination of momentum advection and the curvature of the shelf break (Dinniman and Klinck, 2004). This water mass influences heat and salt budgets (Klinck, 1998; Smith et al., 1999; Smith and Klinck, 2002) and sea ice formation (Smith and Klinck, 2002) on the wAP continental shelf. Observations and numerical circulation modeling studies describe the intrusions of CDW onto the continental shelf as a regular feature that occurs 4-6 times per year (Klinck et al., 2004; Dinniman and Klinck, 2004). The position and variability of the southern boundary of the ACC determines and influences the frequency and extent of CDW intrusions (Orsi et al., 1995; Dinniman and Klinck, 2004). Recent observations of the characteristics of CDW intrusions showed that UCDW intrudes in the form of frequent (four per month)

warm eddy-like structures (Moffat et al., 2009). These observations also showed that LCDW was on several deep depressions, including Marguerite Trough, forming a layer $\approx$95 m of relatively dense water that reached into Marguerite Trough and is renewed approximately every six weeks.

Hydrographic (Stein, 1986, 1988, 1989, 1992; Hofmann and Klinck, 1998a; Smith et al., 1999; Klinck et al., 2004) and surface drifter observations (Beardsley et al., 2004) showed that the circulation over the wAP continental shelf in the Marguerite Bay region consists of a clockwise gyre, the inner limb of which is connected to a southward flowing coastal current, the Antarctic Peninsula Coastal Current (APCC, Moffat et al., 2008). In the SO GLOBEC study region (Fig. 1), this current is a seasonal feature that is driven by wind and buoyancy forcing, such as runoff from land and precipitation (Moffat et al., 2008). During ice-free conditions, the APCC was observed to flow into Marguerite Bay and exit the south side of the Bay along Alexander Island (Beardsley et al., 2004). Subtidal currents in the permanent pycnocline tend to have little vertical shear (Smith and Klinck, 2002; Howard et al., 2004). The flow is weak and is strongly influenced by local topography (Howard et al., 2004).

Hydrographic and direct current meter observations obtained during SO GLOBEC suggest a mean flow of LCDW into Marguerite Bay along the northern flank of Marguerite Trough (Beardsley et al., 2004; Klinck et al., 2004; Moffat et al., 2008), which provides a conduit for the LCDW to enter the innershelf region (Beardsley et al., 2004). Current meter measurements show maximum inflow of 18 cm s^{-1} and outflow velocities of 6 cm s^{-1} along the Trough (Moffat et al., 2008). However, the degree to which the overall shelf circulation is connected with the flow in the Trough and to that in Marguerite Bay remains to be determined (Klinck et al., 2004).

2.1.3 Sea Ice

The wAP continental shelf is mostly covered by sea ice during the austral winter, is ice free in summer north of Marguerite Bay, and the sea ice extent of this region is characterized by considerable interannual variability (Stammerjohn and Smith, 1996). Seasonal ice cover along the Antarctic Peninsula differs from other regions of the Southern Ocean in that the period of ice advance is relatively short compared to the period of ice retreat (Stammerjohn and Smith, 1996). During the past two decades annual mean sea ice extent in the wAP has shown a negative trend (Smith and Stammerjohn, 2001; Parkinson, 2002; Vaughan et al., 2003), which is related to a decrease in the duration of winter sea ice. The timing of sea ice advance and retreat in this region has changed, with the advance occurring later and the retreat occurring earlier (Stammerjohn et al., 2008b).

Recent studies have shown that sea ice advance is more sensitive to climate variability than is sea ice retreat (Ducklow et al., 2007; Stammerjohn et al., 2008a). Changes in sea ice advance have occurred in association with decadal changes in the mean state of the Southern Annular Mode (SAM) and the high latitude response to the El Niño-Southern Oscillation (ENSO). The northerly advance of sea ice in the wAP region is not constrained by any boundary, so rapid ventilation of ocean heat is possible. Thus, less time is needed to grow sea ice than is needed to melt sea ice. La Niña events and the positive phase of SAM have a negative impact in the wAP region, by contributing to a decrease in the duration of the sea ice season. This results in less time for sea ice to thicken, making the sea ice more vulnerable to disturbances from oceanic and atmospheric influences.

2.1.4 Atmospheric Circulation

Atmospheric circulation over the Southern Ocean is dominated by a westerly circumpolar vortex (Trenberth et al., 1990; Thompson and Solomon, 2002). The vortex

is strongest during winter, when polar temperatures are coldest and weakest during summer months. During the summer, the circulation in the upper atmosphere (at 30 hPa) reverses and becomes weakly westward (Thompson and Solomon, 2002). The Southern Ocean atmospheric circulation exhibits considerable month-to-month and interannual variability. The surface wind stress is characterized by annual and semi-annual variability. Semi-annual variability is related to the timing of seasonal heating of the atmosphere south of the 40°S (Large and van Loon, 1989).

Along the wAP, the winds are primarily from the northwest, with the weakest wind stress occurring during summer and the strongest during winter (Trenberth et al., 1990; Hofmann et al., 1996). At smaller spatial scales (tens of kilometers), the topographic features of the Antarctic Peninsula and the katabatic winds (Parish and Bromwich, 1987; Parish, 1992) contribute to the variability of the wind stress. In general, weather along the wAP is milder relative to that of the interior of the Antarctic (Smith et al., 1996; Domack et al., 2003) and the Weddell side (Smith et al., 1996). During winter the wAP is influenced by episodic storms events generated by the passage of low pressure systems (Bromwich and Stearns, 1993; Smith et al., 1996).

2.2 BIOLOGICAL PRODUCTION

2.2.1 Distribution

The wAP supports a rich and diverse ecosystem and is considered one of the most productive areas within the Southern Ocean (Arrigo et al., 1998; Deibel and Daly, 2007), supporting high primary production, enhanced zooplankton abundance, and large populations of high trophic level predators. Observations to date of the distribution and abundance of marine mammals and other predators, obtained as part of the SO GLOBEC program, show that these animals concentrate in specific areas of the wAP continental shelf (Burns et al., 2004; Chapman et al., 2004; Širović et al., 2004; Thiele et al., 2004; Costa et al., 2007).

Variability in phytoplankton biomass, community composition and primary production in the coastal areas of the Southern Ocean is the result of the combined effect of water column stratification, sea ice, advection, temperature, light regulation, and macro-nutrient limitation (Bodungen et al., 1986; Smith and Sakshaug, 1990; Holm-Hansen et al., 1994; Prézelin et al., 1994; Moline and Prézelin, 1996; Prézelin et al., 2000, 2004). A historical review of the phytoplankton biomass and productivity data for the Palmer Long-term Ecological Research (PAL LTER) region of the wAP (Smith et al., 1996), suggest that the shelf-slope system west of the Antarctic Peninsula is fundamentally different from the pelagic areas of the Antarctic marine ecosystem. The observed average productivity of the region is on the order of a few hundred gC m^{-2} y^{-1}, which is roughly a factor of 5 lower than other productive coastal areas of the world's oceans (Chávez and Barber, 1987). Estimates of annual primary production in the Southern Ocean (Arrigo et al., 1998) indicate that the Belligshausen Sea-Amundsen Sea (770 Tg C yr^{-1}) pelagic system has values higher than the South-Indian Ocean (543 Tg C yr^{-1}) and the Southwestern-Pacific Ocean (665 Tg C yr^{-1}) sectors but lower than the Weddell Sea and Ross Sea (858-1076 Tg C yr^{-1})

A combination of environmental and biological factors can regulate primary production in the Southern Ocean. Total annual productivity is dominated by the high production rates associated with episodic spring blooms, whose development may be timed by ice-driven water column stability and favorable meteorological conditions (Smith et al., 1995). Chlorophyll *a* distributions obtained from the Sea-Wide-Field of Viewing (SeaWiFS) satellite sensor between 1997-2004 showed higher concentrations in the Bellingshausen Sea and Marguerite Bay region, which persisted throughout austral spring and summer (Marrari et al., 2008). High concentrations of phytoplankton are important to provide krill with the food levels that are required for successful reproduction and larval survival.

Top predators, especially marine mammals, rely on regional patches of high productivity resulting from localized sources of nutrient influx that occur in upwelling areas, around bottom topography, in divergence zones or, at the sea ice edge (Costa and Crocker, 1996). Top predator populations have patchy distributions and their abundances are good predictors of areas of high prey density (Ainley and DeMaster, 1990; Costa and Crocker, 1996). Marine mammals rely on oceanographic features, such as frontal systems, thermocline depth, and bathymetry, to concentrate or aggregate prey, which may be necessary to enable effective predation (van Franecker, 1992; Whitehead et al., 1992; Kenney et al., 1995; Hunt, 1997).

The SO GLOBEC predator program focused on understanding the distribution, abundance, movements patterns and condition of krill predators, such as crabeater seals (*Lobodon carcinophagus*), Adélie penguins (*Pygoscelis adeliae*), fish and cetaceans [humpback (*Megaptera novaeangliae*), minke (*Balaenoptera bonaerensis*) and blue whales (*Balaenoptera musculus*)]. Understanding distribution and abundance of krill predators is key in understanding the biological factors influencing growth, reproduction, recruitment, and survival of Antarctic krill, which was the focus of the SO GLOBEC program (Hofmann et al., 2004). One of the major findings of this program was that predators are not randomly distributed in the wAP; rather they select habitats based on a combination of biological and physical factors (Burns et al., 2004; Chapman et al., 2004; Širović et al., 2004; Thiele et al., 2004).

The distribution and abundance of seabirds observed during SO GLOBEC indicated that these species selected areas related to sea ice cover, water mass structure, and bathymetry (Chapman et al., 2004). Higher densities of southern fulmar (*Fulmarus galcialoides*), snow petrel (*Pagodroma nivea*) and Antarctic petrel (*Thalassoica antarctica*) were observed in the inner shelf near Alexander Island where a coastal current is present. Other species such as the blue petrel (*Halobaena caerulea*), kelp gull (*Larus dominicanus*) and the southern giant petrel (*Macronectes giganteus*) were

associated with variability of the bottom depth. After the development of the pack ice, seabirds distributions (e.g. snow petrel, Antarctic petrel, Adélie penguin were mainly related to sea-ice characteristics instead of water column processes. Timing, development and extent of sea ice as well as hydrographic processes influenced by bathymetry are important factors structuring sea birds distributions (Chapman et al., 2004). Fraser and Trivelpiece (1996) analyzed distributions of Adélie penguin populations for the wAP and observed that 80% of the breeding population were found in five colony clusters that were associated with deep canyons and basins that intersect the continental shelf.

Other important groups of apex predators such as cetaceans have been found in geographically distinct habitats, particularly coastal areas such as fjords where complex bathymetry may concentrate prey (Thiele et al., 2004). During the SO GLOBEC field experiments, observations of the abundance, distribution and seasonal variability in cetacean distributions (Thiele et al., 2004) showed that humpback and minke whales were the most commonly detected species. These species occupied five geographically distinct spatial divisions in the study area. They were associated with increased sea ice cover and boundaries. Higher concentrations were observed when the ice margins overlapped with food resources in near coastal areas. The availability and abundance of baleen whale prey was affected by variability in sea ice conditions, particularly in regions of the Antarctic where annual sea-ice extent is being reduced or has increased (Zwally et al., 2002). The presence of cetaceans in the wAP has also been addressed using passive acoustic moorings that recorded whales calls for later identification. The presence of blue (*Balaenoptera musculus*) and fin (*Balaenoptera physalus*) whales was studied relative to sea ice. Both species of whales showed negative correlation with sea ice concentration, suggesting an absence of these whales in areas covered with sea ice (Širović et al., 2004).

A third major group of apex predators in the wAP is pinnipeds. The abundance

and distribution of these animals were studied during SO GLOBEC, using standard visual observations during ship-based surveys (Chapman et al., 2004) and satellite tags (Burns et al., 2004, 2008; Costa et al., 2008). These observations showed that crabeater seals and Antarctic fur seals (*Arctocehalus gazella*) were the most common species and that these were abundant in nearshore areas associated with abrupt bathymetry, and in areas of UCDW and high sea ice concentration (Burns et al., 2004, Chapman et al., 2004). Diving patterns of crabeater seals vary in response to habitat characteristics; Burns et al. (2008) interpreted seal behaviors in light of information on the distribution of their primary prey, krill (*Euphausia superba* or *Euphausia crystallorophias*). The study showed different scales for foraging by crabeater seals in different habitats.

Pelagic fishes are important consumers of Antarctic krill and they feed upper trophic predators such as seals and birds (Donnelly and Torres, 2008). During SO GLOBEC two distinct assemblages of pelagic fish were observed on the wAP continental shelf. The oceanic assemblage was characterized by high-diversity indices. The coastal assemblage was characterized by low-diversity indices and dominated by larval and juvenile notothenioids (*Pleuragamma antarcticum*). The overlap between the two assemblages was related to the local hydrographic conditions of the region, offshelf and along the shelf break. The oceanic assemblage was closely related to the presence of CDW. Oceanic icthyofauna was observed in Marguerite Trough and toward the innershelf in areas where CDW intrusions have been observed (Hofmann and Klinck, 1998b; Prézelin et al., 2000; Dinniman and Klinck, 2004; Klinck et al., 2004). The coastal assemblage showed elevated abundances, particularly of *Pleuragramma*, at the northern side of Marguerite Bay. Donnelly and Torres (2008) attribute this to the presence of copepods and krill (Ashjian et al., 2004; Lawson et al., 2004; Zhou and Dorland, 2004), which are primary prey groups for *P. antarcticum*.

The spatial distributions of the major apex predators in the wAP suggest that

animals select areas based on combinations of particular physical and biological characteristics (Burns et al., 2004; Chapman et al., 2004; Donnelly and Torres, 2008; Širović et al., 2004; Thiele et al., 2004). These regions are key for the reproduction and survival of Antarctic predators, and studying the physical constraints that affect these distributions will provide insights into the potential responses of this food web to global changes and climate variability.

2.3 ANTARCTIC KRILL

2.3.1 Distribution

The distribution of Antarctic krill in the Southern Ocean is circumpolar and is characterized by regions of persistent high densities (Baker, 1954; Marr, 1962). The patchiness in krill distribution shows strong seasonal and interannual variability (Brierley et al., 1997; Loeb et al., 1997; Siegel et al., 1998; Siegel, 2005). In the wAP region during winter, krill abundance is low and is confined mainly over the continental shelf (Siegel, 1988). From November and into the austral summer, krill abundance increases and the distribution extends beyond the continental shelf break (Siegel et al., 1990). Krill spawning occurs over the summer period from December to March. There is some interannual variability in this seasonal trend and the period of spawning can shift by approximately 4 weeks to give either an earlier start or later end of the spawning cycle (Spiridonov, 1995). During the austral summer, a spatial succession of krill developmental stages can be observed (Siegel, 1988). Spawning stages of krill migrate offshore to oceanic regions along the continental shelf break, while juveniles and small adults are found in coastal waters (Siegel, 1988, 1992; Hofmann et al., 1992; Lascara et al., 1999).

Several studies have focused on the importance of local and large-scale circulation patterns in the transport and distribution of Antarctic krill, particularly the role of the southern boundary of the ACC in connecting different regions (Priddle et al.,

1988; Siegel, 1992; Everson and Miller, 1994; Siegel and Kalinowski, 1994; Hofmann et al., 1998; Murphy et al., 1998; Fach et al., 2002; Hofmann and Hüsrevoglu, 2003). The large krill population west of the Antarctic Peninsula appears to be maintained by occasional strong year classes, with often poor recruitment in the intervening years (Siegel and Loeb, 1995; Hewitt et al., 2003; Quetin and Ross, 2003). Large differences in abundances of larval and juvenile krill were observed between austral fall-winter 2001 and 2002 during the SO GLOBEC field studies. During 2001, krill larvae were abundant with younger stages dominant offshore and older stages dominant onshore, and only few juveniles were present (Daly, 2004). During fall 2002, a similar distribution was observed for the krill larvae, but juveniles were more abundant on the middle and inner shelf indicating successful recruitment from the previous year (Daly, 2004). Large densities of larval krill were supported by high concentrations of chlorophyll *a* particularly in the vicinity of Marguerite Bay and to the south in the Bellingshausen Sea (Marrari et al., 2008).

Seasonal ice cover is an important factor affecting krill reproductive timing and success (Siegel et al., 1990; Siegel and Loeb, 1995) and the life-cycle of Antarctic krill is related to seasonal sea ice in a number of ways (Mackintosh, 1972, 1973; Marschall, 1988; Daly, 1990; Smetacek et al., 1990; Daly and Macaulay, 1991). Ice edge phytoplankton blooms have been suggested as an important factor influencing krill recruitment in the northern Antarctic Peninsula region (Siegel and Loeb, 1995; Smith et al., 1998). In this region, spring and summer ice edge blooms support krill reproduction and winter sea ice biota provide food for overwintering larvae (Kawaguchi and Satake, 1994; Siegel and Loeb, 1995; Quetin and Ross, 2003). In the southern Peninsula however, ice edge blooms are not a prevalent feature. Observations during the 2001 and 2002 SO GLOBEC fall and winter cruises indicated that sea ice biota concentrations were very low, with a large percentage of the krill larvae not even associated with the under surface of sea ice (Daly, 2004; Marrari et al., 2008). These

results are opposite to previous findings (e.g., Siegel and Loeb, 1995; Smith et al., 1998), indicating that sea is not necessarily a good predictor of food availability for overwintering larvae in the region (Daly 2004; Marrari et al., 2008).

2.3.2 Life cycle and development times

Antarctic krill has a multiyear life cycle, that begins when gravid females migrate offshore to spawn (Siegel, 1988; Ross and Quetin, 1983; Siegel, 1992). Krill spawn during the summer season between mid-December and March (Ross and Quetin, 1986; Hosie et al., 1988). Krill have a long and complex larval sequence that includes development of the egg through Nauplius (2 stages), Metanauplius, Calyptosis (3 stages) and Furcilia (6 stages) (Fraser, 1936) (Table 1). Calyptopis I is the first larval stage to occur at the surface and is the first feeding stage (Marr, 1962). It is then about 18-21 days after hatching (Witek et al., 1980; Ross et al., 1988) and is 1-2 mm in length (Fraser, 1936; Ikeda, 1984). At the end of summer, larvae moult to the early furcilia stages and in early winter they reach an average size of about 4-10 mm (Fraser, 1936; Witek et al., 1980; Siegel, 1989). Observations in the Scotia Sea showed that larval growth seems to continue during winter (Daly, 1990) but slows by late March (Huntley and Brinton, 1991). On the wAP in the Marguerite Bay region larvae growth during winter was slow or nearly absent (Daly, 2004).

Krill embryos are heavier than seawater and sink rapidly out of surface layers (Quetin and Ross, 1984; Ross and Quetin, 1985). Consequently, early developmental stages must return to the surface to feed. After spawning *E. superba* embryos hatch at about 850 m-1000 m, after 4.5 to 6 days, depending on the temperature structure of the water column (Marschall, 1983; Quetin and Ross, 1984; Ross and Quetin, 1985). The first three larval stages (nauplii) occur below 250 m. The calyptopis I larvae, the first stage with mouth and feeding appendages, usually lives in the surface layer where it encounters food (Marr, 1962; Hempel et al., 1979). The entire developmental

sequence takes about four months (Ikeda, 1984) if there is enough food available, or not until nine months (mid-November) under winter conditions of low food and low temperature (Ross et al., 1987). In the ocean, however, furcilia VI larvae are found in the same area both at the beginning of winter, sometimes under the ice (Guzmán, 1983), and in the spring, suggesting that further development is delayed while food levels are low. In the Marguerite Bay region, the abundant overwintering larval stages indicated two reproductive pulses during the previous summer (Daly, 2004). The availability of food is critical once the calyptopis I larvae reach the surface. The hatching larvae have enough energy stores to tolerate about 10 to 14 days of starvation after metamorphosis, but further starvation results in eventual death even if food becomes available later (Ross and Quetin, 1989; Hofmann et al., 1992).

Krill can grow to approximately 15 mm in length before their first winter (see Hofmann and Lascara, 2000) and do not mature until they are about 2 years old (Cuzin-Roudy, 1987a,b; Siegel and Loeb, 1994). During this time they overwinter twice. Adult krill grow to 50 to 60 mm in total length. During the early summer periods, juvenile krill are transported by currents as largely passive particles. Larger, adult krill can swim as well as small fish, moving distances larger than 10 km d^{-1} (Kanda et al., 1982). These stages can maintain speeds of 10-15 cm s^{-1} (Kils, 1982).

Temperature is also a significant variable in the early weeks of Antarctic krill development (Ross et al., 1988; Fach et al., 2002). The waters around Antarctica have a seasonal temperature range between -1.8°C to 2.5°C. Embryos and larvae may encounter nearly this full range during their developmental descent and ascent. Ross and Quetin (1986) found that this narrow temperature range has a significant effect on both embryonic duration and larval development times in the laboratory. They observed that developmental time does not depend linearly on temperature, but can

Table 1

Cumulative developmental time of krill larvae in days obtained from laboratory experiments (Ikeda, 1984), field data analysis (Witek et al., 1980; Ross et al., 1988; Daly, 1990) and modeling studies (Hofmann et al., 1992; Hofmann and Lascara, 2000). The simulated development times are representative of average conditions. Antarctic krill stages are abbreviated as: N = Nauplius (stage I-II), MN = Metanauplius, C = Calyptopis (stage I-III), F = Furcilia (I-VI).

	Krill Stage											
Source	**N1**	**NII**	**MN**	**CI**	**CII**	**CIII**	**FI**	**FII**	**FIII**	**FIV**	**FV**	**FVI**
Witek et al. (1980)[1]	–	–	–	30	45-60	60-75	70-90	75-105	90-120	105-135	120-180	135-240
Ikeda (1984)[2]	8	13	20	30	44	52-55	63-64	75	85-87	98-102	111-114	124-131
Ross et al. (1988)[1,2]	–	14-24	22-41	38-	52-	–	–	–	–	–	–	
Daly (1990)[1,2]	–	–	–	–	–	–	–	–	90-121	95-135	118-164	114-193
Hofmann et al. (1992)[3]	5-8	–	10-16	18-33	33-45	–	–	–	–	–	–	
Hofmann and Lascara (2000)[3]	–	–	–	32	44	50	58	70	100	117	163	258

[1] Field data analysis
[2] Laboratory experiments
[3] Modeling studies

be described with a Belèhradek temperature function (Belèhradek, 1926) of the form:

$$D = a(T - b)^c, \tag{1}$$

where D is developmental time in days, T is temperature, and a, b and c are fitted

constants.

The relationship between temperature and developmental times is curvilinear with a sharp decrease in developmental times between -1.0°C and 0°C. Ross et al. (1988) observed that this relationship was best described by an exponential model of the form:

$$D = B_0 \exp^{B_1 T} + B_2, \tag{2}$$

where D is developmental time in days, T is the temperature, and B_0, B_1 and B_2 are fitted constants. Laboratory experiments indicated that a cold sensitive period exists during early larval development. Developmental times were obtained for embryos, nauplius, metanauplius, and calyptopis stages I and II. The predicted developmental times for the first two feeding stages obtained by Ross et al. (1988) were longer than those obtained from laboratory experiments given in Ikeda (1984).

The relative effect of temperature and food on krill growth rate was estimated for a 2 mm krill (larval size) during transport across the Scotia Sea (Fach et al., 2002). These simulations showed that the effect of temperature is most pronounced when high food concentrations coincided with increased temperature. The short duration growth rates increases that they observed during approximately one year of simulation were sufficient to have an effect on the final size of krill.

2.4 LAGRANGIAN PARTICLE EXPERIMENTS

The advective transport pathways and transit times for Antarctic krill in the Southern Ocean have been studied primarily using numerical Lagrangian particle tracking experiments in which krill are considered as passive particles (Capella et al., 1992; Hofmann et al., 1998; Thorpe et al., 2004; Fach and Klinck, 2006) or by coupled physical and biological models (Murphy et al., 2004; Thorpe et al., 2007). These studies examined the role of advection by ocean currents and sea ice in the distribution

of Antarctic krill and connectivity among krill populations around Antarctica. These studies have focused on regional (Capella et al., 1992; Fach and Klinck, 2006) and circumpolar (Thorpe et al., 2007) connectivity of krill populations.

The frontal regions of the ACC have an important role in the transport of krill in the Scotia Sea (Capella et al., 1992; Hofmann et al., 1998; Murphy et al., 1998; Fach and Klinck, 2006), as they are regions of enhanced current speed. Particle tracking studies showed that transport from the Antarctic Peninsula region via the Southern Antarctic Circumpolar Current Front (SACCF) provides a primary route for bringing krill into the northern region of the Scotia Sea around South Georgia (Capella et al., 1992; Hofmann et al., 1998; Murphy et al., 1998; Murphy et al., 2004). Fach and Klinck (2006) showed that successful transport of krill to South Georgia depended on multiple factors, such as the location of the spawning area, timing of spawning, and variations in the location of the SACCF. Variability in sea ice distribution was also found to be a factor regulating the influx of krill to South Georgia region, from upstream regions in the Scotia Sea (Murphy et al, 1998; Fach et al., 2002). Lagrangian particle experiments in the wAP consist only of the study by Capella et al. (1992), which showed that Bransfield Strait is a region of potentially high larval abundance because it is supplied with larvae that are transported from the surrounding areas and by local production. In these Lagrangian calculations, the surface flow was the primary factor influencing the final location of the embryo-larvae particle and the timing of krill spawning affected the eventual position of the feeding larvae.

2.5 CIRCULATION MODEL

A circulation model has been developed for the wAP (Dinniman and Klinck, 2004; Dinniman et al., 2011), which is based on the Rutgers/UCLA Regional Ocean Model System (ROMS, Shchepetkin and McWilliams, 2005). The wAP model domain covers the continental shelf region in and around Marguerite Bay, has a 4-km horizontal

resolution, and is composed of 24 vertical sigma-layers that concentrate toward the surface and the bottom, allowing a better resolution in near shore areas. The model is forced by surface fluxes of heat, momentum (wind stress), freshwater, and by flow of the ACC along the shelf break in the region. The wAP circulation model is coupled with a dynamical sea ice model developed by Budgell (2005).

The comparisons of the wAP velocity and hydrographic distributions given in Dinniman and Klinck (2004) showed good agreement with general flow characteristics, dynamic topography, mean ADCP current fields, and hydrography described in Klinck (1998), Howard et al. (2004) and Klinck et al. (2004). The simulated seasonal variations in the depth and temperature of the mixed layer also matched observations (Klinck, 1998; Klinck et al., 2004).

Momentum advection and curvature of the shelf break were the two dynamical effects identified in the simulated circulation fields that allowed CDW intrusions to occur (Dinniman and Klinck, 2004). The simulated circulation fields showed a cyclonic gyre over the continental shelf with the ACC at the outer shelf boundary and a southwestward flow along the coast as the inner boundary, similar to observations in Smith and Klinck (2002). The simulated circulation fields also showed that variability in the location of the ACC along the wAP affects the movement of CDW onto the shelf, which has important implications on the heat and salt budgets of the region and also for sea ice formation (Klinck, 1998; Smith and Klinck, 2002).

CHAPTER 3

LAGRANGIAN SIMULATION OF TRANSPORT PATHWAYS AND RESIDENCE TIMES ALONG THE WESTERN ANTARCTIC PENINSULA

3.1 INTRODUCTION

The continental shelf of the western Antarctic Peninsula (wAP) was the primary study site for the U.S. Southern Ocean Global Ocean Ecosystems Dynamics (SO GLOBEC) Program, which had a main scientific goal of understanding the physical and biological factors that contribute to enhanced growth, reproduction, recruitment and survivorship through the year of Antarctic krill, *Euphausia superba* (Hofmann et al., 2002). The U.S. SO GLOBEC field studies took place in the Marguerite Bay region of the wAP (Fig. 1) during austral fall (April-June 2001 and 2002) and austral winter (July-September 2001 and 2002) (Hofmann et al., 2004, 2008). This program provided extensive hydrographic and circulation measurements (Beardsley et al., 2004; Howard et al., 2004; Klinck et al., 2004; Costa et al., 2008) that were coincident with measurements of zooplankton (Daly, 2004; Lawson et al., 2004; Ashjian et al., 2008; Marrari et al., 2011) and top predator (e.g. penguins and seals) distributions (Burns et al., 2004; Chapman et al., 2004; Ribic et al., 2008). A major result from analyses of the environmental and biological distributions was the identification of areas in and around Marguerite Bay that are characterized by sustained higher biomass that is in excess of average conditions (biological hot spots) (e.g. Fig. 1B, Costa et al., 2007). Associated with these regions were enhanced abundances of marine mammals and other top predators.

Predators are not uniformly distributed in the wAP; rather they select habitats

based on a combination of biological and physical factors (Burns et al., 2004; Chapman et al., 2004; Širović et al., 2004; Thiele et al., 2004). They tend to be associated with areas of above average sea ice concentration and shallow but irregular bathymetry (Burns et al., 2004), or coastal areas that have marginal sea ice (Trathan et al., 1996; Chapman et al., 2004; Thiele et al., 2004) and where large zooplankton and adult Antarctic krill are abundant (Lawson et al., 2004; Ashjian et al., 2008). Because of this selective distribution, predator distributions have been used as indices of resource availability to describe regions with localized productivity (Costa, 1991; Trathan et al., 1996) and as indicators of oceanographic features, such as polynyas or gyre circulation areas (Trathan et al., 1993).

The presence of CDW on the wAP continental shelf below the permanent pycnocline (about 120 m) is a dominant feature of this habitat (Smith et al., 1999; Klinck et al., 2004). Intrusions of CDW onto the wAP shelf are persistent, seasonally independent, and arise from interactions of the ACC with the bathymetry of the outer continental shelf (Klinck, 1998; Smith and Klinck, 2002; Dinniman and Klinck, 2004). The CDW intrusions are important to wAP heat, salt (Smith and Klinck, 2002) and nutrient budgets (Serebrennikova and Fanning, 2004) and areas where CDW intrusions occur are characterized by enhanced primary production (Prézelin et al., 2000, 2004). The presence of CDW affects distributions of Antarctic krill (Lascara et al., 1999) and potentially all trophic levels (Burns et al., 2004; Chapman et al., 2004; Daly, 2004; Širović et al., 2004; Thiele et al., 2004). Intrusions of Upper Circumpolar Deep Water (UCDW, potential temperature (θ) >1.5°C, salinity 34.6-34.7) are frequent (3-4 per month) and Lower Circumpolar Deep Water (LCDW, θ 1.3-1.7°C, salinity 34.72) intrusions are observed along deep trenches, such as Marguerite Trough (Fig. 1B), as dense water tongues that fill the depressions below 450 m and reach the inner portion of the wAP continental shelf (Moffat et al., 2009).

The role of the advective circulation in structuring biological populations has been

studied using numerical Lagrangian models, which provide estimates of transport pathways and residence times (see reviews in Hofmann and Lascara, 1998; Carlotti et al., 2000; deYoung et al., 2010). For the Antarctic, numerical Lagrangian particle tracking experiments have been used to determine transport patterns for Antarctic krill embryos and early life stages (Capella et al., 1992) and connectivity of Antarctic krill populations at regional (Hofmann et al., 1998; Murphy et al., 1998; Murphy et al., 2004; Fach and Klinck, 2006) and circumpolar scales (Thorpe et al., 2004; 2007). These studies highlighted the importance of the ACC fronts as primary transport mechanisms for Antarctic krill and potentially other plankton. Lagrangian studies for the wAP region showed that variability in the location of the SACCF relative to the continental shelf edge is an important determinant of plankton export or import (Hofmann et al., 1998; Fach et al., 2006). The wAP region also has local retention of Antarctic krill (e.g. Capella et al., 1992; Lawson et al., 2004), and potentially other plankton, due to clockwise gyres that are part of the continental shelf circulation (Smith et al., 1999; Klinck et al., 2004).

The spatial distributions of the major apex predators along the wAP continental shelf suggest that these animals select areas based on combinations of particular physical and biological characteristics. These regions are key for productivity of the wAP ecosystem, and understanding the processes that produce them will provide insights into the potential responses to global change and climate variability. Therefore, the objective of this study was to determine the role of the circulation in producing observed biological distributions on this shelf. This objective was addressed by using a numerical circulation model developed for the wAP (Dinniman and Klinck, 2004) to do a series of Lagrangian particle tracking experiments to determine sites of across-shelf transport and to obtain quantitative estimates of residence times in specific regions and primary transport pathways.

The following section provides a description of the numerical circulation model

and Lagrangian experiments used in this study. The results from the numerical simulations were used to develop diagnostics of the characteristics of the flow, determine primary transport pathways on the wAP continental shelf, and estimate residence times in areas of the shelf that are characterized by aggregations of top predators. The discussion and summary section places these results in the context of what is currently known about biological distributions on the wAP continental shelf.

3.2 METHODS

3.2.1 Circulation model

The Rutgers/UCLA Regional Ocean Modeling System (ROMS) version 3.0 was implemented for the wAP region (Fig. 1A) and used to provide the circulation distributions for the Lagrangian experiments. This model is a free-surface, terrain-following, primitive equations ocean circulation model (Shchepetkin and McWilliams, 2005; Haidvogel et al., 2008). The version of the circulation model used in this study included a dynamic sea-ice model (Budgell, 2005) and thermodynamically active ice shelves (Dinniman et al., 2007).

The model domain extended along the western side of the Antarctic Peninsula from 72°S to the tip of the Peninsula, covered the entire continental shelf, and extended about 500 km offshore from the shelf break (Fig. 1A). The horizontal grid spacing was 4 km and there were 24 vertical levels, which were concentrated towards the top and bottom of the domain. The flow components u (east-west) and v (north-south) are oriented according to the grid configuration or roughly along the coastline. Therefore east-west component represents along-shelf flow and north-south component represents the flow across-shelf. The bathymetry grid was constructed from sources that included, ETOPO2v2 (2 minute gridded bathymetry, Smith and Sandwell, 1997), Woods Hole Oceanographic Institution SO GLOBEC bathymetry data (Bolmer, 2008), BEDMAP data including bathymetry beneath ice shelves and

ice thickness, a bathymetry developed for simulation of tidal flow under ice shelves (Padman et al., 2002), and bathymetry data given in Maslanyj (1987). The latter data source provided ice thickness and bedrock depth below sea level for the George VI Ice Shelf (Fig. 1A). The wAP model bathymetry was modified over the outer few grid-points of the model domain so that the isobaths were normal to the boundary, which improves performance of open-boundary conditions (e.g. Dinniman et al., 2003; Dinniman and Klinck, 2004). The bathymetry was smoothed with a modified Shapiro filter, which was designed to selectively smooth areas where the changes in bathymetry are large with respect to the total depth (Wilkin and Hedström, 1998). For the wAP model, domain most of the changes to the bathymetry were in the inner shelf around islands, where the bathymetry is steep and the water depths are shallow.

The sea ice was simulated using a dynamic-thermodynamic module coupled with the ocean circulation model. The sea ice dynamics are based upon an elastic-viscous-plastic rheology (Hunke and Dukowicz, 1997; Hunke, 2001), which allows the sea ice to deform as a plastic material, thereby providing increased realism for shorter time scales associated with physical forcing (Budgell, 2005). The sea ice thermodynamics are based on Mellor and Kantha (1989) and Häkkinen and Mellor (1992), which allow one layer of snow and two layers of sea ice. The snow layer is an insulating layer and also absorbs incoming radiation as it melts in the spring. A molecular sublayer at the bottom of the ice layer-ocean allows realistic freezing and melting rates.

At the model boundaries, monthly climatologies derived from the Simple Ocean Data Assimilation (SODA) reanalysis (Carton and Giese, 2008), were used to specify temperature, salinity, and depth-averaged velocities, similar to what was done by Dinniman and Klinck (2004). The baroclinic velocities were specified using pure radiation conditions. The model was initialized with horizontally uniform temperature, salinity and a vertical structure obtained from the average of the SODA climatologies. The horizontal variation was imposed over five days to minimize the initial geostrophic

adjustment of the simulated flow.

The model was forced with daily wind stress and wind speed calculated from 12-hr winds obtained from the Antarctic Mesoscale Prediction System (AMPS, Powers et al., 2003), which were applied as a surface stress. The wind forcing was for September 15, 2003 to September 15, 2005. Monthly climatologies of precipitation, surface pressure, air temperature, and humidity obtained from AMPS were used to specify freshwater and air-sea fluxes. Precipitation and the monthly cloud climatologies were obtained from the International Satellite Cloud Climatology Project (ISCCP, Rossow and Schiffer, 1999). Open ocean momentum, heat, and fresh water (imposed as a salt flux) fluxes for the model were then calculated based on the COARE 3.0 bulk flux algorithm (Fairall et al., 2003).

Evaluation of the simulated circulation fields for the wAP was done using Acoustic Doppler Current Profiler (ADCP) observations made during the SO GLOBEC field studies (Howard et al., 2004) and historical hydrographic observations. Details of these comparisons are given in Dinniman and Klinck (2004).

3.2.2 Flow diagnostics

The characteristics of the advective flow on the wAP were determined first to provide guidance as to space and time scales needed to constrain the Lagrangian particle simulations. The simulated mean surface flow and that from the depth that corresponds to the CDW (model sigma level 15) were analyzed to identify persistent high/low velocity regions, the shape and distribution of circulation gyres, and general flow patterns.

The temporal variability of the wAP circulation was obtained by determining the autocorrelation of the flow at each model grid point. The autocorrelation (ρ_k)

function (Box et al., 1994) for a time lag, k, is defined by:

$$\rho_k = \frac{c_k}{{\sigma_z}^2}, \tag{3}$$

$$c_k = \frac{1}{N}\sum_{t=1}^{N-k}(z_t - \bar{z})(z_{t+k} - \bar{z}) \qquad k = 0, 1, 2, ...k, \tag{4}$$

where c_k is the autocovariance at lag k and ${\sigma_z}^2$ is the variance of the time series, z, of length N and is calculated as

$$\sigma_k^2 = \frac{1}{N}\sum_{t=1}^{N}(z_t - \bar{z})^2. \tag{5}$$

The mean of the values in the time series, z_t, for times $t = 1$ to N is given by $\bar{z}$. For this analysis, the time series (z_t) that were analyzed were the east-west (u) and north-south (v) velocity components obtained from the circulation model at daily intervals. The decorrelation scale of the advective flow at each model grid point was taken to be the time lag prior to crossing the 95% confidence interval.

3.2.3 Lagrangian Experiments

The trajectory followed by a particle in space (x, y, z) and time (t) is described by the equation:

$$\frac{d\vec{X}}{dt} = \vec{U}(\vec{X}, t) + W_{vw}\hat{Z}, \tag{6}$$

where $\frac{d}{dt}$ is the change in the location of a particle along a three-dimensional (x, y, z) trajectory given by $\vec{X}$. The particle location is modified by the advective velocity $\vec{U}(\vec{X}, t)$, and vertical diffusion, which was included by adding a random vertical displacement (W_{vw}), to the vertical ($\hat{Z}$) particle location at each time step (Hunter et al., 1993; Visser, 1997). The maximum value allowed for vertical diffusion 10^{-2} m^2s^{-1} is associated with convective flows. The horizontal (u, v) and vertical (w) velocity components were obtained from the circulation model.

The horizontal and vertical positions of the particles, at each time interval were obtained using a fourth-order Milne predictor (Abramowitz and Stegun, 1964) and a fourth-order Hamming corrector scheme (Hamming, 1973). Vertical displacement resulting from the random walk parameterization of vertical diffusion was obtained with a forward difference scheme. The probability distribution for the vertical displacement is Gaussian and includes a correction for the vertical gradient in the diffusion coefficient. The time step used in the Lagrangian particle tracking experiments was four minutes, but the particle positions were obtained at two-hour and twelve-hour intervals, depending on the experiment.

Lagrangian numerical experiments were designed to focus on sites of across-shelf exchange, particularly areas of CDW intrusions, general transport patterns on the wAP continental shelf, and import/export of particles in specific regions of the wAP. These studies used neutrally buoyant floats that were released at several sites and depths along the outer and mid-regions of the wAP and in arrays of varying density (Fig. 2, Table 2). The horizontal and vertical release points for the particles were determined from the spatial decorrelation scales obtained from analysis of the advective fields. The fine-grid float array provided determination of general transport patterns (Fig. 2). The coarse-grid float array (Table 2) consisted of transects across the shelf break in regions where the flow was onshelf and had higher velocities. Areas where the floats consistently crossed the continental shelf break were used to identify regions of CDW intrusions, and these were used to define a shelf break float array (Fig. 2). The position of the particles for these three grid arrays (coarse, fine, and shelf break) was obtained every two hours; this time interval is shorter than the decorrelation scales obtained from analysis of the advective fields.

The role of circulation in producing the biological hot spots was explored by tracking the origin of particles transported into the regions. Two experiments explored contributions to hot spots (Fig. 2, Table 2); in the first experiment the simulated

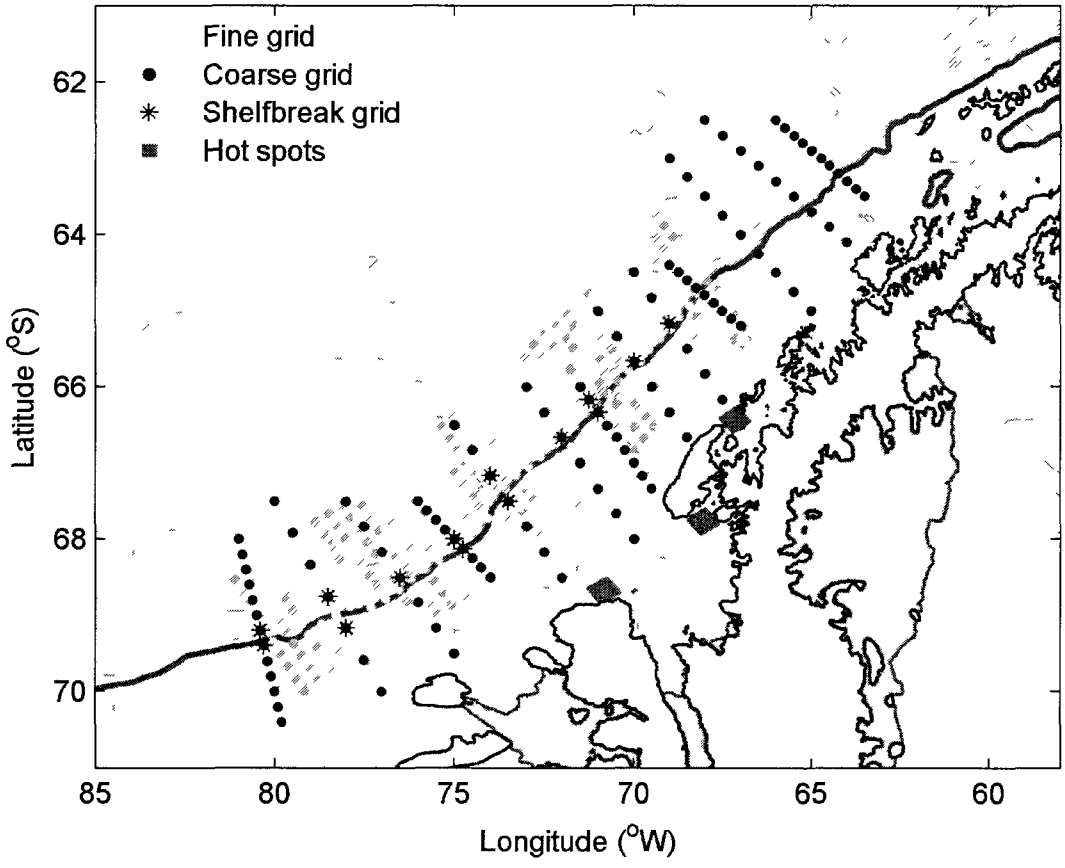

Fig. 2. Distribution of release locations used for the Lagrangian simulations, which included a high resolution grid that covered the outer shelf, shelf break and slope (light gray dots), a coarse resolution grid with transects crossing the shelf in areas of onshelf flow (black dots), and locations along the shelf break (*). Additional Lagrangian release experiments were done in the three biological hot spots, indicated by the gray squares. The region around the hot spot used for the simulated drifter releases are indicated by the gray squares.

Table 2

Summary of the numerical Lagrangian experiments done for the west Antarctic Peninsula region. For each experiment, the grid resolution, description, number of release points, depth of drifter release, release date, and release frequency is given.

Resolution	**Description**	**Number of release points**	**Depth of release (m)**	**Release date**	**Release frequency**
Fine grid	Higher resolution grid, along shelf break	407	300	23 January 2004 to 23 April 2004 at 10 days intervals	Multiple-11 releases
Shelfbreak grid	Pathways for CDW-intrusions	14	250, 300, 350, 400, 450, 500	23 January 2004	One time
Hot spots grid	To determine residence times for hot spots	49	0, 50, 100, 150, 200, 250, 300	15 January 2004 and 15 May 2004	One time
Observations-WOCE drifters	Points of release to compare with observations from WOCE-drifters	17	15	24 January 2005 21 January 2005 29 January 2005 27 January 2005, 2 days before, same day and 2 days after	Multiple-20 releases

floats were released at 300 m at 10-day intervals for 60 days in a grid of transects that extended across the continental shelf break. For the second experiment the simulated floats were released at 300 m at 10-day intervals for 100 days in a high-resolution grid of transects that extended across the continental shelf break (Fig. 2, Table 2).

Residence time estimates were obtained for the hot spot areas of the wAP shelf by releasing one float at each grid point in a 7 $\times$ 7 grid (24 km $\times$ 24 km) between

0 and 300 m at 50-m intervals (7 depths), for a total of 343 floats (Fig. 2, Table 3). The horizontal spacing was defined by the horizontal resolution of the model (i.e. 4 km). The position of the particles was obtained at twelve-hour intervals. Floats were released in the summer (January 15) and in the fall-winter (May 15) and tracked for 354 and 489 days, respectively. The time required for the floats to exit the release area was taken as a measure of the residence time for the region. The fraction of particles that remained within the source region with respect to the initial number of floats released was obtained at each time interval and used to calculate residence time as:

$$f(\tau) = f_o e^{-\lambda\tau}, \tag{7}$$

where f is the fraction of particles that remain within the source region at an elapsed time τ, given in days since release, f_o is the initial fraction of particles at $\tau = 0$, and λ is the decay constant. Residence times were calculated for the e-folding time scale or the time when the fraction of particles was reduced to 0.3679 (Fig. 3). Residence times were calculated for each depth of release and a total mean was calculated for each hot spot region. The significance of differences between the mean residence times obtained for the summer and winter was determined using a t-test with a 95% confidence interval and for 12 degrees of freedom.

3.2.4 Definition of Hot Spots

The top predator biological hot spots (Costa el al., 2007) were defined based on habitat use by seabirds, cetaceans, crabeater seals, and pelagic fish. The Alexander Island hot spot region (Fig. 1B, Table 3) is south of Marguerite Bay and was characterized by densities of southern fulmars (*Fulmarus galcialoides*), snow petrels (*Pagodroma nivea*), and Antarctic petrels (*Thalassoica antarctica*), that were higher than observed in other regions of the wAP before pack ice is formed (Chapman et al., 2004). Crabeater seal sightings and satellite tracks data also showed high densities

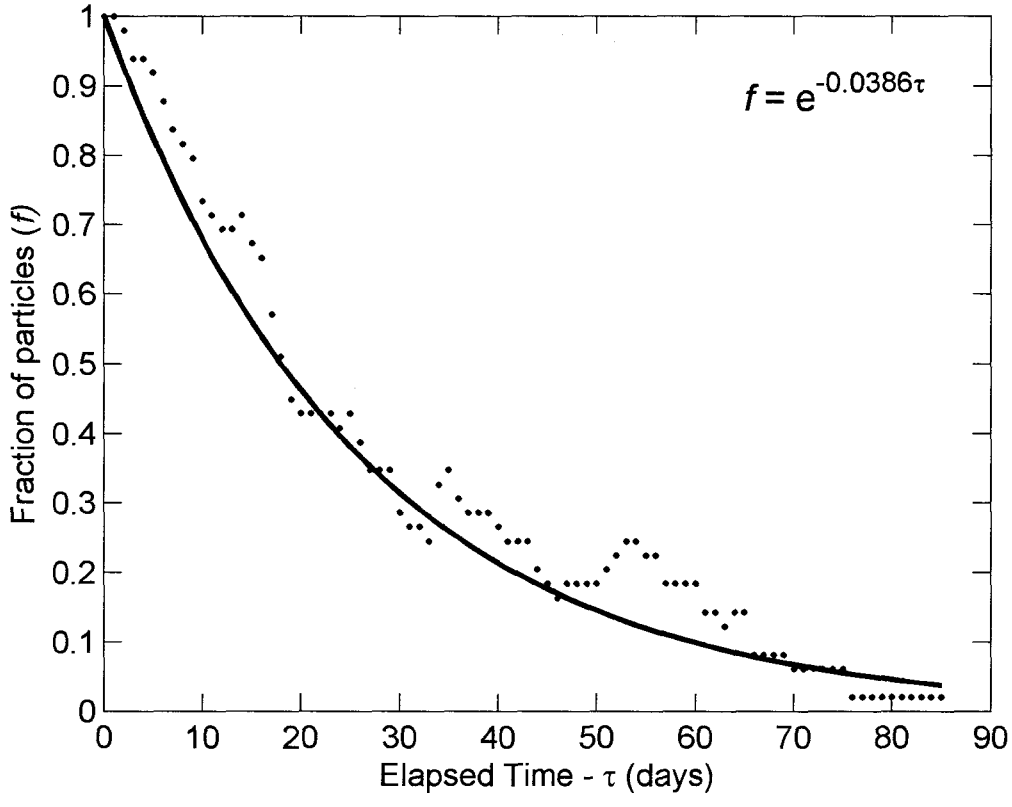

Fig. 3. The fraction of particles that remained within the Laubeuf Fjord hot spot at 50 m after release on 15 May (f) versus elapsed time (τ, in days) since the start of the simulation (•). The model fit to the data (solid line) is shown. Similar analyses were done for other depths and the two other hot spot locations to obtain residence time estimates.

Table 3

Latitude and longitude boundaries used for the Lagrangian experiments for the three biological hot spot regions.

Hot Spot Region	North limit	South limit	East limit	West limit
Crystal Sound	66°16.8′°S, 67°06.3′°W	66°34.9′°S, 67°12.5′°W	66°27.0′°S, 66°46.7′°W	66°24.6′°S, 67°32.0′°W
Alexander Island	68°31.3′°S, 70°45.4′°W	68°49.2′°S, 70°55.1′°W	68°42.0′°S, 70°25.5′°W	68°38.5′°S, 71°14.9′°W
Laubeuf Fjord	67°59.3′°S, 67°37.0′°W	67°55.1′°S, 68°06.1′°W	67°47.4′°S, 67°39.0′°W	67°44.7′°S, 68°26.8′°W

in this hot spot (Burns et al., 2004). This region was also identified as a location for baleen whale feeding during summer and autumn (primarily minke and humpback whales, Thiele et al., 2004). The Laubeuf Fjord hot spot, located south of Adelaide Island inside Marguerite Bay (Fig. 1B, Table 3), was characterized by elevated abundance of pelagic fish (*Pleuragramma antarcticum*, Donnely and Torres, 2008), which may be related to elevated biomass of copepods and krill (Ashjian et al., 2004; Lawson et al., 2004; Marrari et al., 2011) in this area. The Crystal Sound hot spot region, located between Adelaide Island and Renaud Island (Fig. 1B, Table 3) had high densities of crabeater seals (Burns et al., 2004) and krill (Zhou et al., 2004).

For the numerical Lagrangian particle experiments, equal-sized regions were defined around each hot spot (Fig. 1B, Table 3), which allowed the transport pathways and residence times obtained for the three regions from the Lagrangian particle experiments to be compared. Each area was defined to be 24 km × 24 km, which contained a total of 49 grid points in the horizontal and sampled for seven depths from surface to 300 m, was large enough to include the hot spots defined from observations.

3.2.5 Evaluation of Simulated Float Trajectories

Prior to implementing the Lagrangian studies for specific regions of the wAP, the simulated float trajectories were evaluated by comparisons with drifter measurements made as part of the PAL LTER program. In January 2005, World Ocean Circulation Experiment (WOCE)-style drifters were released in Marguerite Bay and tracked via the ARGOS satellite system (Table 4). Details of the methodology for the drifter data are given in Beardsley et al. (2004). To compare observed and simulated drifter trajectories, an array of 16 surface floats was released around the location of the observed drifter, and one float was released at exactly the same release location of the observed drifter. Each of the four arrays was released at three times, two days before, same day and two days after the day of the observed drifter release (Table 4). The frequency of the releases was defined according to the short decorrelation scales observed on the surface flow (see section III.3.1.2). The simulated float trajectories were obtained at twelve-hour intervals; the reporting interval of the satellite-tracked drifters was every 1.2 (located 20 times per day) hours. Simulations of the float trajectories extended until the last day of data return for which the observed floats were still in the region used in this study (Table 4). The WOCE-style drifters provided observations of the surface circulation; therefore, only simulated surface fields were used for comparisons of general circulation pathways and time scales.

3.3 RESULTS

3.3.1 Flow Diagnostics

3.3.1.1 Flow Characteristics

The simulated mean surface circulation along the outer edge of the wAP continental shelf was dominated by the northeasterly flowing ACC. Surface velocities in excess of 0.1 to 0.15 m s^{-1} (Fig. 4A) were associated with the southern boundary of

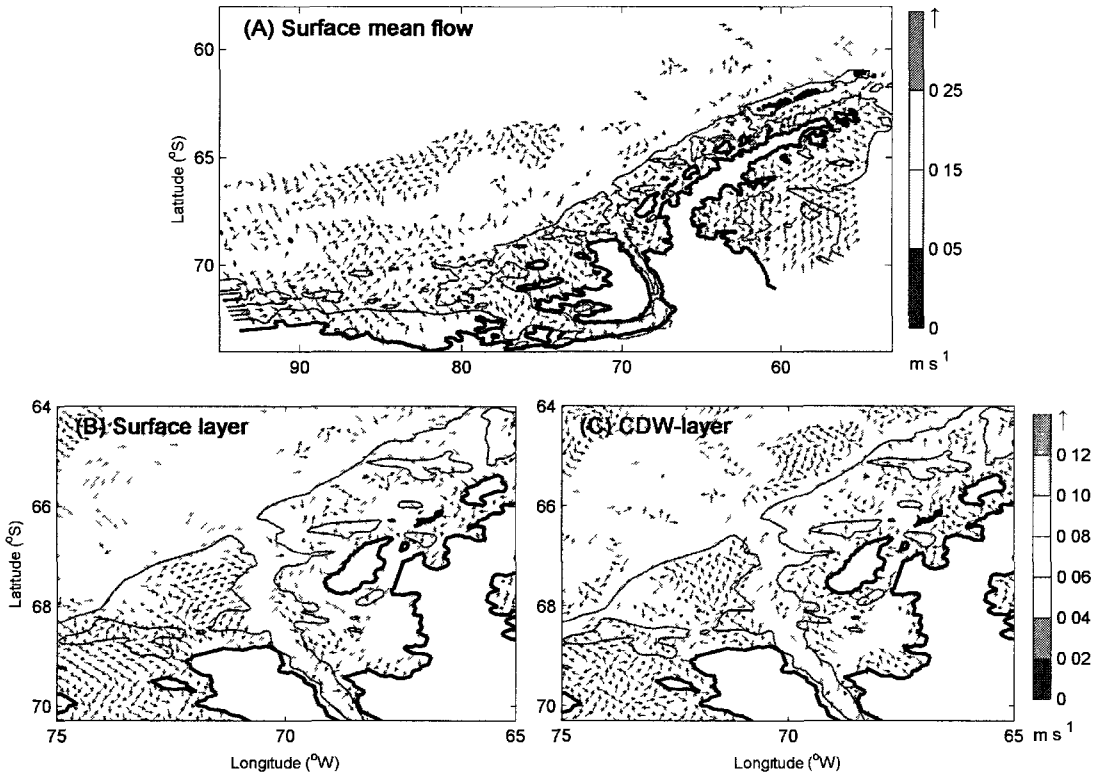

Fig. 4. (A) Simulated surface mean circulation field for the entire western Antarctic Peninsula model domain calculated using approximately 1.7 years of simulated distributions (from model day 1560-December 24 to model day 2190-September 30). The velocity vectors were plotted for every 8^{th} grid point (28 km resolution). Flow speed (m s^{-1}) is indicated by color; equal-length vectors indicate flow direction Simulated mean flow for the SO GLOBEC study area at the (B) surface and at the (C) depth of the Circumpolar Deep Water (CDW) layer (200-500 m). Velocities in excess of 0.12 m s^{-1} were assigned the same color to better resolve the lower flow speeds (<0.1 m s^{-1}) over the continental shelf. Every third velocity vector was plotted (8 km resolution). The land boundaries (thick solid line) and 500 m isobath are shown (thin solid line).

Table 4

Details of the floats deployed on the wAP continental shelf in 2005. The initial and final locations and release date are given for each float. The date of the last float observation used in the comparisons between the observed and simulated floats is also given.

Float designation-Figure number	Initial location	Final location	Release time	Date of last observation used
A50 - 7A-C	67°46.4′°S, 69°58.2′°W	68°16.4′°S, 67°08.6′°W	2005-01-24	2005-02-18
A48 - 7D-F	66°45.6′°S, 69°14.4′°W	68°13.2′°S, 71°32.8′°W	2005-01-21	2005-04-24
A65 - 8A-C	66°26.2′°S, 73°07.4′°W	65°47.3′°S, 67°37.9′°W	2005-01-29	2005-04-25
A49 - 8D-F	67°07.1′°S, 71°29.0′°W	67°44.7′°S, 71°45.8′°W	2005-01-27	2005-02-09

the ACC, which is aligned with the wAP continental shelf break (Orsi et al., 1995). On-offshelf meanders occurred at several locations on the outer shelf along the path of the ACC.

In the SO GLOBEC study region (Fig. 4B), the mean surface circulation associated with the ACC turned onto the wAP shelf along the northern edge of Marguerite Trough and flowed onshelf. Part of this flow continued onshelf towards Crystal Sound. The other part of this flow continued south of Adelaide Island into Marguerite Bay and became part of the cyclonic circulation of the Bay. The flow exited the Bay along the eastern side of Alexander Island, where the velocity increased in magnitude. As it moved offshore the flow meandered and joined the incoming flow, suggesting a cyclonic surface circulation in Marguerite Bay (Fig. 4B). The magnitude and pattern of the simulated surface circulation in the Marguerite Bay area was generally consistent with that produced from hydrographic observations and dynamic heights obtained

during the 2001 SO GLOBEC field program (Klinck et al., 2004). The primary difference in the simulated and observed surface circulation was in the outward flow from Marguerite Bay. Observations show merging of the outward flow at the western side of Marguerite Bay with a dominant southerly flow over the continental shelf south of the Bay. The simulated surface flow west of Marguerite Bay was dominated by a slow northeasterly flow and by mesoscale circulation structures farther west. These discrepancies may be attributed to differences in the space and time scales of the processes, that the observations and the model represent, and to the climatological nature of the forcing fields used with the circulation model.

The general pattern of the flow at the depth of the CDW (200-500 m) was similar to the surface flow (Fig. 4C). The southern boundary of the ACC along the shelf break is indicated by meanders and increased flow speeds. The flow at this depth also turned onshore at the northern edge of Marguerite Trough. In general, the flow over the continental shelf was slower and less organized than the flow at surface but there was a clear cross-shelf flow via the deep depressions that cross the continental shelf, such as off Adelaide Island (66°30′S, 69°W), Anvers Island (65°18′S, 67°W) and Alexander Island (68°S, 73°42′W). The locations where the flow at this level moves onshore are consistent with those identified in hydrographic distributions (Klinck et al., 2004) and previous numerical circulation studies (Dinniman and Klinck, 2004). Over the shelf, the mesoscale structure of the flow reflected the effect of the bathymetry, which exerts strong control on the flow of this region (Dinniman and Klinck, 2004; Klinck et al., 2004).

3.3.1.2 Temporal Decorrelation Scales

Temporal decorrelation scales for the east-west (u) and north-south (v) velocity components were constructed for the flow at surface and at the depth of the CDW (Fig. 5A-D). The decorrelation scales for the surface flow over most of the wAP

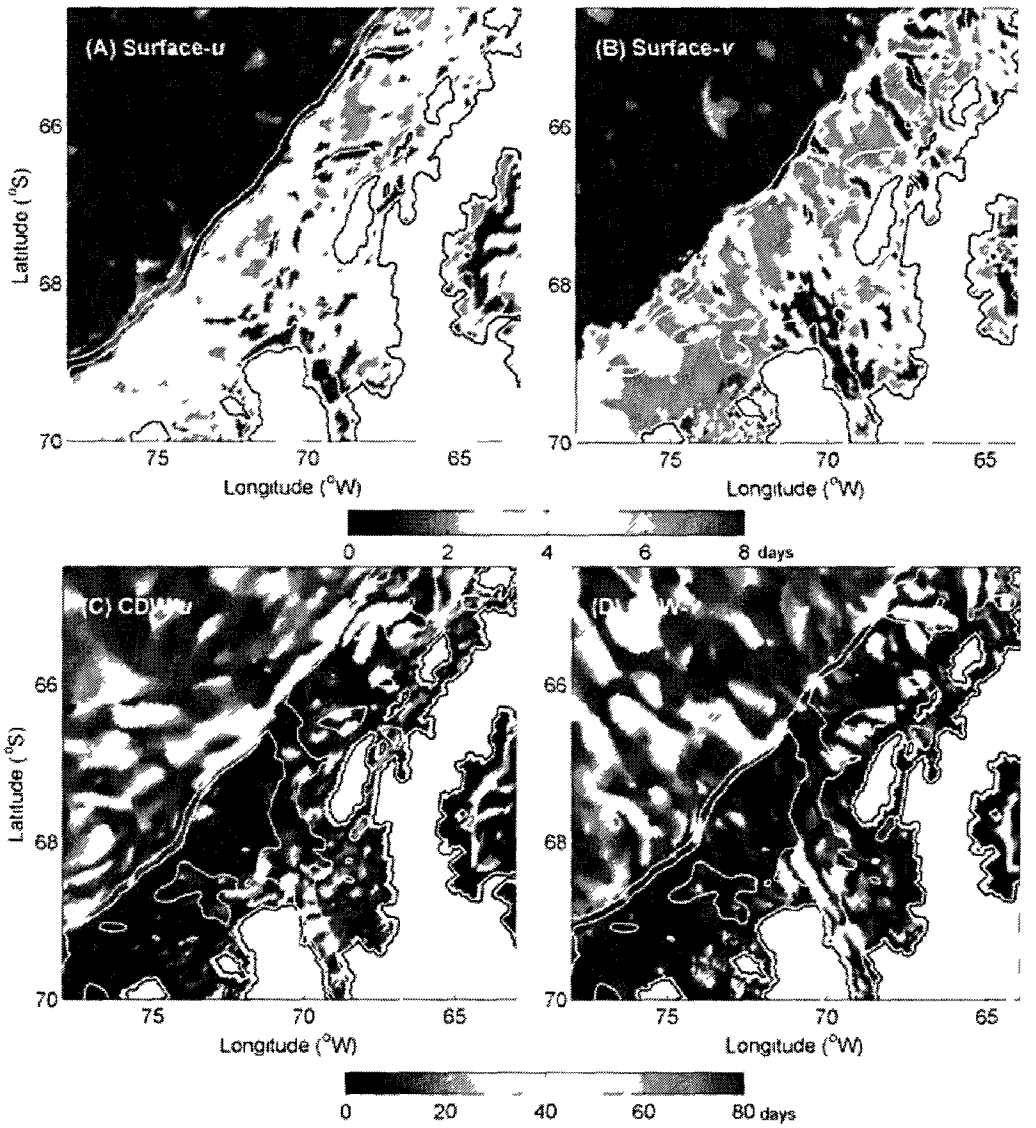

Fig. 5. Temporal decorrelation scales (days) calculated for the simulated (A) east-west component (u) of the surface flow, (B) north-south component (v) of the surface flow, (C) east-west component (u) of the flow at the depth of the Circumpolar Deep Water (CDW), and (D) north-south component (v) of the flow at the depth of the CDW. Only decorrelation scales shorter than 8 days for the surface flow are shown (A and B). The decorrelation scales were obtained for the velocity at each model grid point using 1.7 years of simulated distributions. The confidence interval for the decorrelation scales is 95%. The land boundaries (thick white line), the 500-m and 1000-m isobaths (thin white lines) are shown.

continental shelf were short, between 2-4 days (Fig. 5A, B). This short decorrelation scale is consistent with the scale of the wind stress, which is dominated by synoptic variability at 3 to 6 days (Trenberth, 1991; Bromwich and Stearns, 1993).

Longer decorrelation scales for the u and v components of the surface velocity of about 30 to 40 days were found along the southern part of Marguerite Bay (not shown using present color-scale), which is influenced by outflow from the George VI Sound and George VI Ice Shelf (GVIIS). The outflow of freshwater from basal melting of the GVIIS may result in surface stratification that stabilizes the flow in the southern part of Marguerite Bay (Potter and Paren, 1985). Also the maximum decorrelation scale was consistent with the seasonal influx of the fresh water produced by the retreat and melting of sea ice, which may enhance stratification in southern Marguerite Bay.

Temporal scales for the flow below the permanent pycnocline (Fig. 5C, D) were similar to those estimated for the surface flow offshore of the shelf break. However, over the continental shelf, the temporal decorrelation scales of the deeper flow were more variable than those of the surface flow. Flow decorrelation scales around the depressions that intersect the wAP continental shelf were 30 to 60 days (Fig. 5C, D). In particular, both components of the flow showed decorrelation scales of 30 to 50 days along the extent of Marguerite Trough and into Marguerite Bay. At other locations, such as off Adelaide Island, Anvers Island and the southern side of Alexander Island, the decorrelation scales for the u and v velocity components varied between 40 to 60 days. This temporal scale of variability is consistent with 5-6 CDW intrusions per year (Klinck et al., 2004).

The decorrelation scales associated with the flow in the biological hot spots were variable. The surface flow in all three regions had scales of 2-3 days (Fig. 6A, B), similar to those associated with the surface flow over the continental shelf (Fig. 5A, B). At the depth of the CDW, the mean temporal decorrelation scales were 5-7 days (Fig. 6C, D), and the east-west (u) component of the flow was more coherent (Fig.

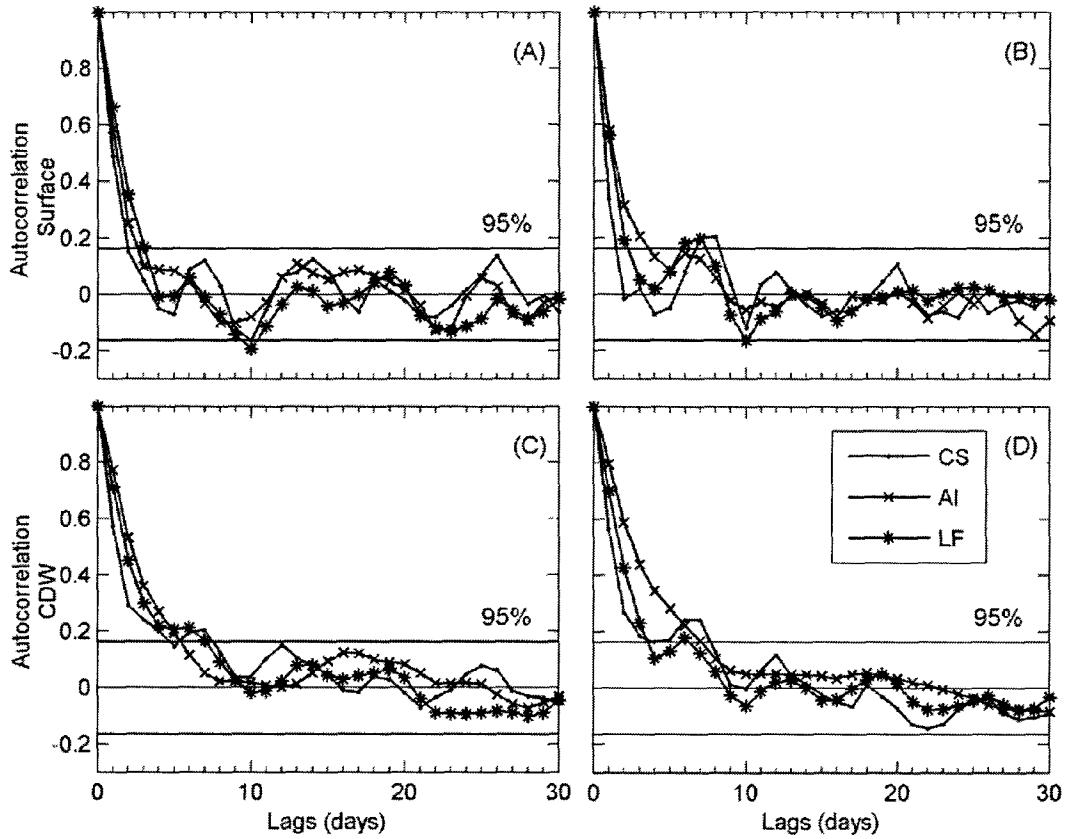

Fig. 6. Mean autocorrelation functions calculated for the simulated (A) east-west component (u) of the surface flow, (B) north-south component (v) of the surface flow, (C) east-west component (u) of the flow at the depth of the Circumpolar Deep Water (CDW), and (D) north-south component (v) of the flow at the depth of the CDW (200-500 m) for the three biological hot spot regions; Crystal Sound (CS), Alexander Island (AI) and Laubeuf Fjord (LF). The 95% confidence intervals are shown by the solid lines.

6C).

3.3.1.3 Evaluation of Simulated Floats

The accuracy of the simulated float trajectory pathways and time scales of flow was evaluated by comparison with trajectories from the drifters deployed on the wAP. Two of the WOCE-style drifters were deployed near Adelaide Island (Fig. 7). The drifter deployed near the entrance to Marguerite Bay (Fig. 7A-C) entered the Bay, moved southward, and after 27 days ended its trajectory in the near shore portion of the Bay (Fig. 7A-C). A part of the array of simulated drifters followed a similar pathway for the three days over which these were released. The trajectories of some the simulated floats also ended in the nearshore region between 23 to 27 days after release (Fig. 7C).

The simulated floats released off the northwest side of Adelaide Island followed trajectories that differed from those of the WOCE-style drifter (Fig. 7D-F). During the first 5 days, the observed and simulated floats remained near the area of release, after which the pathways diverged. The WOCE-style drifter moved along Adelaide Island and turned inside Marguerite Bay, following the path of the Antarctic Peninsula Coastal Current. The simulated floats moved northeastward along the shelf, and some entered Crystal Sound, and eventually moved south along the inner shelf into Marguerite Bay through Laubeuf Fjord (Fig. 7F).

One WOCE-style drifter was deployed off the shelf break. The observed and simulated drifters (Fig. 8A-C), showed similar pathways, moving to the northeast with the ACC, but the simulated floats showed more mesoscale variability. After 40 days, the pathways of the observed and simulated drifters diverged. The observed drifter turned onshore and continued southwest along the shelf. The simulated floats continued along the path of the ACC moving to northeast along the shelf break (Fig. 8A-C). The WOCE-style drifter released in the mid-shelf west of Marguerite Trough

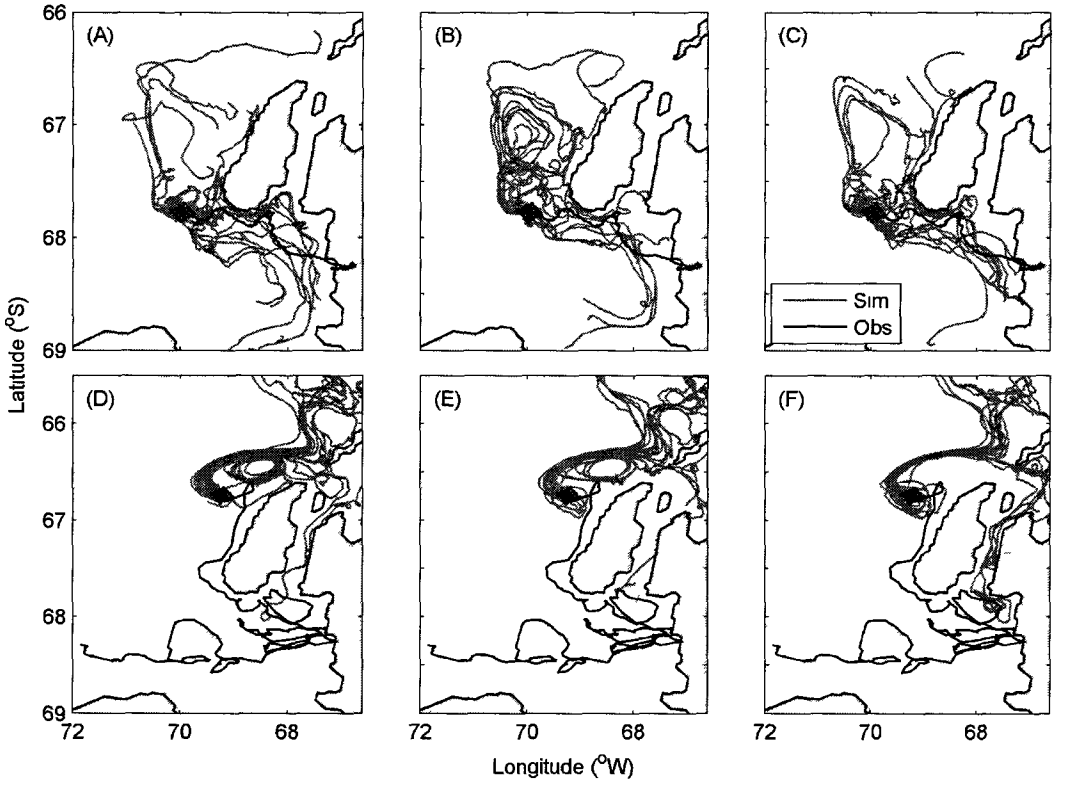

Fig. 7. Comparison of simulated drifter trajectories (light gray lines) with trajectories obtained from two WOCE-style drifters (black lines) deployed on the western Antarctic Peninsula region from 24 January 2005 to 18 February 2005 (A-C) and 21 January 2005 to 24 April 2005 (D-F). The release point for the observed drifters is at the center of the array (black dots, 17 points) used for the release points of the simulated drifters. The simulated drifters were tracked for the same time as the observed drifters. The simulated drifters were released 2 days before (A and D), the same day (B and E), and 2 days after (C and D) the release day of the observed drifter. The 500, 1000, 1500, 2000, 2500 and 3000-m isobaths are shown (light gray lines).

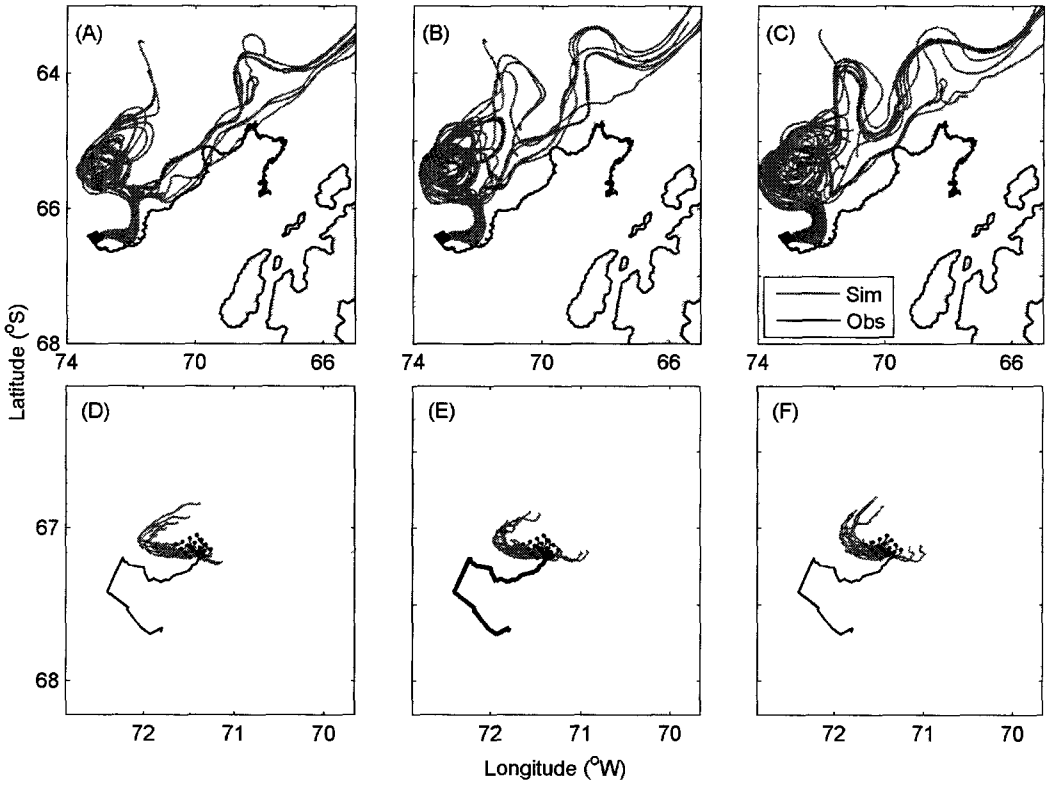

Fig. 8. Comparison of simulated drifter trajectories (light gray lines) with trajectories obtained from two WOCE-style drifters (black lines) deployed on the western Antarctic Peninsula region from 29 January 2005 to 25 April 2005 (A-C) and 27 January 2005 to 09 February 2005 (D-F). The release point for the observed drifters is at the center of the array (black dots, 17 points) used for the release points of the simulated drifters. (The simulated floats were tracked for the same time as the observed drifters. The simulated floats were released 2 days before (A and D), the same day (B and E), and 2 days after (C and D) the release day of the observed drifter. The 500, 1000, 1500, 2000, 2500 and 3000-m isobaths are shown (light gray lines).

provided data for only 14 days (Table 4). The trajectories of the array of simulated floats during this period were similar to the observed pathways (Fig. 8D-F). After release the observed drifter moved more south than west relative to the simulated drifters.

The comparisons of observed and simulated drifter trajectories indicated that the wAP simulated flow fields resolve the spatial and temporal scales of variability. Discrepancies in the comparisons likely result from differences in wind forcing, sea ice conditions, coastal fresh water flux and location of the ACC that result from the forcing fields and climatologies used as input to the circulation model. Thus, the Lagrangian experiments provide realistic estimates of transport pathways and residence times for the wAP continental shelf.

3.3.2 Transport pathways and residence times

3.3.2.1 Pathways

The ACC and CDW intrusions dominated the wAP continental shelf simulated circulation distributions. Thus, the first set of Lagrangian particle tracking experiments was focused in areas where these flows occurred. Particles were released along across-shelf transects that crossed CDW intrusion sites at the outer shelf (Fig. 2, Table 2).

Particles released along the shelf break between 250 m and 500 m, depths that correspond to CDW, were transported to the northeast with the prevailing flow of the ACC (Fig. 9). Mesoscale meanders in the flow retained many of the particles offshore of the shelf break, but the particles eventually continued northeastward along the outer shelf. Floats released at 350 m and below (Fig. 9C-F) showed more transport onto the continental shelf than those released at shallower depths. The release depth of the deeper floats corresponded to the core of CDW, which lies between 300-500 m along the wAP continental shelf edge (Klinck, 1998; Klinck et al., 2004).

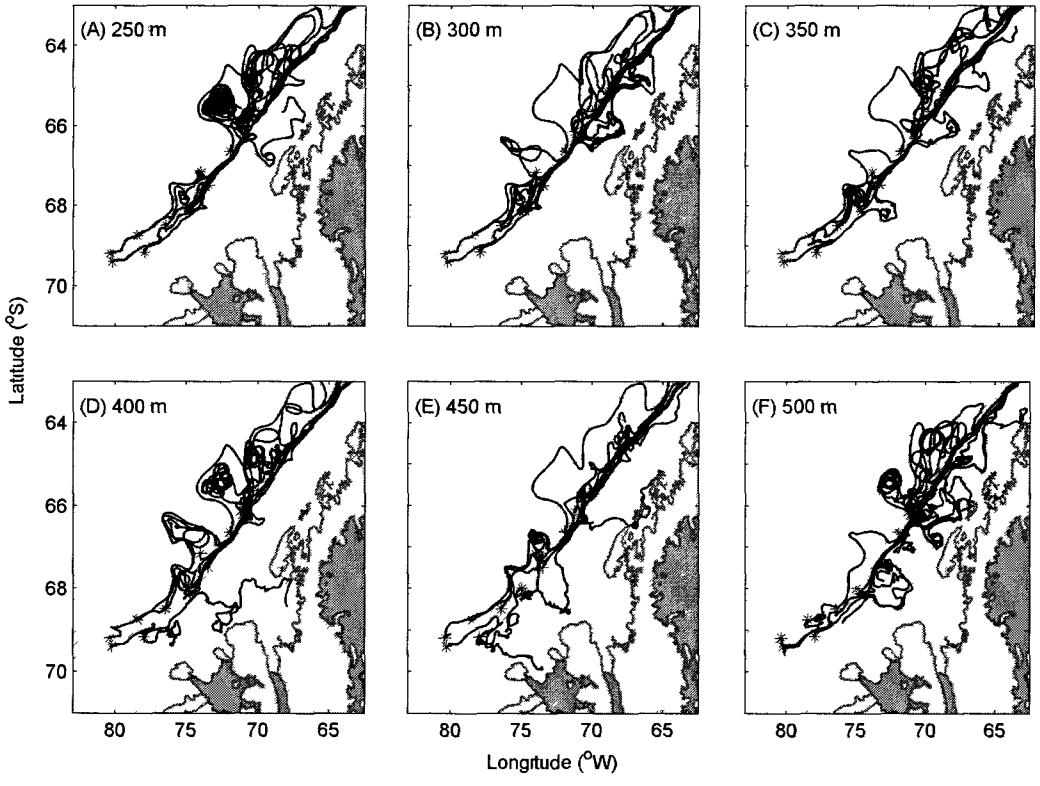

Fig. 9. Trajectories of the simulated floats (black lines) released along the western Antarctic Peninsula shelf break within the CDW layer depth, at (A) 250 m, (B) 300 m, (C) 350 m, (D) 400 m, (E) 450 m, and (F) 500 m. The simulated floats were tracked for approximately 1 year. The release point for the individual floats is indicated (*). The bottom bathymetry (500, 1000, 2000, 3000, and 4000 m) is shown by the light gray lines.

Three locations were identified as persistent sites for onshelf movement of floats. The primary site was Marguerite Trough where onshelf movement of floats occurred at 400 m (Fig. 9D), and increased with increasing depth (Fig. 9E, F). Transport pathways for the floats moving onshelf were either along Marguerite Trough or along the depression northeast of Adelaide Island that extends towards Crystal Sound, where some floats ended their trajectory (Fig. 9E). Some floats moved northward along this depression towards Renaud Island (Fig. 9E, F).

Onshelf movement of floats also occurred south of Alexander Island and north of Marguerite Bay between Anvers and Renaud Islands. These locations were identified as regions of CDW intrusions (Dinniman and Klinck, 2004) and enhanced biological production (Prézelin et al., 2000). Based on the simulated float trajectories, these three sites provide CDW to the inner shelf areas of Crystal Sound and the northern side of Marguerite Bay, the observed biological hot spot regions.

The role of circulation in producing the biological hot spots was explored by tracking the origin of particles that were transported into the regions. Crystal Sound, the northern-most region, received inputs from sites along the shelf break (Fig. 10A). A large percentage of particles that moved into Crystal Sound came from regions to the west that were aligned along the shelf break and showed transport time scales of 117-127 days (Table 5). Particles moved to the northeast along the shelf and the shelf break, and all moved onto the shelf through the same area defined by the intersection of the shelf break with Marguerite Trough (Fig. 10A). Crystal Sound also received inputs from Marguerite Trough and the region offshore and west of Alexander Island. Over 40% of the particles released around Marguerite Trough, along the shelf break off Alexander Island, and over the shelf off Alexander Island reached Crystal Sound (Fig. 10D). Crystal Sound also received inputs from many sources located farther west of Marguerite Bay (about 20-40%, Fig. 10D), with much of the wAP shelf region southwest of the Bay providing a particle source. The movement of these

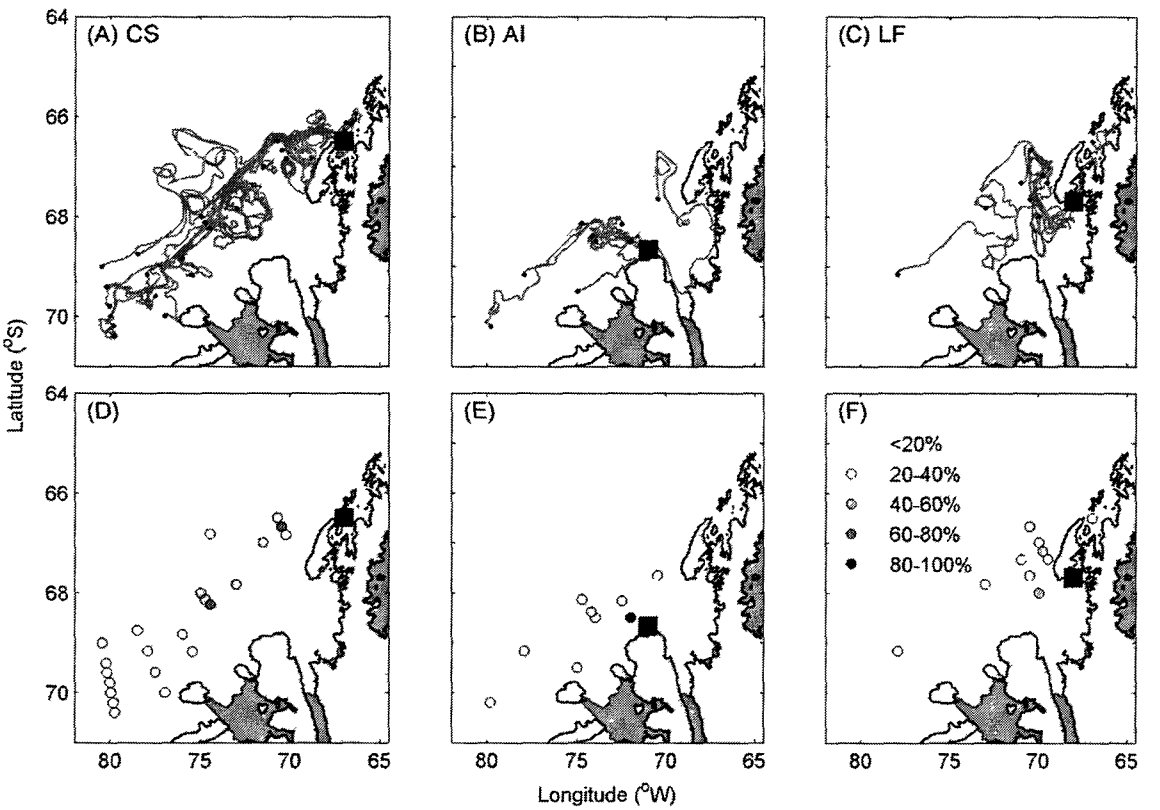

Fig. 10. Trajectories of simulated floats (dark gray lines) that enter the (A) Crystal Sound (CS), (B) Alexander Island (AI), and (C) Laubeuf Fjord (LF) hot spot regions (indicated by filled square). Only the trajectories that originated in areas with contributions to the hot spots greater than 20% are shown. The distribution of the source regions and associated percentage of particles that were provided to (D) Crystal Sound, (E) Alexander Island, and (F) Laubeuf Fjord are shown. The simulated floats were released at 300 m at 10-day intervals for 60 days in a grid of transects that extended across the continental shelf break (shown in Figure 2). The release point of the simulated drifters is indicated (•). The bottom bathymetry is shown by the light gray lines.

particles onto the wAP shelf is primarily through Marguerite Trough (Fig. 10A).

The Alexander Island hot spot region received inputs from the continental shelf area to the west and south of Marguerite Bay (Fig. 10B). The highest inputs (between 80-100%) characterized by short time scales (Table 5) were from the nearby shelf region (Fig. 10E), with lesser inputs originating from the continental shelf southwest of the area (20-40%) and time scales of 191 days (Table 5).

Laubeuf Fjord received inputs primarily from areas along Marguerite Trough and the local continental shelf around Marguerite Bay (Fig. 10C). Between 20-60% of the particles initialized in Marguerite Trough and about 20-40% of the particles released from some sites over the continental shelf moved into Laubeuf Fjord (Fig. 10F). The mean transport time scale of particles initialized in Marguerite Trough that reached Laubeuf Fjord is 115 days (Table 5).

A series of particle tracking simulations using a more highly resolved spatial initialization was done to provide comparisons with the above patterns. The release sites were homogeneously distributed along the shelf break, the slope and over the continental shelf. The input sources for the biological hot spots were similar to those obtained in the previous simulations (Fig. 11). Crystal Sound inputs (Fig. 11A) were primarily from locations around Marguerite Trough (more than 80% of floats), and over 60% of floats entering Crystal Sound were from sites over the continental shelf southwest of Marguerite Trough (Fig. 11D). Particles released west and along Marguerite Trough, moved along the northern flank of the Trough. The transport time scales for particles originated farther west (mostly 40-80% of floats) were 206-322 days (Table 5). Input sources for Alexander Island (Fig. 11B) were primarily from the surrounding continental shelf (Fig. 11E), with mean transport time scales of 150 days (Table 5) and smaller (20-40%) inputs from the mid-shelf area. No source areas were identified along the inner section of Marguerite Trough. The regions providing the largest inputs to Laubeuf Fjord were near Marguerite Trough (Fig. 11F).

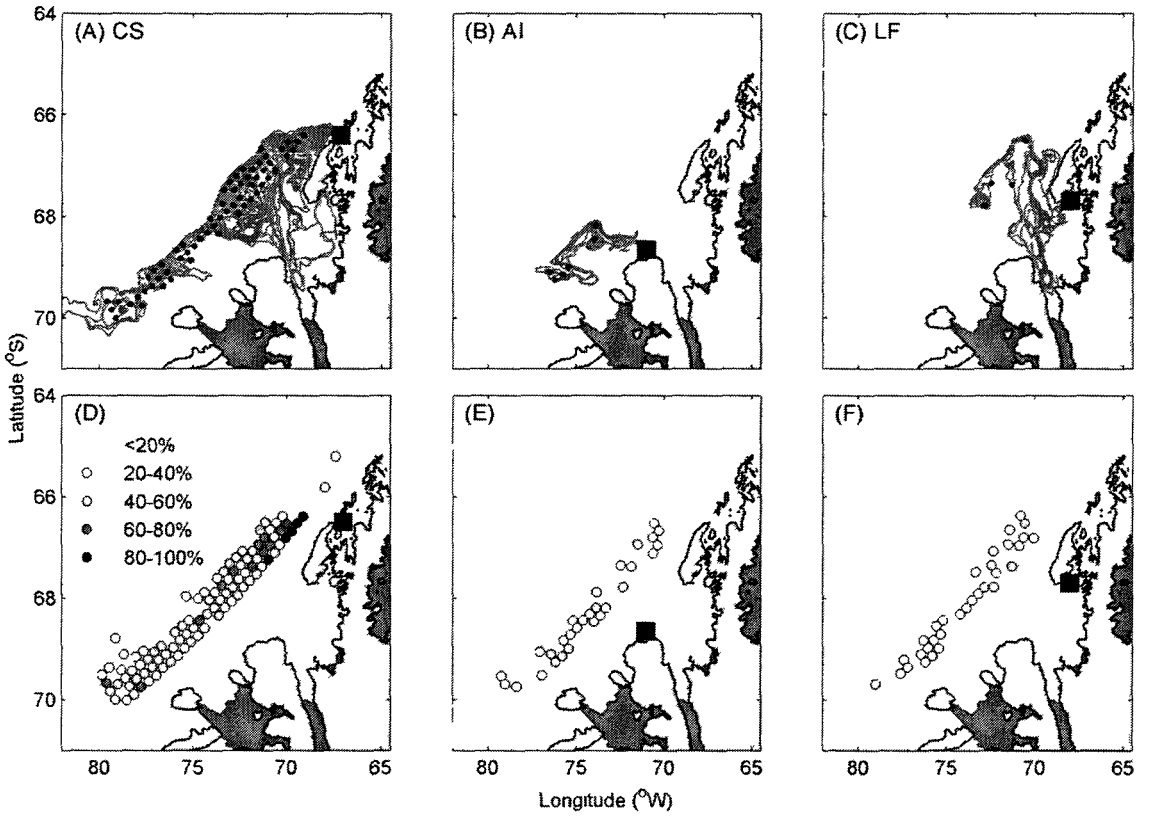

Fig. 11. Trajectories of simulated floats (dark gray lines) that enter the (A) Crystal Sound (CS), (B) Alexander Island (AI), and (C) Laubeuf Fjord (LF) hot spot regions (indicated by filled square). Only the trajectories that originated in areas with contributions to the hot spots greater than 40% are shown. The distribution of the source regions and associated percentage of particles that were provided to (D) Crystal Sound, (E) Alexander Island, and (F) Laubeuf Fjord are shown. The simulated floats were released at 300 m at 10-day intervals for 100 days in a high-resolution grid of transects that extended across the continental shelf break (light gray dots in panels D-F). The release point of the simulated drifters is indicated (•). The bottom bathymetry is shown by the light gray lines.

Table 5

Mean transport time scales of the particles reaching the hot spots (Crystal Sound-CS, Alexander Island-AI and Laubeuf Fjord-LF) for the coarse and fine grid simulations. Only the trajectories that originated in areas with contributions to the hot spots greater than 40% are shown. The average for all the transport time scales to hot spot regions is given. No input of particles to the hot spots is indicated by NI.

Coarse Grid		
Hot spot	**Contribution (%)**	**Transport time scales (days)**
CS	40-60	117
	60-80	127
	80-100	NI
AI	40-60	191
	60-80	NI
	80-100	23
LF	40-60	115
	60-80	NI
	80-100	NI
Fine Grid		
Hot spot	**Contribution (%)**	**Transport time scales (days)**
CS	40-60	206
	60-80	322
	80-100	52
AI	40-60	150
	60-80	NI
	80-100	NI
LF	40-60	235
	60-80	NI
	80-100	NI
Mean	All	154

About 40-60% of the floats released in this region reached this hot spot through a pathway defined by the inner limb of the shelf break and Marguerite Trough (Fig. 11C). The mean transport time scales averaged 235 days (Table 5). Overall, many of the outer shelf particles released to the southwest of Marguerite Trough contributed

significantly to the three hot spot regions. The mean transport time scale for inputs to biological hot spots was 154 days. Transport pathways to Crystal Sound and Laubeuf Fjord were similar, with across-shelf transport of particles occurring only in Marguerite Trough. For inputs to the Alexander Island hot spot region, across-shelf transport of particles was from the wAP to the west, and also through Marguerite Trough via the cyclonic circulation of Marguerite Bay.

3.3.2.2 Residence times

The residence times of particles in the three biological hot spots was estimated by calculating the fraction of particles (Eq. 7) leaving the hot spots in a specified time interval (Table 6).

Table 6

Estimated residence times (τ) in days for the Alexander Island (AI), Crystal Sound (CS) and Laubeuf Fjord (LF) hot spot regions at several depths for winter and summer particle releases. The residence time at each depth was calculated from the fraction of particles that remained within the hot spot area when the number of particles was reduced to a specified percentage of the initial number of particles that were released (see equation 7 and Fig. 3). The number of days that elapsed to reach this fraction is a measure of the residence time. The elapsed time was calculated by fitting an exponential decay model (equation 7) to the fraction of particles that remained at a given elapsed time. The decay coefficient (λ) and the correlation coefficient (R^2) obtained for each residence time calculation is shown. The average summer and winter residence time for each hot spot region is given.

Region	**Depth (m)**	τ **(days)**	λ **(days^{-1})**	R^2
		Summer		
	0	10.20	0.05	0.80
	50	30.49	0.02	0.60

Table 6 Continued

Region	Depth (m)	τ (days)	λ (days^{-1})	R^2
	100	26.74	0.02	0.71
CS	150	16.23	0.03	0.49
	200	13.59	0.04	0.45
	250	15.34	0.03	0.56
	300	13.89	0.04	0.59
	Mean	18.07		
	0	6.12	0.08	0.72
	50	9.71	0.05	0.88
	100	15.02	0.03	0.96
AI	150	19.76	0.03	0.95
	200	18.94	0.03	0.94
	250	27.47	0.02	0.90
	300	38.46	0.01	0.97
	Mean	19.35		
	0	16.72	0.03	0.92
	50	26.04	0.02	0.71
	100	20.83	0.02	0.66
LF	150	18.45	0.03	0.93
	200	31.06	0.02	0.97
	250	46.30	0.01	0.95
	300	56.82	0.01	0.85
	Mean	30.89		
Region	**Depth (m)**	**(τ days) Winter**	**(λ days^{-1})**	R^2
	0	16.56	0.03	0.56
	50	15.77	0.03	0.63
	100	20.75	0.02	0.56
CS	150	43.48	0.01	-0.75
	200	37.88	0.01	0.35
	250	33.78	0.01	-0.49
	300	22.12	0.02	-0.73
	Mean	27.19		
	0	8.88	0.06	0.84
	50	9.31	0.05	0.73
	100	23.92	0.02	0.59
AI	150	15.92	0.03	0.93
	200	11.66	0.04	0.93
	250	26.18	0.02	0.85
	300	29.94	0.02	0.75
	Mean	17.97		
	0	6.27	0.08	0.93

Table 6 Continued				
Region	**Depth (m)**	τ **(days)**	λ **(days^{-1})**	R^2
	50	12.95	0.04	0.89
	100	15.24	0.03	0.97
LF	150	23.59	0.02	0.91
	200	48.08	0.01	0.93
	250	74.63	0.01	0.75
	300	64.94	0.01	0.93
	Mean	35.10		

Mean residence times were calculated for all the depths (0-300 m) used for particle releases. The particles released in winter were tracked for approximately 1.3 years and those released during the summer were tracked for 1 year to determine if there is a seasonal bias in the residence time estimates. No significant difference was obtained for the estimated summer and winter mean residence times (Table 7). Laubeuf Fjord

Table 7

Results from the t-test conducted to compare summer and winter mean residence times for the biological hot spot regions. The values of t and p for 12 degrees of freedom and confidence interval of 95% are given.

Hot spot region	$t(12)$	$p < 0.05$
Crystal Sound	1.796	2.18
Alexander Island	0.262	2.18
Laubeuf Fjord	0.356	2.18

had the longest residence times of 31 days during summer and 35 days during winter (Table 6). This area is constrained to the north by bathymetry, by Adelaide Island to the west, and by the Antarctic Continent to the east. The cyclonic circulation in Marguerite Bay advects the particles from this region southward along the coast, with limited dispersion into Marguerite Bay proper (Fig. 12A, 13).

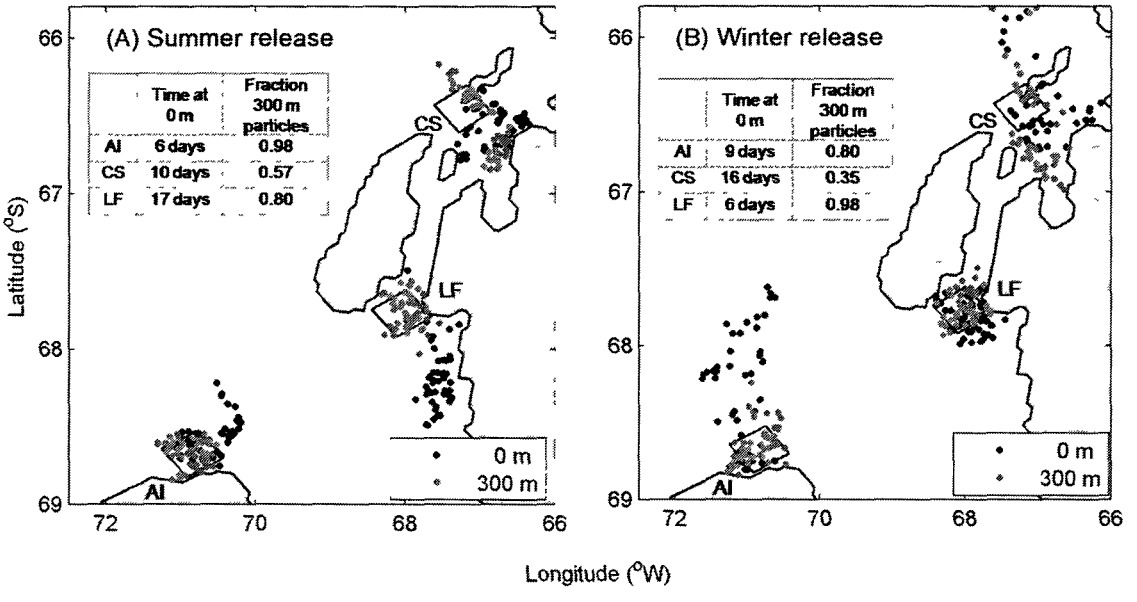

Fig. 12. Distribution of particles as a function of the surface (0-m release) residence time for the Alexander Island (AI), Crystal Sound (CS) and Laubeuf Fjord (LF) biological hot spot regions (indicated by box). Particles were released at 0-m (black dots) and 300-m (gray dots) in the (A) summer and (B) winter. The residence time for the surface particles and fraction of particles remaining within the source region at 300-m are shown for the summer and winter releases (inset tables).

The residence time in Crystal Sound was between 18-27 days, which is larger than the time scales of the synoptic wind forcing (Trenberth, 1991; Bromwich and Stearns, 1993). Despite a shorter residence time compared with Laubeuf Fjord, Crystal Sound was a retentive site. After one year of simulation, a small percentage (10-18%) of the particles remained in the area (Table 8). This percentage was consistent for summer and winter particle releases in Crystal Sound. In contrast, about 4% of the particles were retained in Laubeuf Fjord and none were retained for the Alexander Island region. Analysis of the origin of the particles remaining in Crystal Sound indicated that these were primarily from releases below 200 m (Table 8). These floats were retained between the bathymetric features northeast of Adelaide Island and the islands south of Lavoisier Island (Fig. 12, see Fig. 1 for Lavoisier Island location). The Crystal Sound and Laubeuf Fjord hot spot regions have similar bathymetric characteristics. Both sites are partially surrounded by land, are not directly exposed to the general circulation of the continental shelf, and are located close to deep depressions. Bathymetric features, such as depressions, may favor longer residence times by trapping the particles and/or creating local retention gyres. Retention of the particles was higher for the 300-m floats (Fig. 12), relative to the surface floats. A larger fraction of the deeper particles (0.35-0.98) remained within the hot spot regions relative to the surface particles (Fig. 12).

The Alexander Island hot spot region received inputs primarily from the adjacent shelf area and residence times averaged 18 days during winter and 19 days in summer (Table 6). The Alexander Island hot spot region has no obvious bathymetric constraint and is more open to the effects of the shelf circulation. Both may favor shorter particle residence times. A large portion of the particles that exited this hot spot were dispersed north along Marguerite Trough (Fig. 13A), but a portion of the particles moved southward (Fig. 13B).

Table 8

Percentage of the particles that remained within the Alexander Island (AI), Crystal Sound (CS) and Laubeuf Fjord (LF) hot spot regions at specific release depths after 1 year of simulation for the winter and summer numerical Lagrangian experiments.

	Depth						
Hot spot	**0 m**	**50 m**	**100 m**	**150 m**	**200 m**	**250 m**	**300 m**
Winter							
AI	0.0	0.0	0.0	0.0	0.0	0.0	0.0
CS	8.2	10.2	8.2	8.2	10.2	14.3	18.4
LF	2.0	4.1	4.1	4.1	4.1	4.1	4.1
Summer							
AI	0.0	0.0	0.0	0.0	0.0	0.0	0.0
CS	8.2	8.2	10.2	8.2	10.2	12.2	8.2
LF	2.0	2.0	4.1	2.0	2.0	2.0	4.1

3.4 DISCUSSION AND SUMMARY

3.4.1 Flow characteristics in hot spot regions

The simulated circulation fields showed the importance of the ACC to the wAP continental shelf circulation. The shelf circulation is bounded by the northeastwardly flowing ACC (Klinck, 1998; Klinck et al., 2004; Dinniman and Klinck, 2004) and interaction of this current with the rugged bathymetry of the outer shelf sets up conditions that produce onshelf intrusions of CDW (Dinniman and Klinck, 2004). The onshelf intrusion sites were apparent in the simulated flow fields, with Marguerite Trough a primary site. The long temporal decorrelation scales of the flow at the intrusion sites indicated the persistence of these features. The permanence of the intrusion sites provides dependable movement of heat, salt, nutrients, and planktonic organisms from the outer to the inner shelf. Crystal Sound is located at the terminus of one of the branches of Marguerite Trough and, as a result, receives continual inputs from the outer and middle parts of the wAP continental shelf.

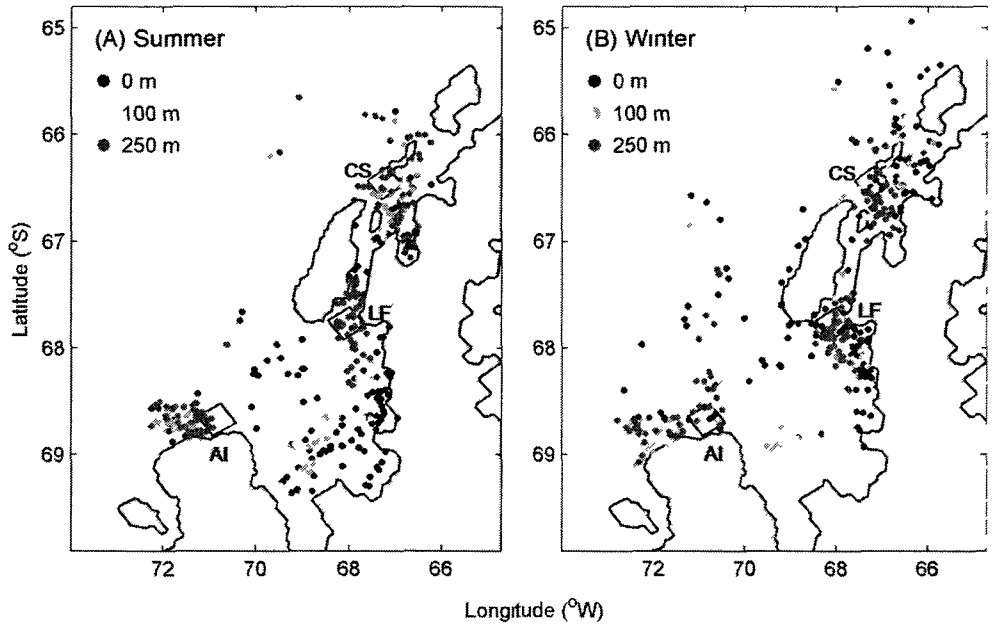

Fig. 13. Dispersion of simulated particles released at three depths in the three hot spot regions (indicated by the box), Alexander Island (AI), Crystal Sound (CS), and Laubeuf Fjord (LF), 50 days after release in the (A) summer and (B) winter.

The large-scale flow over the wAP shelf is generally cyclonic (Stein, 1992; Smith et al., 1999; Klinck et al., 2004) in which are embedded smaller-scale cyclonic gyres. A schematic of the wAP surface horizontal circulation (Hofmann et al., 1996) constructed from hydrographic observations that took place during the BIOMASS Program (Stein, 1981, 1983, 1986) and the dynamic height fields constructed from observations during the Second International BIOMASS Experiment (Stein, 1992) indicated two cyclonic gyres over the wAP shelf; one off Anvers Island and one near Adelaide Island. The annual mean simulated surface circulation reproduced the main dynamic features in the schematic circulation. However, the simulated patterns reveal small-scale important features of the shelf circulation. One such feature occurs off Adelaide Island, where the flow follows two pathways; one defined by the northern side of Marguerite Trough and a second that follows the bathymetric depression that

extends towards Renaud Island. The across-shelf velocities along the northern flank of Marguerite Trough of 0.04-0.06 m s^{-1} agree with velocity estimates of 0.05 m s^{-1} made from analysis of ADCP transects made on the wAP since 1997 (Savidge and Amft, 2009). The onshore flow associated with Marguerite Trough and the smaller cyclonic gyre over the adjacent shelf to the north combine to produce a retention region in the Crystal Sound area. The residence times of 18-27 days and the high retention of particles (up to 18%) after one year of simulation, estimated for this region, are consistent with a retention region.

The simulated onshelf flow along Marguerite Trough continues into Marguerite Bay and reaches George VI Sound in the southern part of the Bay, as observed (Dorland and Zhou, 2008). Surface flow in the northern part of Marguerite Bay is cyclonic and is continuous with that over the wAP shelf. The flow in the region near Laubeuf Fjord was characterized by long decorrelation scales and inputs to this area tended to be from the local region. The lack of exchange between this region and the rest of Marguerite Bay and long particle residence times suggest that it is a retention area. The area off Alexander Island is influenced by flow out of Marguerite Bay along the southern flank of Marguerite Trough in George VI Sound (Potter and Paren, 1985; Dorland and Zhou, 2008). The northeasterly flowing shelf currents along the middle shelf off of Alexander Island turn across the wAP shelf along the southern flank of Marguerite Trough south of the hot spot off Alexander Island. The simulated circulation fields showed seaward flow with surface velocities less than 0.05 m s^{-1} in this region. The direction and magnitude of the simulated flow agrees with estimates made from ADCP data (Savidge and Amft, 2009). The intersection of the outward flow from Marguerite Bay with the offshelf-turning flow, combined with the small velocities, may contribute to formation of a retention area off Alexander Island.

3.4.2 Particle transport pathways and residence times

Lagrangian particle tracking experiments have been used to estimate advective transport pathways and transit times for planktonic organisms in a range of marine environments (e.g. Capella et al., 1992; Werner et al., 1993; Carlotti and Wolf, 1998; Hofmann et al., 1998; Miller et al., 1998; Batchelder et al., 2002; Thorpe et al., 2004; Murphy et al., 2004; Thorpe et al., 2007). A general result from these studies is that particle transport and distributions are strongly controlled by circulation. Moreover, structures associated with the circulation, such as fronts and eddies are important in determining local patterns of dispersion and/or retention of particles (e.g. Werner et al., 1996.

The transport patterns and residence times estimated for the wAP region showed that the circulation over the wAP continental shelf is important in producing areas where particles are preferentially retained. Crystal Sound and Laubeuf Fjord retain particles for over a year (e.g. Table 8). Particle retention in the Alexander Island hot spot is shorter. The circulation dynamics contributing to these retention regions differ, which results in different estimated residence times. The variable residence times potentially affect the structure of the local food web. Net samples from the austral fall and winter showed that the zooplankton biomass in the Laubeuf Fjord region was dominated by krill between 50 and 100 m (Ashjian et al., 2004). This site was the only one of those sampled with nets that showed krill to be the biomass dominant. This area also showed some of the highest backscattering returns, which are related to zooplankton abundance, from acoustic surveys made during the SO GLOBEC field studies (Lawson et al., 2004). Similar high backscattering returns were observed in the Alexander Island hot spot region (Lawson et al., 2004).

Zhou et al. (2004) combined acoustic backscattering with *in situ* observations (Optical Plankton Counter and nets) made during the SO GLOBEC field studies to estimate growth and removal rates for zooplankton biomass. These estimated rates

provide a time scale of about 20 days for local growth of the mesozooplankton populations. The winter residence times estimated for the Laubeuf Fjord and Crystal Sound regions are longer than this time scale, which suggest that these hot spot regions may be produced by the combination of biological as well as physical processes. The values estimated by Zhou et al. (2004) were for the austral winter. Equivalent values for the austral summer may be shorter, because of higher overall productivity during this time. Thus, the relative contribution to the hot spot regions from biological processes may be higher at this time. An analysis of net-derived zooplankton distributions along the wAP (Marrari et al., 2011) showed large differences in the zooplankton assemblages in the three hot spot regions. For the Laubeuf Fjord and Alexander Island regions, *Thysanoessa macrura* accounted for almost 100% of the krill biomass; whereas, in Crystal Sound, Antarctic krill accounted for about 50% of the krill biomass. The mesozooplankton composition in the three hot spot regions included many of the same species, but differences in relative abundance between the regions and between seasons within regions occurred (Marrari et al., 2011). The hot spot regions include different suites of predators (Section III.2.4), which have different diets. The differences in the type and amount of krill and relative abundance of the mesozooplankton available in the three hot spot regions may contribute to the selection of these predators. For example, the Crystal Sound region was dominated by crabeater seals, which are Antarctic krill predators (Burns et al., 2004) and these predators were not found in regions were this prey was not abundant. However, attributing cause and effect is difficult, because of the lack of diet information for the predators that were concurrent with the zooplankton observations.

Analysis of the trajectories of particles at a range of depths (surface to 500 m) showed that each wAP hot spot received inputs via the advective circulation from differing source regions. Crystal Sound received particle contributions from higher latitude regions of the Bellingshausen Sea, as well as from the adjacent wAP shelf.

Laubeuf Fjord received particles from Marguerite Bay and the local wAP shelf region and Alexander Island received inputs primarily from the adjacent shelf region. The circulation in each hot spot region is largely controlled by factors that are persistent over time, such as bathymetry, outflow from the GVIIS, and the prevailing wind patterns. Thus, the circulation structure that provides these inputs is relatively constant over the year. The persistence of the circulation maintains conditions that provide a dependable planktonic prey supply for the hot spot predator assemblages. Variability in biological production of these regions is likely controlled by the strength of the circulation and the particular source regions, which will affect the rate and type of input, respectively.

The particle trajectories indicated limited exchange between the hot spot regions for the time encompassed by the simulations, suggesting that these regions are relatively isolated. An implication of this result is that much of the biological production of the wAP occurs in small localized areas that support different food web structures.

3.4.3 Relationship to predators

The effect of local and regional retention and aggregation as a result of circulation on top predator assemblages has been studied in several environments. In the southeastern Gulf of Maine, the abundance and proportion of older Calanus life stages advected into the region correlated with right whale (*Eubalaena glacialis*) occurrence (Wishner et al., 1995). Observations from the Ross Sea show that seabirds occurred in large numbers along the Antarctic Slope Front, presumably feeding on prey that was aggregated by the frontal circulation (Ainley and Jacobs, 1981). Subsequent observations indicated that oceanic fronts influenced seabird distributions the most, both for species that tend to stay in the sea ice and those that prefer ice free waters (Ainley et al., 1998).

The Lagrangian simulations show that the circulation of the wAP continental shelf

transports particles to the predator hot spot regions. However, predator abundance and composition in the hot spots depends on the volume, type, and quality of prey transported to these regions. Marrari et al. (2008) suggested that changes in chlorophyll (food) concentrations in the Bellingshausen Sea, which is west and south of the wAP region, affect the productivity and growth of zooplankton, especially Antarctic krill, on the wAP. The simulated drifters show inputs to the wAP from regions to the west and south with mean time scales of 154 days (e.g. Table 6), which are consistent with the time required for development of Antarctic krill from an embryo to late stages of Furcilia (Ikeda, 1984; Hofmann and Lascara, 2000; Daly, 2004). Thus, although the hot spot regions receive inputs from different regions, each region is still connected to the larger region via the circulation of the ACC. Hence, each region maintains a connection and is influenced by processes produced by larger scale variability.

Alternative pathways in the wAP food web (e.g. reduced presence of Antarctic krill and increased copepod abundance) may provide a diet that can sustain predator assemblages in the short term, but if these conditions persist the result may be a change in the abundance and type of resident predator assemblages in the hot spot regions. A system in which viable prey conditions are restricted to limited regions that are imposed by the circulation field is perhaps more sensitive to climate-induced changes in circulation and prey growth than one with broadly distributed predator-favorable conditions. Thus, the wAP ecosystem merits further monitoring, especially during the rapid changes that are now occurring in regional atmospheric, ocean, and sea ice conditions (e.g. Meredith and King, 2005; Clarke et al., 2007).

CHAPTER 4

MODELING THE REMOTE AND LOCAL CONNECTIVITY OF ANTARCTIC KRILL (*Euphausia superba*) POPULATIONS ALONG THE WESTERN ANTARCTIC PENINSULA

4.1 INTRODUCTION

The wAP region of the Antarctic supports large and persistent populations of Antarctic krill (Marr, 1962; Huntley et al., 1991; El-Sayed, 1994; Atkinson et al., 2004). However, the biomass of Antarctic krill over this shelf undergoes seasonal variations in horizontal and vertical distributions (Siegel, 1988; Siegel et al., 1997, 1998; Lascara et al., 1999). Acoustic observations showed that in austral summer, krill occurred throughout the wAP shelf region and were concentrated in the upper 50 m (Lascara et al., 1999). Winter distributions were characterized by reduced presence over the mid and outer shelf, high concentrations in the inner shelf, and large aggregations below 100 m (Lascara et al., 1999).

The net and acoustic measurements that were made as part of the U.S. SO GLOBEC field studies have refined the understanding of fall and winter patterns of krill distribution over the wAP continental shelf. Multi-frequency acoustic surveys (Lawson et al., 2008b) showed that fall-winter distributions of Antarctic krill were characterized by small, closely spaced aggregations, interspersed with large aggregations that accounted for the majority of the biomass (Lawson et al., 2008a). These aggregations were mostly located along the inner shelf (Lawson et al., 2008b). Zooplankton distributions obtained from video plankton recorder observations (Ashjian et al., 2008) and net tows (Daly, 2004; Ashjian et al., 2004; Wiebe et al., 2011) showed that larval krill were present over the SO GLOBEC study region. However, there was

an across-shelf gradient in krill stage and relative abundance. Larval krill (C2-F2, F4-F5) were most abundant along the outer shelf and calyptopis and early furcilia stages were more abundant on the shelf. An implication of these observations is that the wAP region supports local retention of krill and/or this region receives a continuous supply of krill from other areas. The former implies that the wAP provides a habitat that supports successful reproduction, recruitment, and retention of Antarctic krill. The latter implies connectivity of the wAP via the circulation to other regions that support Antarctic krill populations.

Evidence for local reproduction, recruitment, and subsequent retention of krill on the wAP is provided by length frequency analysis of the krill in diets of Adélie penguins. Diet samples collected from wAP Adelie penguins showed a systematic increase in krill size that is consistent with the progression of identifiable cohorts through the population with a 4-5 year periodicity (Fraser and Hofmann, 2003). This led to the hypothesis that the local circulation maintains the krill population in restricted regions of the wAP continental shelf. This is consistent with circulation distributions derived from hydrographic observations (Stein, 1992; Smith et al., 1999; Klinck et al., 2004) and numerical circulation models (Dinniman and Klinck, 2004) that show closed gyres over the wAP.

In contrast, recent studies have linked recruitment of krill on the wAP with inputs from upstream regions in the western Bellingshausen Sea. Observations of the vertical abundance of Antarctic krill obtained from net tows made as part of the U.S. SO GLOBEC field studies in the fall and winter of 2001 and 2002 provided detailed information about the horizontal and vertical distribution of the dominant modes of Antarctic krill larvae. The younger krill stages (C2, F1) were found primarily along the shelf break off Marguerite Bay near the offshore end of Marguerite Trough and older krill life stages were dominant on the shelf (Daly, 2004). The German SO GLOBEC survey in the wAP region that occurred in April 2001 just prior to the

U.S. field study, also showed higher abundances of krill larvae over the shelf break and slope offshore of Marguerite Bay (Pakhomov et al., 2004). These distributions suggested that the younger krill stages were transported to the wAP region via the currents associated with the ACC which flows along the outer shelf.

In a follow-on study, Marrari et al. (2008) suggested a connection between the region of high chlorophyll *a* (>10 mg chl m^{-3}) concentration observed in the Bellingshausen Sea during the summer of 2001, prior to the 2001 fall SO GLOBEC field studies, and the high abundance (~15 ind m^{-3}) of krill larvae offshore of Marguerite Bay. If the high chlorophyll *a* region is coincident with a krill spawning area, then embryos originating in this area could provide krill to the outer wAP continental shelf. Marrari et al. (2008) estimated that normal developmental times over the summer and fall (~3 months) and a transport velocity of 0.1 m s^{-1} (characteristic of ACC speeds) would result in the arrival of krill larvae at the wAP outer shelf by fall.

The objectives of this study were to investigate the influence of the circulation in supporting local and remote inputs of krill to the wAP continental shelf and to provide an analysis of the relative contribution of each mechanism to structuring and maintaining Antarctic krill populations of this region. To address these objectives, numerical Lagrangian tracking experiments were done in a region that extends from the western Bellingshausen Sea to the tip of the Antarctic Peninsula (Fig. 14). The following section describes the series of particle tracking experiments used in the study. The results are presented next and these focus on the influence of inputs from Bellingshausen Sea (remote connectivity), the role of Marguerite Trough as a conduit for transport of larvae onto the wAP shelf, and local retention of krill. The discussion and summary provides a comparison of the numerical results to observations and other modeling studies of krill distribution along the wAP and Scotia Sea region.

4.2 METHODS

4.2.1 Model Implementation

Lagrangian tracking experiments were used to simulate the passive transport of *Euphausia superba* larvae along the wAP. The Rutgers/UCLA Regional Ocean Modeling System (ROMS) version 3.0 (see Chapter III for details of the model configuration), implemented for the wAP region (Fig. 1A) provided the circulation distributions for the Lagrangian tracking simulations. The model domain covers the continental shelf region in and around Marguerite Bay, has a 4-km horizontal resolution, and is composed of 24 vertical sigma-layers that concentrate toward the surface and the bottom, allowing a better resolution in nearshore areas. The model is forced by surface fluxes such as heat, momentum (wind stress), and freshwater, and is dynamically forced by the ACC that flows along the wAP shelf break. The circulation model includes a dynamic sea-ice model (Budgell, 2005) and thermodynamically active ice shelves (Dinniman et al., 2007).

4.2.2 Lagrangian simulations

Three sets of numerical Lagrangian experiments were conducted to determine the role of ocean circulation on the connectivity of Antarctic krill populations along the wAP (Fig. 14, Table 9). The first set of experiments was designed to test the potential for krill embryos spawned in the Bellingshausen Sea to reach the wAP continental shelf. Particles were released in the simulated circulation fields along four transects (83°W, 85°W, 89°W and 92°W) that extended seaward across the shelf break (Fig. 14). The release locations coincided with the observed high chlorophyll *a* concentrations (Marrari et al., 2008), and encompassed the region suggested to be the source area for the krill larvae observed offshore of Marguerite Bay (Daly, 2004).

Particles were released at 25 to 50-m intervals over depths of 0-350 m at 10-day

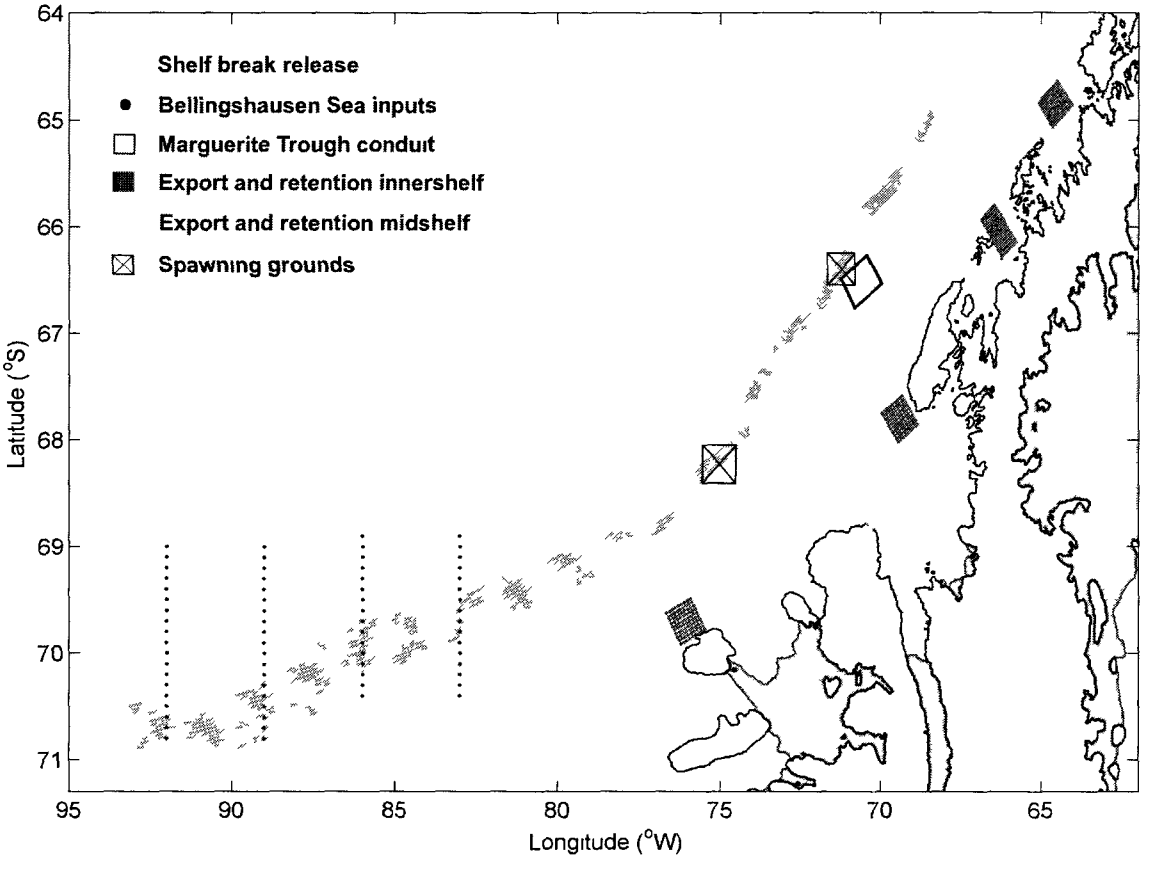

Fig. 14. Map of the study area showing the release locations for the Lagrangian particle experiments in the Bellingshausen Sea (across-shelf transects, black dots), along the shelf-break (light gray dots), Marguerite Trough (unfilled black box), mid-shelf (light gray boxes), inner shelf (dark gray boxes), and potential spawning grounds (x-marked rectangles).

Table 9

Summary of the Lagrangian particle tracking simulations conducted in the Bellingshausen Sea, along the shelf-break, the Marguerite Trough region, and along the wAP continental shelf.

Release region	Number of release points	Depth of release	Time and frequency of release
Bellingshausen Sea	70	0, 25, 50, 100, 125, 150, 175, 200, 250, 300, 350	24-Dec to 12-Feb, every 10 days
Shelf-break	2258	50, 150, 300	29-Dec, 13-Jan, 2-Feb
Marguerite Trough	120	25, 100, 200, 300, 500	24-Dec to 24-Jan, every day
Mid-shelf	624	50, 120, 150, 300	24-Dec
Inner shelf	360	25, 50, 100, 300	15-Nov, 24-Dec, 13-Jan

intervals starting from 24 December until 12 February (see Table 10 for details). The time period corresponds to peak krill spawning in this region of the Antarctic (Spiridonov, 1995) and the interval is consistent with krill spawning for this region (Quetin and Ross, 1991). Trajectories of particles that moved onto the wAP in the vicinity of Alexander Island and Marguerite Bay, provided estimates of potential connectivity of the wAP and upstream regions. These two sites are where intrusions of CDW occur (e.g. Fig. 9 in Chapter III and Fig.11 in Dinniman and Klinck, 2004) and have persistent onshelf flow. Transport times were mapped to development times for several larval stages, assuming normal development (see Table 10) and this was used to identify possible krill spawning grounds.

The second set of experiments was designed to examine the role of Marguerite Trough as a conduit for onshelf transport of particles. A high resolution array of floats was released at the intersection of the Trough with the shelf break (Fig. 14).

Floats were released at 1-day intervals for 32 days at depths between 25 and 300 m (Table 10). The number of particles following particular pathways was calculated and used to determine dominant transport pathways.

The third set of experiments was designed to explore local retention and export of krill larvae. Particles were released between 0 and 300 m over the mid-shelf south of Charcot Island, the southern entrance of Marguerite Bay along the Trough, and north of Renaud Island (Fig. 14). These areas correspond to regions where high krill abundance has been observed. Export from the shelf was defined as the number of particles that crossed the 800-m isobath, defined to be the outer shelf edge (Bolmer, 2008).

Connectivity along the inner shelf was investigated by releasing particles at several depths (Table 9) close to shore near Charcot Island, Adelaide Island, Renaud Island and Anvers Island (Fig. 14) on November 15, December 24 and January 13. These times correspond to peak spawning over the wAP continental shelf (Ross and Quetin, 1986; Spiridonov, 1995). Connectivity along the inner shelf was determined by calculating the number of furcilia 6 larvae, determined from transport and developmental times, exchanged between each release site. The surface distribution of furcilia 6 larvae was determined and the number of these larvae in regions of the wAP with equal surface area (e.g. 40 km^2) was calculated. The resultant particle counts provided a representation of the connectivity and the export from the four sites to other parts of the shelf.

4.2.3 Development times for Antarctic krill

Antarctic krill early life stages have a sequence that includes development of the egg through Nauplius (2 stages), Metanauplius, Calyptosis (3 stages) and Furcilia (6 stages) (Fraser, 1936). Development times obtained from modeling studies (Hofmann et al., 1992; Hofmann and Lascara, 2000), laboratory experiments (Ikeda, 1984) and

field observations (Witek et al., 1980; Ross et al., 1988; Daly, 1990) were used in this study (see Table 1 in Chapter II for details of the studies included to determine development times) to define a time interval for the development of each larval stage and the median of each time interval was used to define the time span for the Lagrangian simulations (Table 10).

Table 10

Intervals for the cumulative developmental time of krill larvae (e.g. Table 1) obtained from laboratory experiments (Ikeda, 1984), field data analysis (Witek et al., 1980; Ross et al., 1988; Daly, 1990) and modeling studies (Hofmann et al., 1992; Hofmann and Lascara, 2000). The simulated development times are representative of average conditions. Antarctic krill life stages are abbreviated as: N = Nauplius (stage I-II), MN = Metanauplius, C = Calyptopis (stage I-III), F = Furcilia (I-VI).

Stage	Intervals (days)	Median (days)
NI	5-8	7
NII	13-24	19
MN	10-41	26
CI	18-38	28
CII	33-60	47
CIII	50-75	63
FI	58-90	74
FII	70-105	88
FIII	85-121	103
FIV	95-135	115
FV	111-180	146
FVI	114-258	186

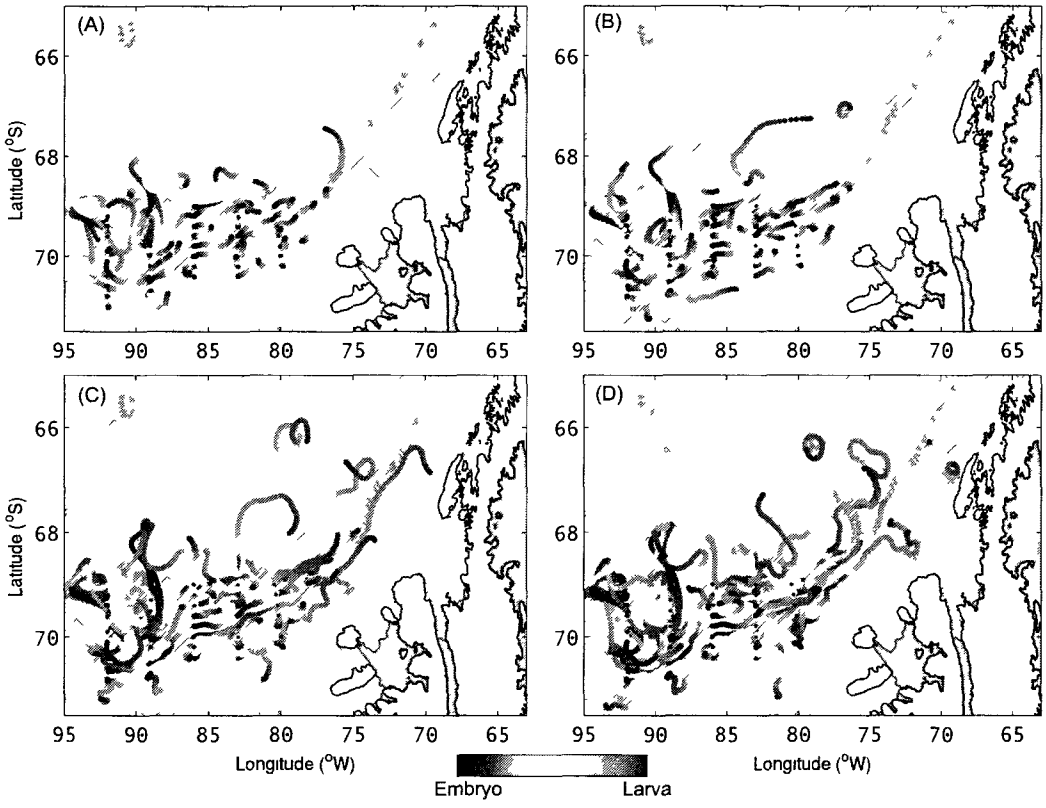

Fig. 15. Transport pathways of particles released at 25 m in the Bellingshausen Sea after (A) 47 days, (B) 88 days, (C) 115 days, and (D) 186 days. Transport time was mapped to development time to show the distribution of the calyptopis 2 (A), furcilia 2 (B), furcilia 4(C) and furcilia 6 (D) larval stages. The individual trajectories provide a representation of the age for each developmental stage.

4.3 RESULTS

4.3.1 Bellingshausen Sea inputs

Particles released near surface (Fig. 15) and at depth (Fig. 16) in the Bellingshausen Sea were transported to the northeast with the prevailing flow of the ACC or moved further offshelf and retained in the region The trajectories showed considerable meandering, especially in the offshelf region. The trajectories associated with

the calyptopis 2 stage (Fig. 15A) reached the outer portion of the wAP towards the end of the developmental time associated with this stage. Onshelf movement of this developmental stage occurred upstream of the U.S. SO GLOBEC study region. Similarly, onshelf movement of the furcilia 2 stage (Fig. 15B) occurred over the upstream shelf regions. Particle trajectories associated with furcilia 4 (Fig. 15C) and furcilia 6 (Fig. 15D), however, moved onto the wAP in the region of Marguerite Trough and off of Alexander Island. The furcilia 6 trajectories reached the inner part of the wAP shelf just off of Adelaide Island (Fig. 15D). The trajectories for the particles released at 125 m showed similar patterns (Fig. 16). Only the older furcilia stages were transported onto the wAP continental shelf in the Marguerite Bay region.

The percent of furcilia 2 and 6 larvae released in the upper 25 m that was transported onto the continental shelf was 5-7% (Fig. 15C, D, Table 11). The percentage of older larvae provided to the shelf increased with depth (Fig. 16). Also, the releases at depths greater than 100 m resulted in more of the younger larval stages (calyptopis 2) moving onto the continental shelf. The maximum percentage of larvae that moved onto the shelf occurred between 150 and 200 m for all larval stages (Table 11).

After one year of simulation, the percentage of the particles released in the Bellingshausen Sea that moved onto the shelf showed that all depths between 0 and 350 m can provide krill larvae to the continental shelf (Table 11). These percentages indicate that about 15 to 25% of the embryos spawned in the Bellingshausen Sea have the possibility of reaching the continental shelf along the wAP and that these will arrive in different stages of development.

Particles released along the shelf break showed that all depths (50, 150 and 300 m) can provide krill larvae to the continental shelf of Marguerite Bay (Table 12). About 7 to 10% of the krill embryos spawned along the shelf break on the wAP will enter the shelf as early calyptopis, and between 18 to 26% will reach Marguerite Bay as furcilia 6. These percentages are coherent with the simulations done for the Bellingshausen

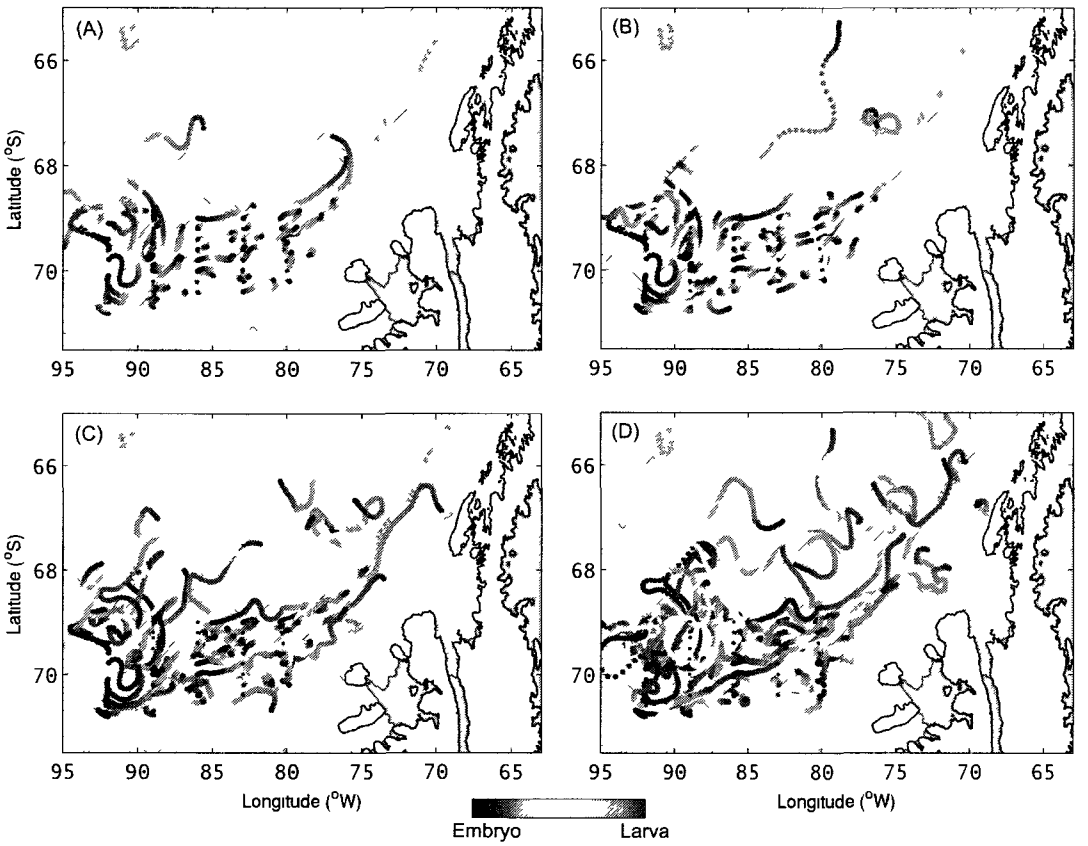

Fig. 16. Transport pathways of particles released at 125 m in the Bellingshausen Sea after (A) 47 days, (B) 88 days, (C) 115 days, and (D) 186 days. Transport time was mapped to development time to show the distribution of the calyptopis 2 (A), furcilia 2 (B), furcilia 4(C) and furcilia 6 (D) larval stages. The individual trajectories provide a representation of the age for each developmental stage.

Sea, and serves as additional support that a remote connectivity for krill larvae is possible for the wAP.

The particle transport pathways showed two preferred sites for intrusions to the shelf independent of the depth or date of release; the depression off Alexander Island (hereafter AI depression) and the intersection of Marguerite Trough with the shelf break (hereafter MT intersection). These are areas where CDW intrusions are known

Table 11

Percentage (%) of different developmental stages of krill larvae that originated in the Bellingshausen Sea that were transported onto the continental shelf. Larval stages are abbreviated as: C2 = Calyptopis 2, C3 = Calyptopis 3, F3 = Furcilia 3, F6 = Furcilia 6, 1y = 1 year old.

Depth (m)	Total-1y	C2 (%)	C3 (%)	F3 (%)	F6 (%)
0	11.4	0.6	1.5	5.3	5.8
25	12.3	3.2	4.1	7.3	7.3
50	16.1	4.7	6.1	8.2	9.1
100	21.1	6.1	9.1	14.3	15.5
125	21.9	7.3	9.4	13.7	15.8
150	26.6	8.5	11.1	16.1	17.5
175	26.3	10.2	12.6	16.1	17.5
200	24.9	8.8	11.7	16.4	18.1
250	22.5	8.5	9.7	13.7	16.1
300	20.5	6.1	7.6	11.1	12.3
350	19.3	3.8	7.0	10.5	12.9

to occur (Dinniman and Klinck, 2004; Klinck et al., 2004). The source areas for the particles that move onto the wAP continental shelf at these sites were tracked back to their source regions and the transport time was converted to developmental time for the calyptopis 2 and furcilia stages (Fig. 17).

The three larval stages that arrived at the Alexander Island location originated mostly along the shelf break, either near the bathymetric depression, for the calyptopis 2 stage, or from further west (~90°), for the late furcilia stages (Fig. 17A). Some calyptopis and furcilia 2 and 3 originated offshore of the AI depression. The origination regions for the larvae observed in the Marguerite Through area were more widely distributed (Fig. 17B). Some of the particles originate along the shelf break but a large portion also came from the region off the shelf offshore of Marguerite Bay. Most of the calyptopis 2 and early furcilia larvae observed in the Marguerite Trough

Table 12

Percentage (%) of different developmental stages of krill larvae that originated along the shelf break of the wAP that were transported onto the continental shelf of Marguerite Bay. Larval stages are abbreviated as: C1 = Calyptopis 1, F3 = Furcilia 3, F6 = Furcilia 6.

Simulation day - depth (m) of release	C1 (%)	F3 (%)	F6 (%)
Dec-29 - 50 m	7.7	14.1	20.5
Dec-29 - 150 m	7.0	13.7	21.1
Dec-29 - 300 m	7.4	14.4	22.0
Jan-13 - 50 m	10.0	14.7	22.2
Jan-13 - 150 m	10.9	18.2	24.8
Jan-13 - 300 m	10.6	17.4	23.7
Feb-2 - 50 m	8.7	12.6	17.8
Feb-2 - 150 m	8.4	14.9	25.1
Feb-2 - 300 m	9.3	16.8	25.7

intersection derived from the region along and across the shelf break in an area east of 80°W (Fig. 17B). In contrast, most of the late furcilia stages came from the area west of 80°W along the shelf break and offshore in the 3000-4000 m region.

The depth distribution of the larvae arriving at the Alexander Island depression and Marguerite Trough intersection differed for the two regions. At the Alexander Island depression, the highest percentage (~40%) of the larvae were observed at 400 m (Fig. 18A). However, the percentage of particles arriving at 100 m and 200 m was higher (~46%). A small percentage of particles moved onshore above 50 m (<5%).

At the Marguerite Trough intersection over 50% of the particles moved onto the shelf at 100 m (25%) and 200 m (30%) (Fig. 18B). These particles derive mostly from the shelf break, the open ocean off Marguerite Bay, or from the outer shelf south of Marguerite Bay (Fig. 17B).

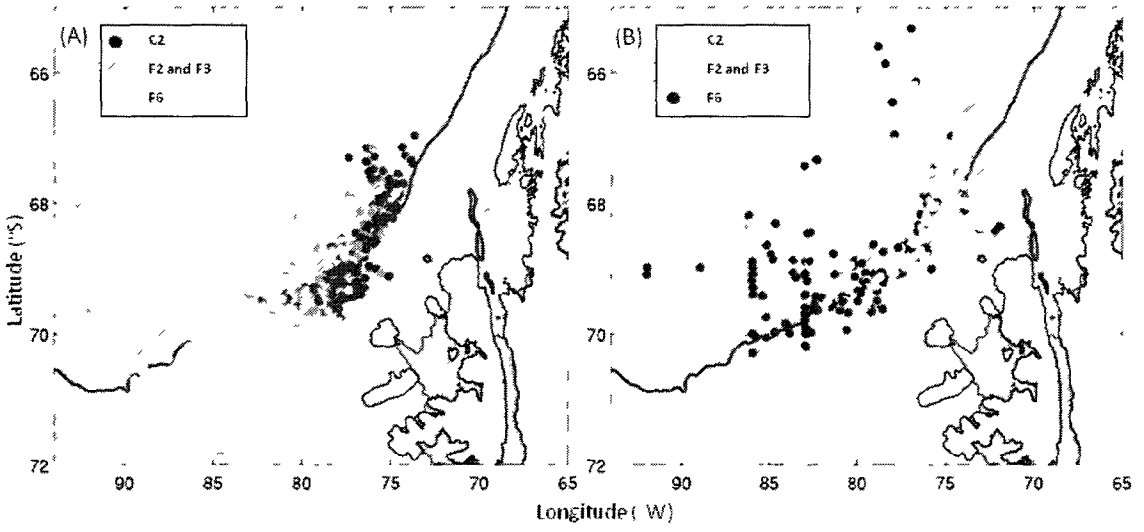

Fig. 17. Origination regions for the simulated particles that arrived at (A) Alexander Island and (B) Marguerite Trough. The particle transport time was converted to larval age/stage using the developmental times given in Table 10.

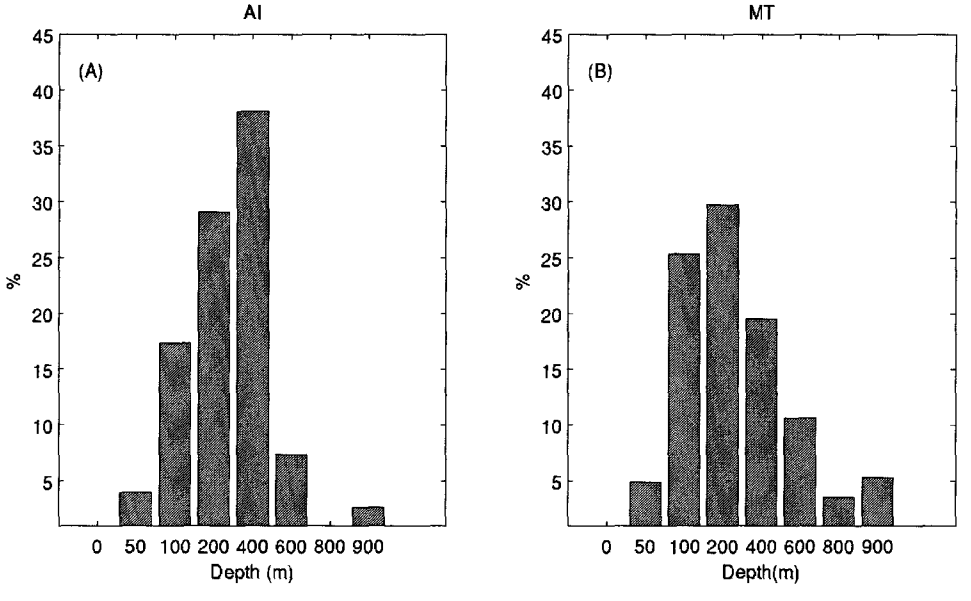

Fig. 18. Percentage (%) of particles at different depths that arrived at the (A) Alexander Island intersection and the (B) Marguerite Trough intersection. The depth intervals used to apportion the particles correspond to those used for net tows made during the US SO GLOBEC field studies.

4.3.2 Role of Marguerite Trough

The shelf break region and slope off Marguerite Bay have been identified as a suitable areas for local recruitment of Antarctic krill (Pakhomov et al., 2004), by providing a conduit for Antarctic krill larvae to enter the wAP continental shelf (Pakhomov et al., 2004). This was investigated by releasing a grid of floats at the intersection of Marguerite Trough and the shelf break (Fig. 19). The dominant depth of arrival of Antarctic krill from the Bellingshausen Sea was 100 m to 200 m, therefore the time sequence of the horizontal distribution of the transport pathways is shown for releases at 100 m. Once released, the floats were clearly apportioned into specific pathways determined by the origination point. The subsequent transport of the floats showed three dominant pathways (Fig. 19A). The first was a downstream pathway, which flows along the shelf break to the northeast away from Marguerite Bay and the shelf. The second pathway extended along the depression off Adelaide Island, which reaches the inner shelf region north of Marguerite Bay towards Crystal Sound. The third pathway was along Marguerite Trough towards Marguerite Bay (Fig. 19A). The downstream pathway dominated the west side of the Marguerite Trough region (Fig. 19B-F) and with time also dominated the offshore east side (Fig. 19G-I).

The particles that entered the wAP continental shelf north of Marguerite Bay were mostly from the region east of Marguerite Trough. These particles continued along the depression off Adelaide Island into the inner shelf towards Crystal Sound or continued to the northeast on the shelf. Particles entering Marguerite Bay moved along the east flank of the Trough from the center side of the release region (Fig. 19).

In addition to spatial and temporal variability, the depth distribution of the percentage of particles associated with the three dominant pathways differed (Fig. 20). The highest percentage of particles followed the Marguerite Trough pathway, with the second highest percentage associated with the onshelf pathway (Fig. 20A). Particles released above 25 m tended to follow the downstream pathway and be transported

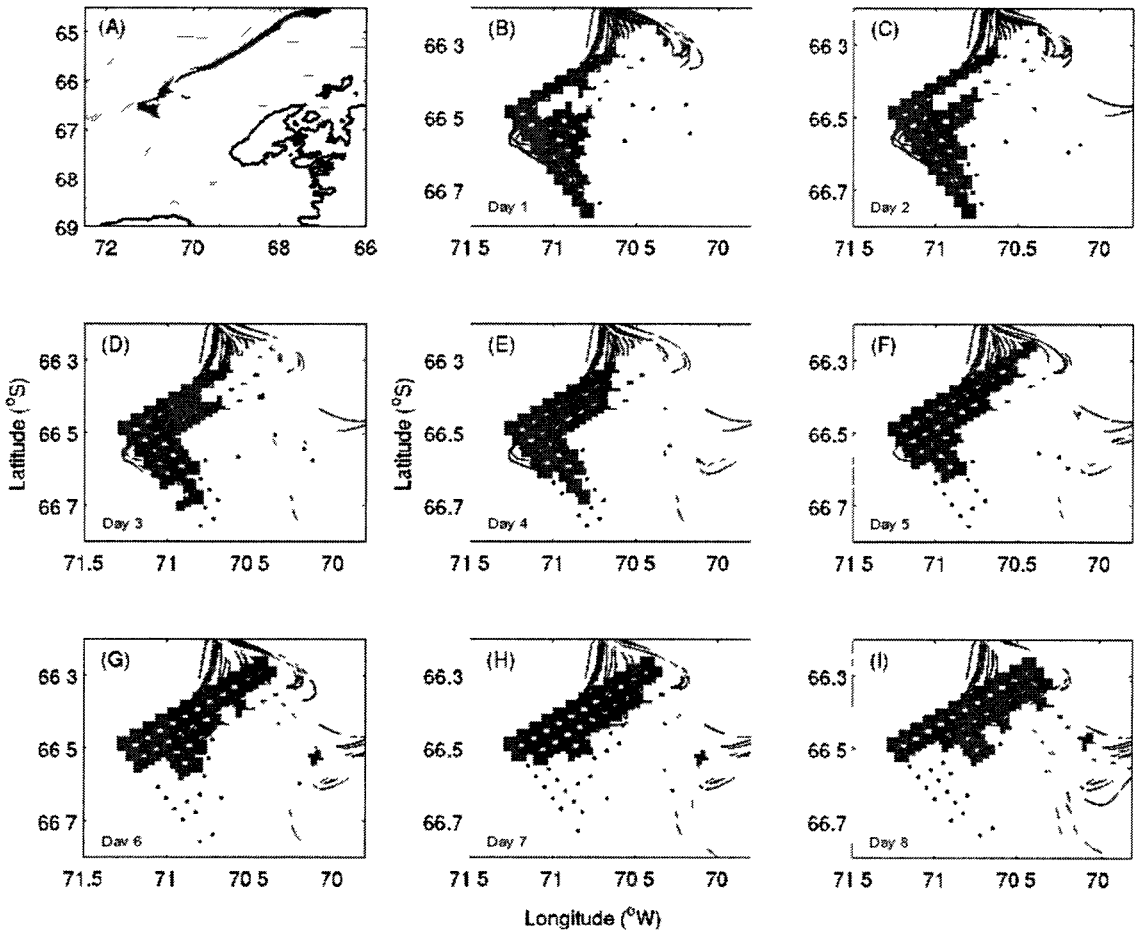

Fig. 19. (A) Release sites and simulated transport pathways obtained for particles released at the outer end of Marguerite Trough at 100 m at daily intervals for 8 days. Colors indicate the three transport pathways, downstream (blue), onshelf (light-blue), and Marguerite Trough (yellow). The origination points for the particles contributing to the three transport pathways on days 1 to 8 are shown in panels B-I, respectively.

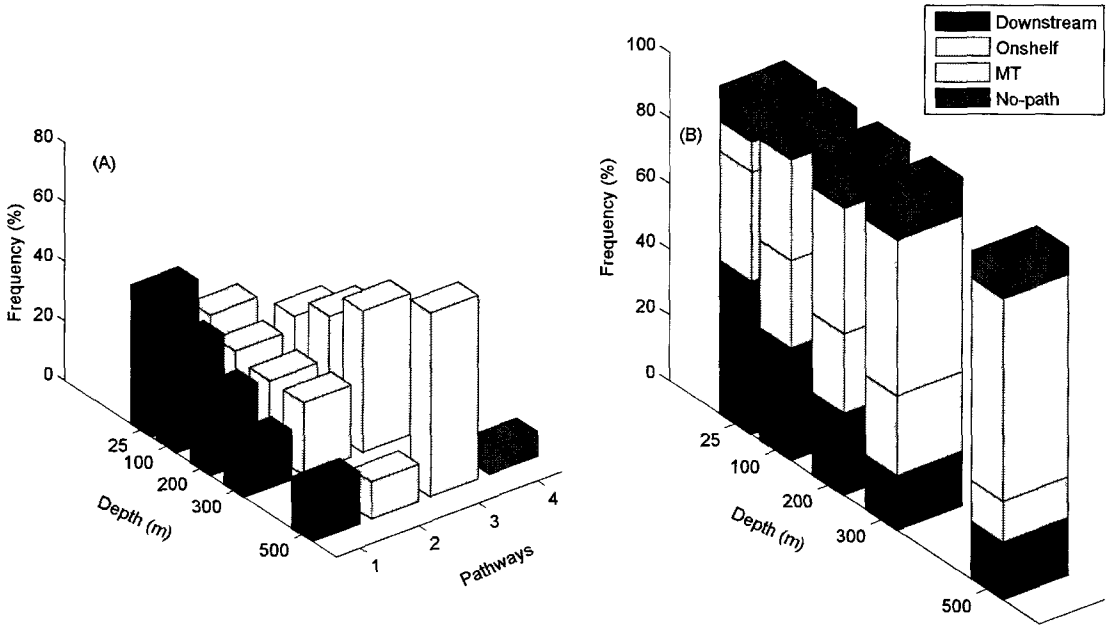

Fig. 20. Depth distribution of the percentage of total particles released along the outer end of Marguerite Trough that followed the (A) three dominant transport pathways and (B) the relative percentage at each depth along the transport pathways. The percentage particles that followed no pathway are also shown.

to the northeast with the prevailing flow of the ACC. This tendency decreased with depth, especially below 200 m where only <10% of the larvae are transported away from Marguerite Bay (Fig. 20B). At 100 m, the percentage of particles that followed any of the three dominant pathways was approximately the same (Fig. 20B). However, only two of the three pathways provide sources of potential larvae to shelf sites in Marguerite Bay and Crystal Sound (Fig. 20B). Below 200 m, there was a clear tendency for the particles to follow the Marguerite Trough pathway especially at 300 m where ~40% of the total entered the shelf via this pathway (Fig. 20A). The percentage of particles that did not follow one of the dominant pathways (Fig. 20B) was low (<15%) for all depths.

The temporal variability of the transport pathways was determined by releasing particles at daily intervals for one month (Fig. 21). At 25 m the particles tended to follow the downstream pathway (Fig. 21A), being more than 40% for 22 of the 32 days. During the other 10 days, six days at the start of the time series and 4 days around day 20, there was a preference for the particles to continue onshelf along the depression off Adelaide Island. During the first 10 days of the month at 100 m (Fig. 21B), the particles were as likely to continue along the downstream or onshelf pathway. However, during the beginning around day 12 and at the end of the time series there was clear dominance of the downstream pathway. The downstream pathway was the dominant pathway at depths above 300 m during most of the time series. Below 300 m the Marguerite Trough pathway dominated (Fig. 21C-E). Particle transport at 500 m (Fig. 21E) was predominately along the Marguerite Trough pathway.

4.3.3 Local reproduction and retention

Simulated trajectories for floats released on the wAP shelf at a site to the north between Renaud and Anvers Island and at a site to the south of Marguerite Bay showed that these regions exported particles to the north and south and that the particles remained mostly on the shelf (Fig. 22). Particles released at a central site just off the southern entrance of Marguerite Bay moved across the shelf and entered the northeasterly flow of the ACC. Other particles entered Marguerite Bay or moved southward along Alexander Island.

Apportioning the (Fig. 22A, D) trajectories into times that correspond to the calyptopis 2 larval stage (47 days, Fig. 22A, D) suggested that these larvae, if spawned on the southern wAP shelf, would be found in Marguerite Bay and along Marguerite Trough. Similarly, spawns to the north would result in calyptopis 2 larvae on the inner shelf west of Renaud Island. Export from the shelf occurred after larvae developed to the furcilia 2 and 3 stages (Fig. 22B, E). Only a small percentage of the larvae crossed

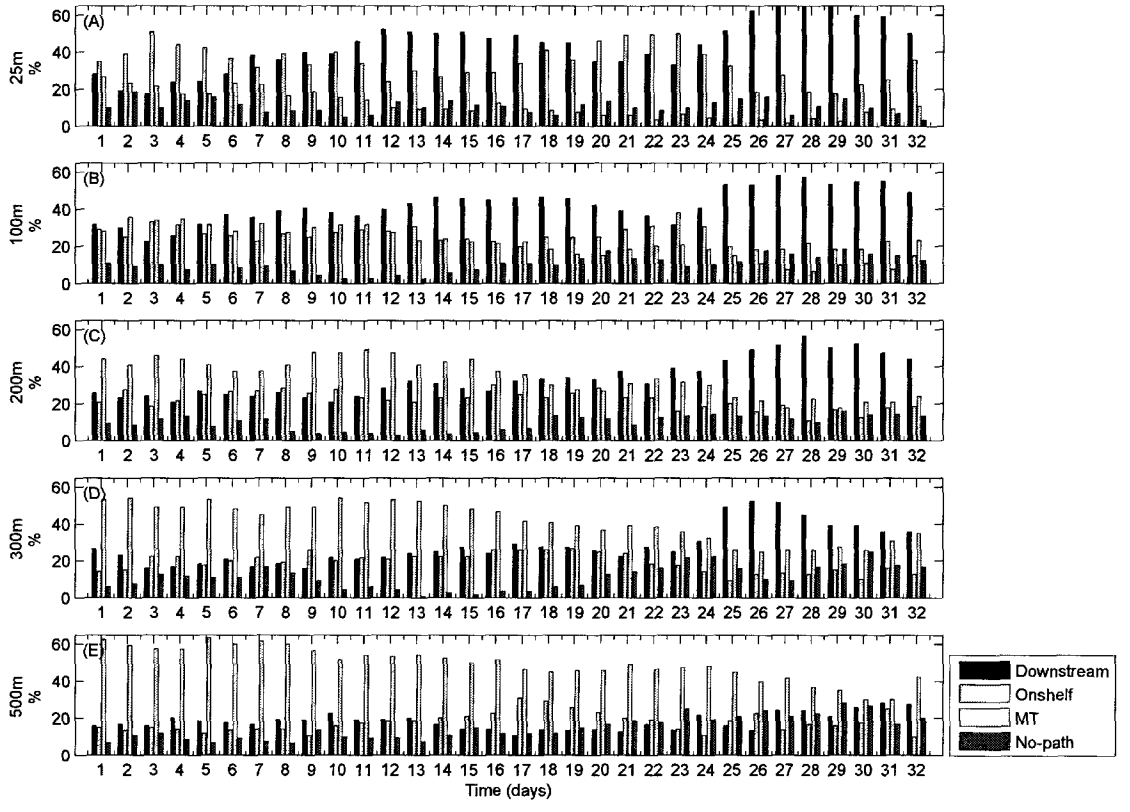

Fig. 21. Time series of the percentage of particles that followed the three dominant transport pathways after release at the offshore end of Marguerite Trough at (A) 25 m (B) 100 m (C) 200 m (D) 300 m, and (E) 500 m. The percentage of particles following on pathway are shown for comparison. The percentages were calculated relative to the total number of particles released.

the 800-m isobath and moved offshore before the furcilia 3 stage was completed (Table 13). However, export increased after 150 days, at which point the larvae correspond to the furcilia 6 stage. At 300 m furcilia 6 larvae coming from the southern portion of the wAP shelf (Fig. 22F) reached the vicinity of Marguerite Bay. However, at 100 m, particles were retained on the mid-shelf, preventing larvae from reaching Marguerite Bay (Fig. 22C).

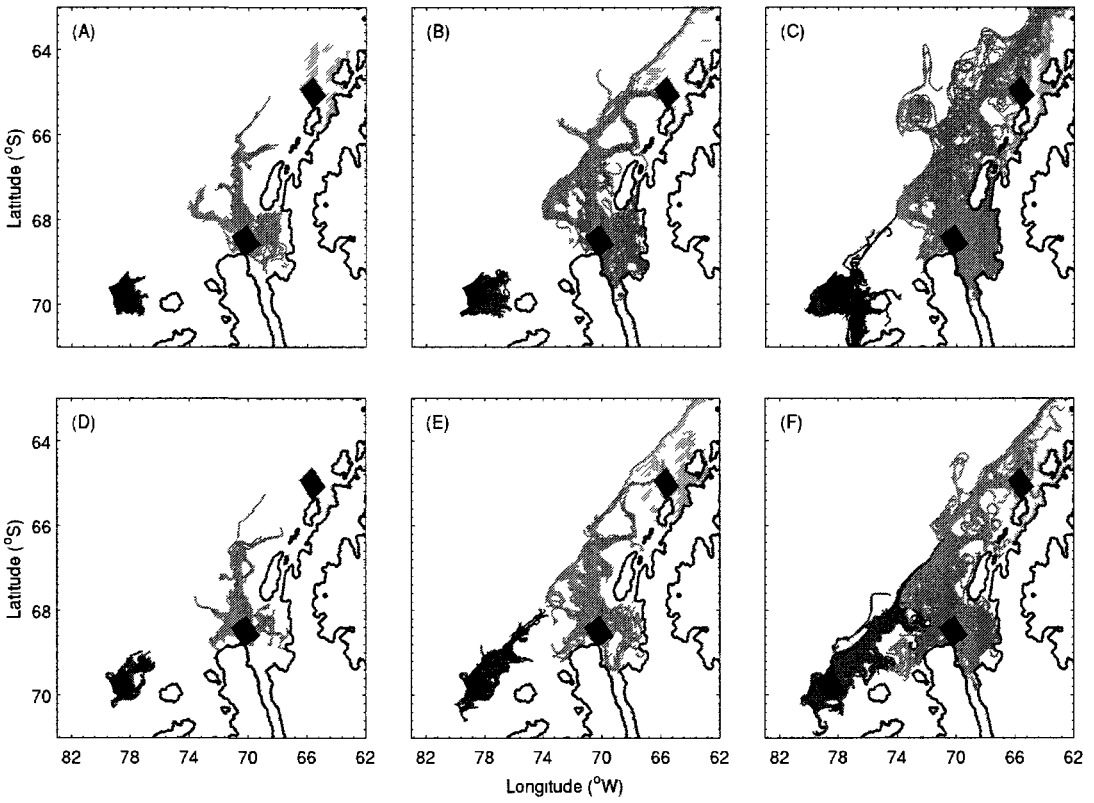

Fig. 22. Dispersion of simulated particles released at 100 m (top panels) and 300 m (bottom panels) at three sites (black boxes) over the wAP continental shelf. The particle trajectories were mapped to the (A, D) calyptopis 2, (B, E) furcilia 3, and (C, F) furcilia 6 larval stages using the developmental times given in Table 10.

Dispersion, export, and connectivity of krill populations along the inner portion of the wAP shelf was determined by releasing particles at four locations at times that correspond to when spawning occurs (Fig. 23).

Table 13

Percentage (%) of particles released at 50, 120, 150 and 300 m that were exported from the continental shelf from the sites on the southern (S), central (C) and northern (N) portions of the wAP (see Fig. 22 for site locations). At each site and depth 208 particles were released. The trajectories were apportioned into times that correspond to Antarctic krill larval stages using the developmental times given in Table 10. The total percent export for each depth and site over one year (1 y) is given in the last column. The larval stages are abbreviated as: Nauplius 1 and 2 (N1, N2), Metanauplius (MN), Calyptopis 1-3 (C1, C2, C3) and Furcilia 1-6 (F1, F2, F3, F4, F5, F6).

Area of release	**N1**	**N2**	**MN**	**C1**	**C2**	**C3**	**F1**	**F2**	**F3**	**F4**	**F5**	**F6**	**1 y**
50 m													
S	0	0	0	0	0	0	0	0	0	0	1	0	9
C	0	0	0	0	3	6	13	9	9	10	17	19	47
N	0	0	0	0	1	1	6	13	18	22	35	44	83
120 m													
S	0	0	0	0	0	0	4	5	6	8	8	12	27
C	0	0	0	0	0	0	2	2	4	4	4	6	32
N	0	0	0	0	0	3	4	10	14	16	18	25	66
150 m													
S	0	0	0	0	0	0	2	3	6	5	8	9	25
C	0	0	0	0	0	0	0	1	1	1	1	3	19
N	0	0	0	0	0	1	4	7	10	13	19	25	50
300 m													
S	0	0	0	0	0	0	0	1	3	3	3	6	22
C	0	0	0	0	0	0	2	3	3	4	5	9	39
N	0	0	0	0	0	1	2	5	10	12	14	19	76

Early in the reproductive season (15 November) export of calyptopis 2 larvae from the inner shelf was low at the three southern-most release sites (Fig. 23A, D, G) and furcilia 3 (Fig. 23B, E, H) larval stages. Export of calyptopis 2 larvae occurred only at the northern release site near Anvers Island (Table 14). For the 24 December release,

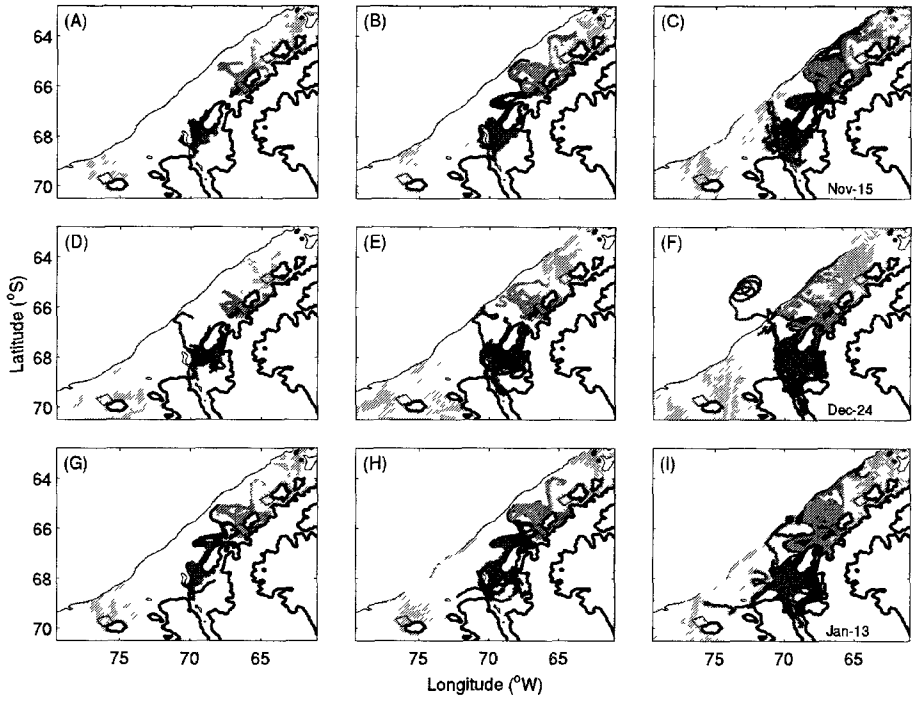

Fig. 23. Dispersion of simulated particles released at 50 m along the inner portion of the wAP continental shelf on (A-C) 15 November, (D-F) 24 December, and (G-I) 13 January. The particle trajectories were mapped to the (A, D, G) calyptopis 2, (B, E, H) furcilia 3, and (C, F, I) furcilia 6 larval stages using the developmental times given in Table 10. Releases sites were (from south to north) near Charcot Island, Adelaide Island, Renaud Island and Anvers Island.

the sites off Charcot Island, Adelaide Island, and Renaud Island showed essentially no export. Particles exported from the Charcot Island site were returned to the shelf by the prevailing circulation (Table 14). Export of the late stage larvae exceeded 20%, but only for the northernmost release site. By mid-January, there was some exchange of particles between the three northern sites, but the southern-most site remained essentially self contained (Fig. 23C, F, I, Table 14).

The connectivity among the inner shelf release sites showed that the export tended

to be to the north along the shelf, but that the number of particles that were exchanged was low (Fig. 24). The number of particles exchanged between sites (Table 15) at the time corresponding to the first larval feeding stage (calyptopis 1) and the time before completion of the last larval stage (furcilia 6) provided a measure of potential import and export of individuals from a location. There was no connectivity among these sites at the calyptopis 1 larval stage and the degree of connectivity for the last larval stage was low (Table 15). A small percentage of individuals from Marguerite Bay (Adelaide Island) reached Renaud Island and there was limited exchange between Renaud Island and Anvers Island (Fig. 24, Table 15). The December and January releases showed similar dispersion patterns. The furcilia 6 larvae from Charcot Island occupied the shelf south of Alexander Island and only a small number of individuals were observed along the shelf north of Marguerite Bay. The release sites near Charcot Island and Adelaide Island showed no direct connectivity (Fig. 24A, B). The Adelaide Island release site showed higher retention and some connectivity with the region near Renaud Island (Fig. 24C, D). The largest number of particles were found either on the mid-shelf north of Marguerite Bay or in the fjords southeast from Anvers Island (Fig. 24C, D). Larvae from the Renaud Island site was observed on the inner wAP shelf and around the Anvers Island release site (Fig. 24E, F).

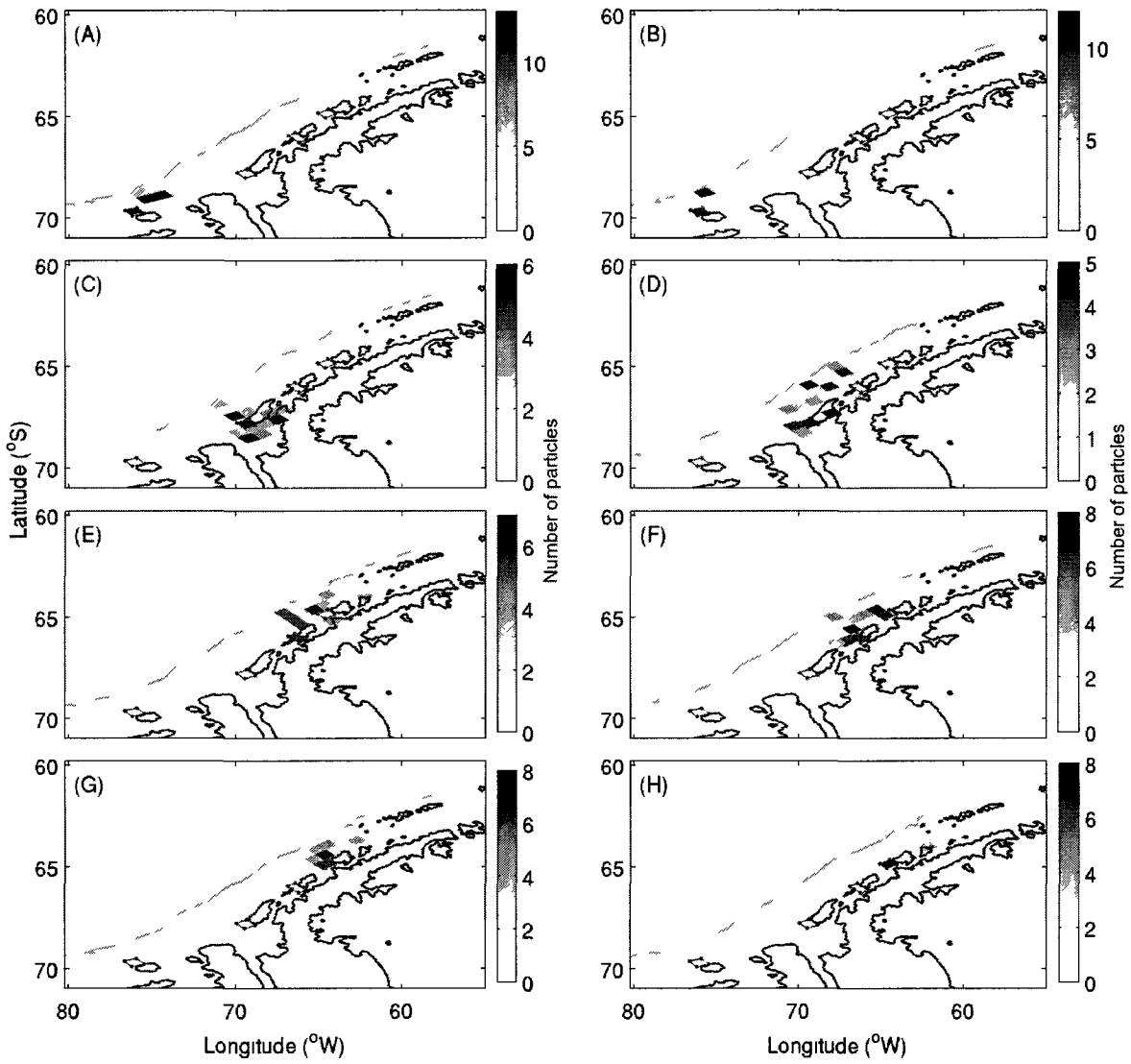

Fig. 24. Distribution of particles released at four sites (unfilled blue squares) near Charcot Island (A, B), Adelaide Island (C, D), Renaud Island (E, F) and Anvers Island (G, H) along the inner wAP shelf in December (left panels) and January (right panels). Release site is indicated (filled blue square) in each panel. The number of particles (indicated by scales) in 40 km by 40 km gridded regions of the shelf after development to furcilia 6 larvae.

Table 14

Percentage (%) of particles released at 25, 50, 100 and 300 m that were exported from the shelf from the sites near Charcot Island (CH), Adelaide Island (AdI), Renaud Island (RI) and Anvers Island (AI). At each site and depth 90 particles were released. The trajectories were apportioned into times that correspond to Antarctic krill larval stages using the developmental times given in Table 10. The total percent export for each depth and site over one year (1 y) is given in the last column. The larval stages are abbreviated as: Nauplius 1 and 2 (N1, N2), Metanauplius (MN), Calyptopis 1-3 (C1, C2, C3) and Furcilia 1-6 (F1, F2, F3, F4, F5, F6).

Area of release	**N1**	**N2**	**MN**	**C1**	**C2**	**C3**	**F1**	**F2**	**F3**	**F4**	**F5**	**F6**	**1 y**
25 m													
CH	0	0	0	0	0	0	0	0	0	0	0	0	0
AdI	0	0	0	0	0	0	0	0	0	0	0	0	2
RI	0	0	0	0	0	0	0	0	0	0	0	2	18
AI	0	0	0	0	0	0	0	0	6	12	23	38	51
50 m													
CH	0	0	0	0	0	0	0	0	0	0	0	0	0
AdI	0	0	0	0	0	0	0	0	0	0	0	2	17
RI	0	0	0	0	0	0	0	0	0	0	0	2	17
AI	0	0	0	0	0	0	0	0	3	12	20	31	56
100 m													
CH	0	0	0	0	0	0	0	0	0	0	0	0	0
AdI	0	0	0	0	0	0	0	0	0	0	0	0	1
RI	0	0	0	0	0	0	0	0	0	0	0	1	17
AI	0	0	0	0	0	0	0	0	3	14	26	43	56
300 m													
CH	0	0	0	0	0	0	0	0	0	0	0	0	1
AdI	0	0	0	0	0	0	0	0	0	0	0	0	3
RI	0	0	0	0	0	0	0	0	0	0	0	0	20
AI	0	0	0	0	0	0	0	1	7	18	24	40	56

Table 15

Number of particles released at 50 m that were exported to the sites near Charcot Island (CH), Adelaide Island (AdI), Renaud Island (RI) and Anvers Island (AI) for the release of December 24. At each site 90 particles were released. The trajectories were apportioned into times that correspond to the first feeding stage (Calyptopis 1, C1) and late larval stage (Furcilia 6, F6) of Antarctic krill using the developmental times given in Table 10.

C1 larvae				
Sites	**CH**	**AdI**	**RI**	**AI**
CH	–	0	0	0
AdI	0	–	0	0
RI	0	0	–	0
AI	0	0	0	–
F6 larvae				
Sites	**CH**	**AdI**	**RI**	**AI**
CH	–	0	0	0
AdI	0	–	1	0
RI	0	0	–	3
AI	0	0	1	–

The number of particles originating near Renaud Island that reached Anvers Island was low (Table 14), but dispersion and retention occurred along and between the inner shelf between these two areas. Most of the furcilia 6 larvae released near Anvers Island in January were exported from the shelf (Fig. 24H). In contrast a December release at this site resulted in a larger number of particles being retained east of the release site (Fig. 24G).

4.4 DISCUSSION AND SUMMARY

4.4.1 Western Bellingshausen Sea Inputs

A circumpolar, one-dimensional temperature-dependent model of the descent-ascent cycle of Antarctic krill (Hofmann and Hüsrevoğlu, 2003) showed that the Bellingshausen Sea is a region where this portion of the reproductive cycle can be successfully completed. Embryos released over the deep water reach CDW, which provides a suitable habitat for development. The embryos hatch at depth and the larvae return to the surface to start feeding (Marr, 1962; Marschall, 1983; Quetin and Ross, 1984). The Lagrangian tracking experiments showed that particles released in upstream regions of the Bellingshausen Sea were entrained in the north-northeasterly flowing ACC and transported along the outer shelf, reaching the wAP shelf in 120-150 days. In areas where the alongshelf flow is deflected onshore, such as Marguerite Trough and the depression off Alexander Island, the particles moved onto the wAP continental shelf. These numerical results correspond to aspects of krill reproduction and life history. Gravid females of Antarctic krill migrate to the outer shelf area to spawn (Marr, 1962; Siegel, 1988), which provides a source of embryos that can be transported by the ACC towards the wAP region. The transport time scales correspond to developmental times associated with the early to late larval stages of Antarctic krill. The locations of the onshelf movement of the krill larval stages in the wAP region are consistent with observed distributions and with areas where persistent krill populations have been observed, such as Crystal Sound and Laubeuf Fjord.

The limited observations available from the Bellingshausen Sea and wAP continental shelf support the patterns obtained from the numerical Lagrangian experiments. Acoustic observations of the abundance and distribution of Antarctic krill in the marginal ice zone of the Bellingshausen Sea area showed large krill swarms in the open sea between 84°W-86°W south of 67°S in an area characterized by mesoscale

eddies and high chlorophyll concentrations (>6 mg chl a m^{-3}) were observed (Murray et al., 1995; Savidge et al., 1995). The area sampled during these studies is consistent with potential spawning grounds inferred from the Lagrangian experiments that resulted in furcilia larvae that are transported onto the wAP shelf via Marguerite Trough (e.g. Fig. 17B). Additional net-based observations showed that Antarctic krill size/age groups were spatially segregated along a gradient from the shelf break to offshore waters in the Bellingshausen Sea area (Siegel and Harm, 1996). Large mature krill size groups were found mostly in open water, and younger krill (age group +1) were predominant near the shelf break and over the southern shelf. Most of the females observed belonged to the prespawning stage, which indicated that early phase of spawning. Larvae resulting from spawns from krill either along the shelf break or on the outer shelf represent potential inputs to the wAP shelf.

Net-based observations from the U.S. SO GLOBEC field studies showed that early furcilia stages, including the furcilia 6 stage, were the dominant modes of krill larvae between 50-200 m at the outer portion of Marguerite Trough along the shelf break (Daly, 2004). Additional net-based observations (0-300 m) from the German SO GLOBEC field studies in fall 2001 (Pakhomov et al., 2004) also showed a high abundance of furcilia 1 and 2 at locations over the shelf break and slope around Marguerite Trough. The depth distributions of the simulated particles showed that approximately 55% of the particles that arrived at the outer end of Marguerite Trough were in the 100-200 m depth range, which roughly agrees with the depth distribution observed by Daly (2004) and Pakhomov et al. (2004). Moreover, the predominant transport pathways (see Fig. 18A) moved these particles towards the inner shelf, through the depression off Adelaide Island reaching Crystal Sound or through Marguerite Trough to the inner portions of Marguerite Bay, such as Laubeuf Fjord. These latter two sites correspond to biological hot spot regions (Costa et al., 2007).

Marguerite Trough is an important conduit for the transport of particles (and

larvae) originating in upstream regions onto the shelf. The numerical simulations showed that 40-60% of the particles that arrived at Laubeuf Fjord were released over the outer portion of Marguerite Trough (intersection of the shelf break with Marguerite Trough) and followed transport pathways along the inner limb of the shelf break and the Trough (see Fig. 11C, F). The estimated residence times for inner shelf regions, such as Laubeuf Fjord (e.g. Table 7 in Chapter III), are long enough for the larvae originating in upstream regions to be retained and recruit to the shelf krill populations by fall when the seasonal pack-ice closes. Observations show that larval and postlarval krill are more likely to occupy the inner shelf areas of the wAP late in the fall season (Siegel, 2005; Nicol, 2006).

The Lagrangian particle experiments also showed that the shelf area south of Alexander Island (around 76°W) is a potential source region of larval krill to the Marguerite Bay region. This is an area where the descent-ascent portion of the krill reproductive cycle can be successfully completed (Hofmann and Hüsrevoğlu, 2003). The particle transport times indicated that this region is a potential spawning area for the calyptopis 2 larvae that were transported to the outer portion of Marguerite Trough. Analysis of video plankton recorder data obtained from surveys made during the U.S. SO GLOBEC 2001 field studies showed high abundances of larval krill of size appropriate for calyptopis 2 on the outer and mid portions of the wAP shelf (Ashjian et al., 2008). The vertical distribution of dominant taxon placed larval krill in an area of the outer shelf and shelf break, where inputs from the Bellingshausen Sea could supply larvae to the Alexander Island region (e.g. Fig. 17A). The estimated upstream spawning ground that would result in inputs of krill larvae that would move onto this portion of the wAP shelf is in an area where high chlorophyll *a* concentrations have been observed (Marrari et al., 2008).

4.4.2 Local reproduction and export from the shelf

The deeper portions of the wAP inner and mid shelf are areas where the descent-ascent reproductive cycle can be successfully completed (Hofmann and Hüsrevoğlu, 2003). Reproduction of Antarctic krill in shelf environments has been suggested for the northern portion of the Antarctic Peninsula (Brinton, 1991). From net-based observations, the Gerlache-Bransfield Strait region was described as a nursery area for immature krill and early summer larvae. The local circulation was assumed to increase the larval retention times in the near shore waters that favored continued development and growth (Huntley and Brinton, 1991).

The residence times estimated from the particle trajectories on the wAP continental shelf were about 3 months. Moreover, the degree of connectivity between sites on the mid and inner shelf was low. These results suggest that local reproduction and development can contribute to maintenance of krill populations on the wAP shelf.

The larval krill distributions observed in the Marguerite Bay region during the U.S. SO GLOBEC field studies suggested that onshore and offshore reproduction by Antarctic krill occurred. Net samples obtained inside Marguerite Bay during fall 2001 and fall 2002 (Daly, 2004) showed high abundances of older stage larvae concentrated in a narrow layer near the surface. Younger larval stages were observed at offshelf locations. The simulated dispersion of older stage larvae (furcilia 6) that originated along four release locations on the shelf (e.g. Fig. 24), showed distributions similar to the onshelf observations given by Daly (2004). The numerical experiments suggest that if local reproduction occurs around Marguerite Bay, the furcilia 6 larval stage will be found either on the mid-shelf north of Adelaide Island or in the fjords inside Marguerite Bay (e.g. Fig. 24C). Larval krill hatched from embryos released in summer within the inner shelf environments north of Marguerite Bay, would enter winter as late larvae (furcilia 6) and occupy the mid and outer shelf region between Adelaide Island and Anvers Island.

Additional support for local reproduction comes from net-based observations made on the wAP shelf during fall 2001 prior to the U.S. SO GLOBEC observations (Pakhomov et al., 2004). These distributions showed that the furcilia 2 and 3 stages accounted for 60% of the total larval abundance. This implies that local reproduction is possible. Embryos spawned on the shelf could develop into furcilia 3 before being exported or retained on the shelf and provide the source of the furcilia 6 larvae observed later in the fall.

Ashjian et al. (2004) showed that the greatest abundance and biomass of larval krill on the wAP shelf were associated with a persistent clockwise gyre located to the west of Adelaide Island. This is also the region where high numbers of simulated particles with time scales that correspond to furcilia 6 larvae accumulated (e.g. Fig. 24D). Ashjian et al. (2004) also observed high abundance and biomass of juvenile and adult krill in Laubeuf Fjord during fall 2001. During winter 2001, larger larval krill were found over the wAP shelf. The Video Plankton Recorder observations from the 2001 fall and winter surveys showed larval krill present across the entire shelf with high abundances at the shelf break (Ashjian et al., 2008). The SO GLOBEC observations are consistent with those made during the SIBEX programme of BIOMASS (Siegel, 1989), which showed winter distributions of furcilia 3 to furcilia 5 larvae along the wAP continental shelf break and mid shelf. The highest abundances were towards the area off of Adelaide Island (the southwestern area covered by that survey).

Wiebe et al. (2011) showed that the distribution of Antarctic krill and other euphausiids was associated with the deep troughs and depressions of the wAP, and suggested that local reproduction is a contributing factor in maintaining these distributions. They also showed an across-shelf gradient in the abundance of Antarctic krill with higher abundances of calyptopis and furcilia over the shelf. Comparison with distributions of numerical Lagrangian particles led Wiebe et al. (2011) to conclude that the observed distribution of larval krill on the wAP shelf could result from

local onshelf reproduction. These results are consistent with the recognition that Marguerite Bay is a potential "hotpot" (Pakhomov et al., 2004) in Antarctic krill recruitment along the Antarctic Peninsula.

Local reproduction does not necessarily imply local retention. The simulated trajectories for particles released at inner shelf sites north of the Marguerite Bay region showed that older larval krill could be transported as far north as Elephant Island (Fig. 24H). Several modeling studies have shown that transport of Antarctic krill from the Antarctic Peninsula does occur and that krill populations in downstream regions, such as South Georgia are sustained by inputs of individuals from the Antarctic Peninsula (Hofmann et al., 1998; Murphy et al., 1998; Fach et al., 2002; Fach et al., 2006).

4.4.3 Implications for wAP krill populations

The results of this study suggest that Antarctic krill populations along the outer and mid wAP shelf receive significant (~25%) and consistent inputs from upstream sources. The extent to which the wAP populations are dependent on these inputs is likely variable and dependent on season and location. The Lagrangian tracking results presented in this and the previous chapter showed that particles are transported to particular regions of the wAP, with time scales that were consistent with that required for development of an Antarctic krill from an embryo to late furcilia stages (186 days).

The preferred transport pathways for particles released over Marguerite Trough at the surface and at depth (e.g. Fig. 20 and 21) resulted in inputs to inner shelf regions, such as Crystal Sound and Laubeuf Fjord. Crystal Sound supports high densities of crabeater seals (Burns et al., 2004). Also, Adélie penguins distributions along the wAP shelf are linked to regions of enhanced krill abundance (Fraser and Trivelpiece, 1996). Adélie penguins depend on Antarctic krill as a primary food source. During the U.S. SO GLOBEC field studies, Adélie penguins were found near or over Marguerite

Trough and in areas associated with CDW (Ribic et al., 2008). Humpback and minke whales distributions on the wAP have a positive relationship with high zooplankton acoustic volume backscatter in the upper and mid water column, they are able to locate physical features and oceanographic processes that enhance prey aggregation (Friedlaender et al., 2006). The distributions of these predators coincided with areas highlighted in the Lagrangian tracking simulations, that showed retention and/or received consistent and significant inputs from other regions. The implication is that the top trophic level predators target these locations because of access to a dependable food supply (Costa et al., 2007). Thus, the spatial separation in dependence on local versus remote inputs has implications for predators that depend on Antarctic krill as the primary prey.

A sequence that may result in maintenance of krill populations that are needed as prey by the top trophic level predators can be constructed from the Lagrangian particle simulations. Furcilia larvae that arrive in the Marguerite Bay region from other source regions can be transported to the inner shelf areas by the shelf circulation during the late summer and fall. By winter, sea ice covers these regions, providing an overwintering habitat for the Antarctic krill with sufficient available food (from sea ice) and retention due to local circulation (see retention times in Table 7). The next summer 1-year-old krill (juveniles) would be found in the inner shelf region. Support for this scenario is provided by krill length frequency distributions collected in summer, which showed small krill (33-37 mm) throughout the inner shelf region of the wAP between Anvers Island and Renaud Island (Lascara et al., 1999). Larger krill (>40 mm) were restricted to the outer shelf. Summer size compositions of Antarctic krill collected in the deeper shelf waters (140 m) between Renaud Island and Adelaide Island showed length classes that ranged from 18-27 mm with a modal value of 22 mm (Siegel, 1985). These individuals were categorized as small juveniles and accounted for 91% of the total individuals that were sampled.

The occurrence of juvenile and medium size krill along the inner shelf may result from local reproduction in areas of the shelf where the shelf is deep and CDW is present, which allows completion of the descent-ascent cycle (Prézelin et al., 2000). The clockwise surface circulation over the shelf and onshore flow at depth (Smith et al. 1999; Dinniman and Klinck, 2004) facilitate transport of krill larvae to the inner shelf.

Reproduction of krill along the wAP continental shelf break has been shown to result in the spreading and transport of larval krill by the frontal regions of the ACC (Capella et al., 1992; Hofmann et al., 1992; Fach et al., 2002; Thorpe et al., 2004; Thorpe et al., 2007). Export of the krill that result from local reproduction in and around Marguerite Bay may account for the larvae observed at the outer shelf end of Marguerite Trough (Wiebe et al., 2011). The Lagrangian tracking simulations showed that about 40% (25-100 m) and <20% (below 200 m) of the particles in this region were transported northeast away from Marguerite Bay (e.g. Fig. 21). This export may be important for krill predators in regions north of Marguerite Bay such as Bransfield Strait and South Georgia (Brierley et al., 1997).

The Bransfield Strait is known to support high biomass and to be an area of krill reproduction and recruitment (Siegel, 1988; Brinton, 1991; Huntley and Brinton, 1991; Hofmann et al., 1992; Ichii et al., 1998). The wAP shelf region south of Bransfield Strait has high krill biomass in all seasons (Lascara et al., 1999). The results from this study showed that particles released in the Marguerite Bay region provided inputs to the wAP shelf area south of Bransfield Strait. An earlier particle tracking study (Capella et al., 1992) showed that particles released on the northern part of the wAP shelf were transported to Bransfield Strait. Thus, there is connectivity among the krill populations that extend from the southern wAP to Bransfield Strait.

Populations of Antarctic krill at South Georgia are sustained by inputs from other

regions (Marr, 1962; Siegel, 1988; Hofmann et al., 1998; Murphy et al., 1998). Acoustic estimates of krill density in the Elephant Island and South Georgia regions showed similarities at both locations that suggested that krill densities are coupled and may be impacted by similar physical and biological factors over similar spatial and temporal scales (Brierley et al., 1999). Years of low krill density corresponded to major breeding failures for numerous krill predators in South Georgia (Brierley and Watkins, 1996). Differences in the length frequency distributions of the krill sampled on the western and eastern side of South Georgia suggested two different krill sources (Watkins et al., 1999). Krill from the western side were larger and were assumed to come from Bellingshausen Sea. On the eastern side of South Georgia krill were smaller and were assumed to originate in the Weddell Sea. The size of krill across the Scotia Sea from the wAP to South Georgia increases (Marr, 1962; Siegel, 1992; Tarling et al., 2007). Observations of krill size frequency distributions from South Georgia suggested that the younger 1+ (2 yr old) and 2+ (3 yr old) size class krill enter the region mainly from the east, as either pulses or continuous recruitment events (Murphy et al. 1998).

Transport of krill across the Scotia Sea to South Georgia is possible due to currents associated with the ACC (Hofmann et al., 1998; Murphy et al., 1988; Fach et al., 2002; Fach et al., 2006; Thorpe et al., 2007). The simulated trajectories showed that >30% of the particles originating on the wAP shelf are exported from the shelf (Table 15) and that many of these may reach Elephant Island when completing the furcilia 6 stage (e.g. Fig. 24H). About 70% of the one year old krill reproduced between Renaud Island and Adelaide Island will be exported from the wAP shelf and may continue transport across the Scotia Sea (Fach et al., 2006; Thorpe et al., 2007). Simulations of krill growth during transport showed that larval and juvenile krill originating along the western Antarctic Peninsula can grow to 1+ and 2+ age classes during transport to the South Georgia region. The observed distribution of krill furcilia larvae during the winter (Siegel, 1989) showed highest concentrations in the oceanic waters north

of the South Shetland Islands towards Elephant Island, providing additional support for export from the wAP to the Scotia Sea.

CHAPTER 5

MODELING EARLY LIFE STAGES OF ANTARCTIC KRILL (*Euphausia superba*) IN CONTINENTAL SHELF ENVIRONMENTS ON THE WEST ANTARCTIC PENINSULA

5.1 INTRODUCTION

The Antarctic krill populations along the wAP continental shelf are maintained at some level by local inputs, as suggested by observational (Lascara et al., 1999; Fraser and Hofmann, 2003; Prézelin et al., 2004; Pakhomov et al., 2004; Wiebe et al., 2011) and modeling studies (Piñones et al., 2011; Chapter IV). The extent to which local inputs support the Antarctic krill stocks depends on the availability of spawning stock and the ability to complete the descent-ascent portion of the reproductive cycle on the wAP continental shelf.

The distribution of Antarctic krill spawning stock and spawning grounds on the wAP continental shelf was inferred from observations that showed spatial separation of the life stages and seasonally varying distributions in biomass (Siegel, 1988, 1992). Juveniles and early subadults were observed in the inner shelf region and gravid and spent females were found along the outer shelf and in oceanic waters. The latter observation suggested that the primary spawning region was along the outer portion of the wAP continental shelf (Siegel, 1988). The observed spatial separation of the krill maturity stages led Siegel (1988) to postulate a seasonal on-offshelf migration by Antarctic krill. Adult krill moved offshore in summer to spawn, after which they moved onshore to the inner portion of the shelf. This migration extended over distances of 50-100 km and occurred in 5 to 10 days (Kanda et al., 1982). The onshore migration was coincident with sea ice formation, which provided a winter habitat for larvae (Daly, 2004) and resulted in larvae in the inner shelf region the next spring

when the sea ice retreated (Nicol, 2003). This sequence explained observed distribution patterns of larval, juvenile, and adult krill (Siegel, 2000) and observations of seasonal shifts in Antarctic krill biomass towards the inner wAP shelf (Lascara et al., 1999).

Successful completion of the descent-ascent cycle portion of Antarctic krill reproduction requires that embryos be released in regions where hatching will occur at depths that are shallow enough to allow the first larval feeding stage to ascend to the surface waters before depleting its carbon stores (Ross and Quetin, 1989). Modeling studies of the descent-ascent cycle (Hofmann et al., 1992; Hofmann and Hüsrevoğlu, 2003) showed that the depth of CDW controls the success of the descent-ascent cycle. Encountering CDW accelerates development and hatching of the embryo, which allows the larva to return from shallower depths and to ascend faster (Hofmann et al., 1992; Hofmann and Hüsrevoğlu, 2003). The outer wAP continental shelf and regions of the mid and inner shelf that are deeper than 400 m and are influenced by CDW support successful completion of the descent-ascent cycle (Hofmann et al., 1992; Hofmann and Hüsrevoğlu, 2003).

The wAP continental shelf, therefore, has spawning stock of Antarctic krill and provides a habitat that supports successful completion of the descent-ascent cycle. However, recent studies have shown that biological production may be supported by limited regions (e.g. hot spots) of the wAP continental shelf (Costa et al., 2007; Hofmann et al., 2009). The extent to which the regions associated with hot spots, spawning, and successful descent-ascent cycles coincide is unknown. Thus, the objective of this study is to investigate connectivity of these regions. A one-dimensional, temperature-dependent model (Hofmann et al., 1992) was used to simulate the descent-ascent cycle of the embryos and early larval stages of Antarctic krill to determine which regions of the wAP continental shelf support successful reproduction. Additional simulations considered the extent to which these regions will be

modified by changing environmental conditions that may result from climate change. The areas where the descent-ascent cycle was successful were related to hot spot and spawning areas to obtain an estimate of the potential for local production to support krill populations of the wAP continental shelf.

The model used in this study is described in the next section. This is followed by results from the descent-ascent cycle for current and future conditions. The discussion section summarizes these results in terms of the Lagrangian particle tracking results (Chapters III, IV) and current understanding of Antarctic krill distributions on the wAP continental shelf.

5.2 METHODS

5.2.1 Embryo-larvae krill model

A one-dimensional temperature-dependent model (Hofmann et al., 1992) was used to simulate the descent-ascent cycle of an Antarctic krill embryo-larvae on the continental shelf of the wAP. The embryo sinking velocity and larva ascent rate depend on developmental stage, ambient temperature, and water density. The time-dependent sinking rate ($Sr(t)$, m s^{-1}) of the released embryo is given by:

$$Sr(t) = \frac{Dm^2}{18\nu} g(\frac{\rho_e}{\rho_w} - 1) \tag{8}$$

where Dm is the diameter of the embryo (μm), ν is the kinematic viscosity (1.787×10^{-6} m^2 s), g is the gravitational acceleration, ρ_e is the density of the embryo and ρ_w is the density of the ambient sea water (both in g cm^{-3}). The embryo changes it initial diameter (Dm_0) as it develops through the five embryonic stages of single cell to early gastrula (SC-eG), early gastrula to gastrula (eG-G), gastrula to early limb bud (G-eLB), early limb bud to late limb bud (eLB-lLB) and late limb bud to hatch (lLB-NI). The diameter for each stage is calculated as:

$$Dm_i(fD) = \begin{cases} Dm_0 + 6.605 + 104.936fD - 247.258fD^2 + 192.003fD^3 & \text{if } T < 0^oC \\ Dm_0 + 1.557 + 153.305fD - 355.408fD^2 + 260.204fD^3 & \text{if } 0^oC \leq T < 1^oC \\ Dm_0 + 0.460 + 150.220fD - 334.003fD^2 + 238.811fD^3 & \text{if } 1^oC \leq T < 2^oC \\ Dm_0 + 1.505 + 138.389fD - 325.546fD^2 + 260.204fD^3 & \text{if } 2^oC \leq T \end{cases}$$

where fD is the fraction of the embryonic development that has been completed and T is the ambient water temperature (°C). The initial diameter of the embryo (Dm_0) used in this study was 620 μm (Hofmann et al., 1992). Time step (t) used for the descent-ascent model is 1 h.

The developmental time for the embryonic stages was estimated as:

$$De_i(T) = \begin{cases} 1.22e^{-2.351T} + 24.147 & \text{for } SC \text{ to } eG \\ 33.3 - 10T & \text{if } T \text{ is } < 0^oC \text{ for } eG \text{ to } G \\ 33.3 & \text{if } T \text{ is } \geq 0^oC \text{ for } eG \text{ to } G \\ 11.851e^{-1.123T} + 62.404 & \text{for } G \text{ to } eLB \\ 110.15 - 14.8T & \text{for } eLB \text{ to } lLB \\ 37.258e^{-0.907T} + 108.644 & \text{for } lLB \text{ to } NI \end{cases}$$

where i designates the different embryonic stages.

The density of the embryo was calculated from the wet weight (Ww) and the diameter of each developmental stage (i) as:

$$\rho_e = \frac{6Ww_i}{\pi Dm_i^3}, \tag{9}$$

and wet weight was calculated using the diameter of the embryo as:

$$Ww_i(Dm) = \begin{cases} 0.6146Dm - 250.4528 & \text{for } SC \text{ to } eG \\ 0.4963Dm - 175.1451 & \text{for } eG \text{ to } eLB \\ 0.7539Dm - 340.0911 & \text{for } eLB \text{ to } lLB \\ 0.7539Dm - 311.4229 & \text{for } lLB \text{ to } NI \end{cases}$$

After the embryo hatches, the larva ascends with an ascent rate (m s^{-1}) that depends on ambient temperature and was calculated as:

$$Ar(t) = \begin{cases} -(0.011T + 0.208)Ps & \text{if } T \text{ is } < 0^oC \\ -(0.043T + 0.208)Ps & \text{if } T \text{ is } \geq 0^oC \end{cases}$$

where Ps is the fraction of time the larvae spends swimming, which was set to 30% (Hofmann et al., 1992; Hofmann and Hüsrevoğlu, 2003). As the larva ascends it develops from metanauplius through the nauplius stages and into a calyptopis I, the first feeding stage, and then into a calyptopis II stage. The development time is dependent on ambient temperature

$$Dl_i(T) = \begin{cases} 38.36e^{-1.41T} + 225.29 & \text{for } NI \text{ to } MN \\ 78.26e^{-1.53T} + 417.93 & \text{for } NI \text{ to } CI \\ 320.58e^{-1.1T} + 752.22 & \text{for } NI \text{ to } CII \end{cases}$$

During ascent, the larva is dependent on its internal carbon stores for energy because it is not feeding. The rate at which these are used is dependent on respiration rate. Embryo and larval respiration rates are given in $\mu l O_2$ h^{-1} and are expressed as a function of fraction of total development (fD) and are given by:

$$R_{embryo} = 0.8368 \times 10^{0.7195fD} \tag{10}$$

$$R_{larva} = 11.1030 \times 10^{0.8489fD} \quad (11)$$

Estimates of carbon used by the embryo and larva were calculated with a standard conversion constant of 0.385 μg carbon used per 1 μl of oxygen consumed (Quetin and Ross, 1989; Hofmann et al., 1992)

The one-dimensional ascent-descent model was implemented using temperature and density fields obtained with the wAP numerical circulation model (see Chapter III) for the time corresponding to the Antarctic krill reproductive season, which extends from December to March (Ross and Quetin, 1986; Spiridonov, 1995). Monthly averages of daily values were used as inputs for the descent-ascent model and the model was implemented at each grid point in the circulation model domain (e.g. 4-km resolution). Model diagnostics were the vertical displacement of the embryo-larvae particle in the water column and the development time from hatching to the calyptopis II stage. The time step (t) used for the descent-ascent model was 1 hour.

5.2.2 Present and future environmental simulations

The embryo-larvae descent-ascent model was used to simulate the effect of perturbed environmental conditions that may potentially occur on the wAP continental shelf as the result of climate warming. These conditions include increased wind speed (i.e. the westerlies) and increased transport of the ACC, both of which affect the volume of CDW transported onto the wAP continental shelf (Dinniman et al., submitted). For these simulations, the present day winds (1 January 2000–31 December 2002) were scaled by a constant factor, which increased wind speed by 20%. The ACC transport was increased by imposing a modified temperature and salinity gradient along the lateral open boundaries (Dinniman et al., submitted). The temperature and density fields obtained from the combined 20% wind increase and enhanced ACC transport simulations were input to the descent-ascent model.

5.3 RESULTS

5.3.1 Temperature and density during the present day reproductive season

The mean simulated surface temperature for the months corresponding to the Antarctic krill reproductive season showed that warming begins in the southwestern inner portion of Marguerite Bay in December and progresses northwards (Fig. 25). The maximum surface temperatures, 1-2°C, occurred in February (Fig. 25C). By March, surface temperatures in Marguerite Bay had cooled to just above 0°C. Surface temperatures in regions outside and to the north of Marguerite Bay remained above 1°C.

Simulated surface density remained relatively constant from December to March (Fig. 26). Freshwater inputs from sea ice melting and heating from solar radiation control the surface ocean density during the summer. The simulated vertical temperature and density profiles reproduced the three water masses that contribute to the hydrographic structure of the wAP continental shelf (Fig. 27). The AASW is characterized by potential temperatures between (-1.8 - 1.0°C) and densities < 27.4 (Klinck et al., 2004) and is present in the upper water column over the shelf. The temperature minimum, which indicates WW occurs below the AASW between 100 and 200 m. Below WW, CDW, characterized by temperatures above 1°C, floods the wAP shelf.

5.3.2 Descent-ascent cycle and hatching depth

The density of krill embryos is higher than that of seawater (Marr, 1962; Quetin and Ross, 1984) and, as a result, the embryos begin sinking immediately after spawning. The sinking velocity of the simulated embryo was variable, which is reflected in the pattern of the vertical trajectory (Fig. 28). Initial sinking rates were fast, 184.9

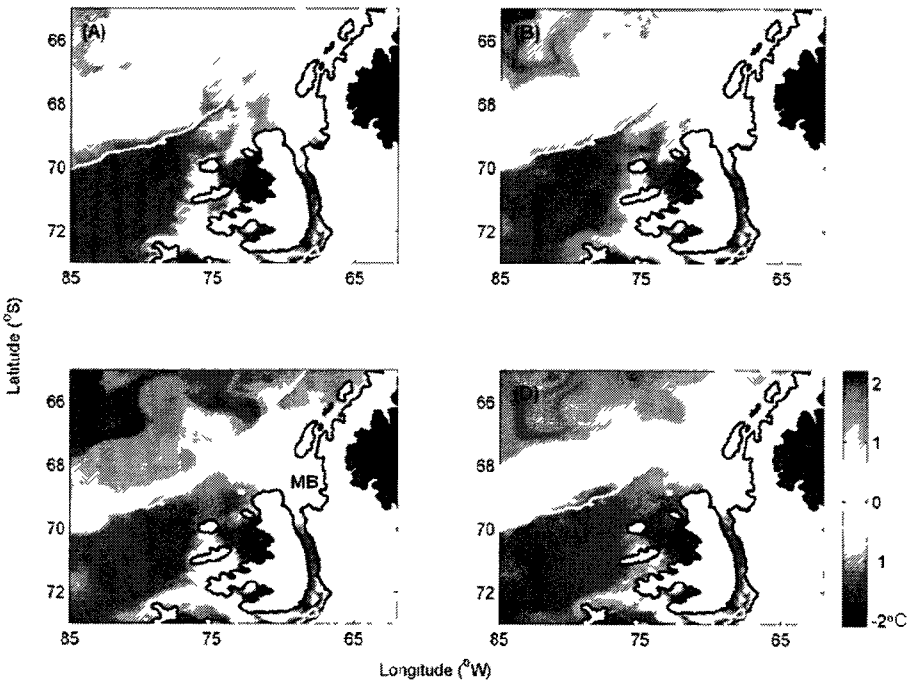

Fig. 25. Monthly-averaged simulated sea surface temperature distribution for (A) December, (B) January, (C) February, and (D) March. The 800-m isobath (white line) indicates the location of the shelf break and the deep areas along Marguerite Trough.

to 190.1 m d^{-1}, which moved the embryo to depths of about 250 m in 2-3 days (Fig. 28B-E). At this point, the embryo had reached the gastrula stage and the sinking rate decreased, thus retaining the embryo in the upper part of CDW (see Fig. 27). The embryo remained in the warmer CDW for 3-4 days where developmental rate was increased. During the last 2-3 days of embryonic development, the sinking rate again increased to 181.4 to 185.8 m d^{-1}. Hatching depths of the embryo were between 600 m and 700 m (Fig. 28B-E).

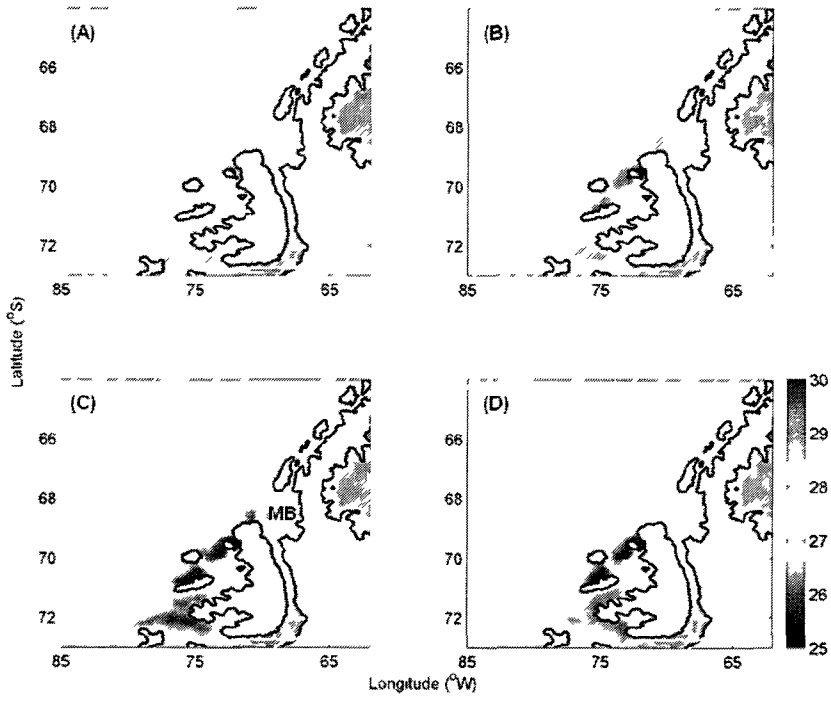

Fig. 26. Monthly-averaged simulated sea surface density (kg m^{-3}) distribution for (A) December, (B) January, (C) February, (D) March. The 800-m isobath (white line) indicates the location of the shelf break and the deep areas along Marguerite Trough.

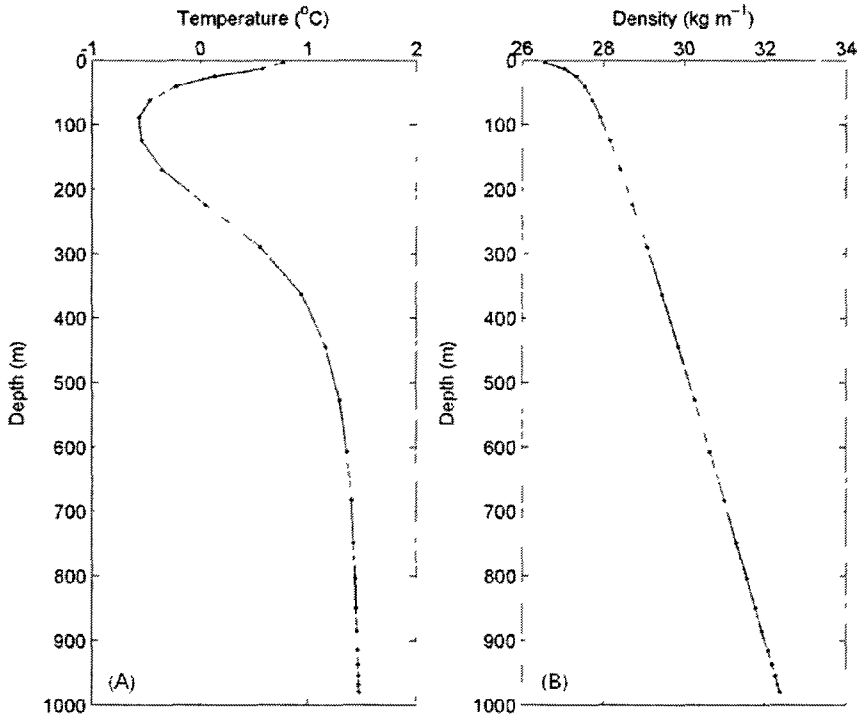

Fig. 27. Simulated vertical distribution of (A) temperature and (B) density from a site at Marguerite Bay on the wAP continental shelf. This profile represents the mean for the austral summer (December to March).

Following hatching the larva ascended, reaching the sea surface in 10 to 13 days. For an embryo spawned inside Marguerite Bay, the descent-ascent cycle took approximately 14 days (Fig. 28A, D, E). The embryo portion of the cycle took 4-5 days and hatching occurred around 600 m, which is above or just at the bottom for most of this region of the wAP continental shelf. After hatching larval ascent took about 10 days and the larva reached the surface as a calyptopis I stage or first feeding stage. South of Marguerite Bay the descent-ascent cycle took approximately 3 days more. The simulated for carbon content showed that internal carbon stores sustain the embryo

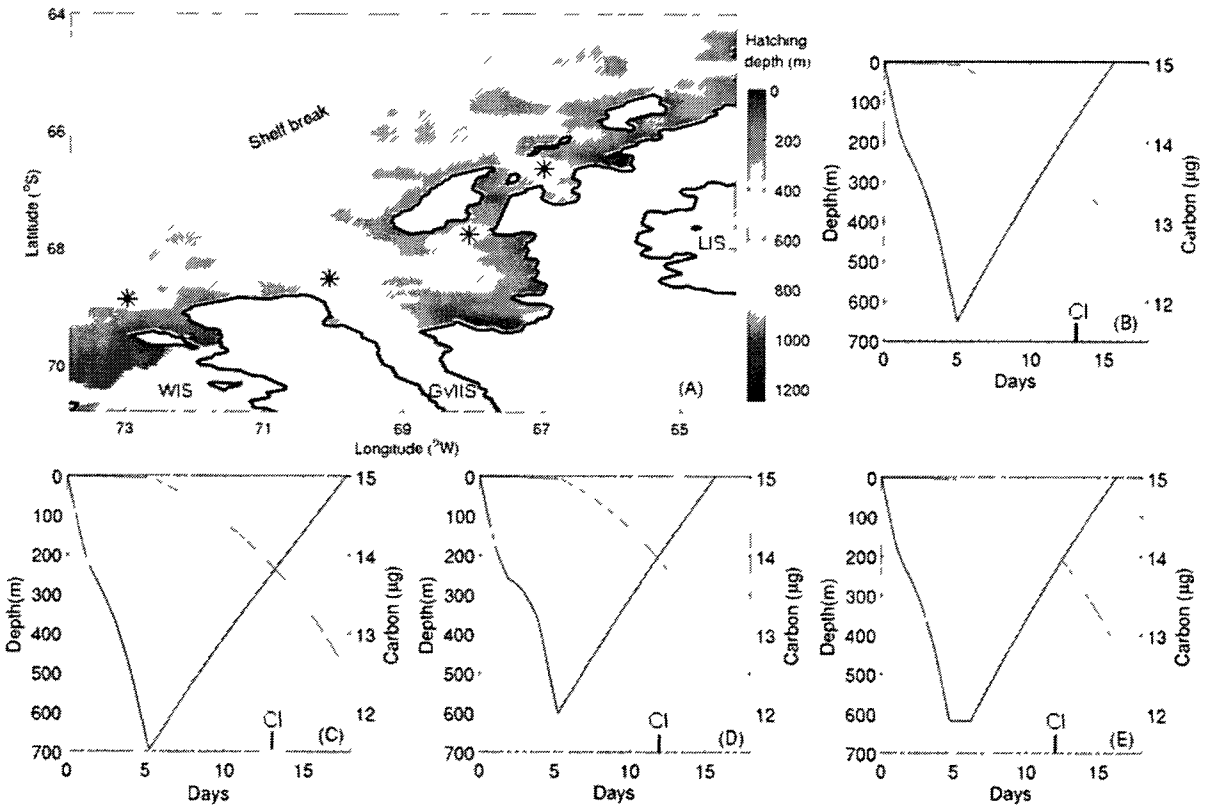

Fig. 28. (A) Distribution of simulated hatching depths for krill embryos released over the wAP continental shelf at each point of the circulation model and the locations of the vertical profiles for the descent-ascent cycle for embryo-larva particles released in (B) Crystal Sound, (C) west of Alexander Island, (D) Marguerite Trough, and (E) Laubeuf Fjord. The Wilkins Ice Shelf (WIS), George VI Ice Shelf (GVIIS) and Larsen Ice Shelf (LIS) and 800-m isobath (solid gray line) are shown. The calyptopis I stage is abbreviated as CI.

and larvae throughout its descent-ascent until is able to begin feeding. Water temperatures in this area are 0.5°C colder (Fig. 29), which showed the embryo development and hence sinking rate. The result was that hatching occurs deeper at about 700 m (Fig. 28C). The ascent time was longer because of slower development, resulting in the cycle being completed in 18 days (Fig. 28C). The Crystal Sound region on the inner shelf north of Marguerite Bay supported completion of the descent-ascent cycle in 15.5 days (Fig. 28B). This region of the wAP continental shelf has warmer temperatures in the upper water column and is influenced by warm CDW below 200 m (Fig. 29).

The simulated hatching depth was relatively uniform along and beyond the shelf break (Fig. 28A). The bottom depth in these regions is deeper than the hatching depth and does not provide a constraint to successful completion of the descent-ascent cycle. For some parts of the wAP continental shelf, the sinking embryo can encounter the bottom before hatching. The descent-ascent cycles along the shelf resulted in hatching around 450 and 700 m (Fig. 28B-E). Over Marguerite Trough where depths are more than 900 m, the embryo hatched at 600 m and cycle was completed in 15 days. At the Laubeuf Fjord site inside Marguerite Bay (Fig. 28A, E), water column depth is 620 m and the embryo reached the bottom before hatching and hatched after 24 hours on the bottom.

The time required for an embryo-larvae particle to reach calyptopis I was 13-15 days along Marguerite Trough and in the deeper regions of the wAP continental shelf (Fig. 30). Shelf regions with shallow bathymetry limited development to 10 days and the sinking embryo encountered the bottom before hatching.

In the biological hot spot regions, development from embryo to calyptopis I took 14-15 days (Fig. 30). The bathymetry and circulation of these regions favors retention, especially below 200 m. Residence times for particles at 300 m (inset table, Fig. 30) are longer than those at the surface. The deeper residence times for the

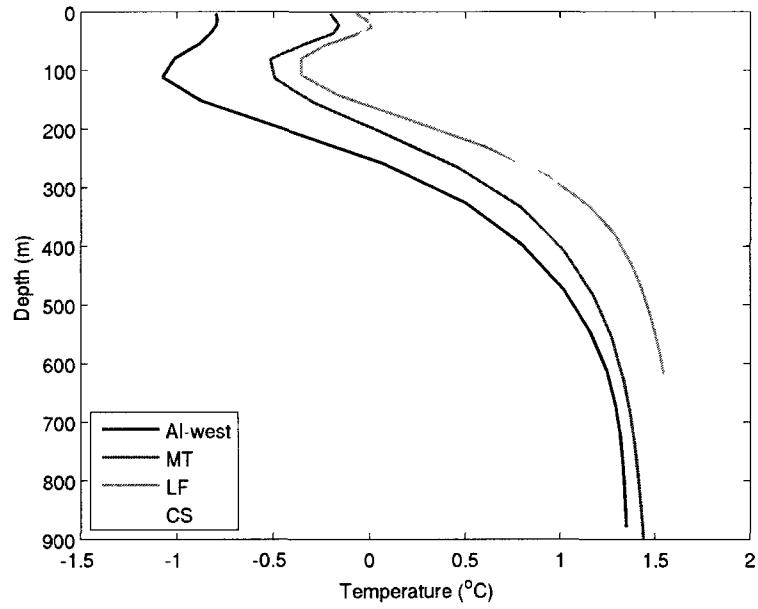

Fig. 29. Simulated vertical temperature profiles at the four locations that correspond to the descent-ascent cycles shown in Fig. 28.

Alexander Island and Laubeuf Fjord areas are almost 3 to 4 times the required time to complete development to calyptopis I. Thus, the retention times for these regions allowed the descent-ascent cycle to be completed. The average summer residence time for the Crystal Sound biological hot spot region was 18 days (see Table 6, Chapter III), which is longer than the time needed to complete development to calyptopis I and may also favor local retention.

Under current environmental conditions, regions where the sea floor depth exceeded hatching depth highlighted areas of the wAP continental shelf where the descent-ascent cycle can be completed prior to the embryo reaching the bottom (Fig. 31). In regions offshore of the shelf break, in Bransfield Strait at the northern tip of the Antarctic Peninsula, and an area south of Elephant Island, bathymetry does not constrain the descent-ascent cycle. However, the Bransfield Strait and Elephant

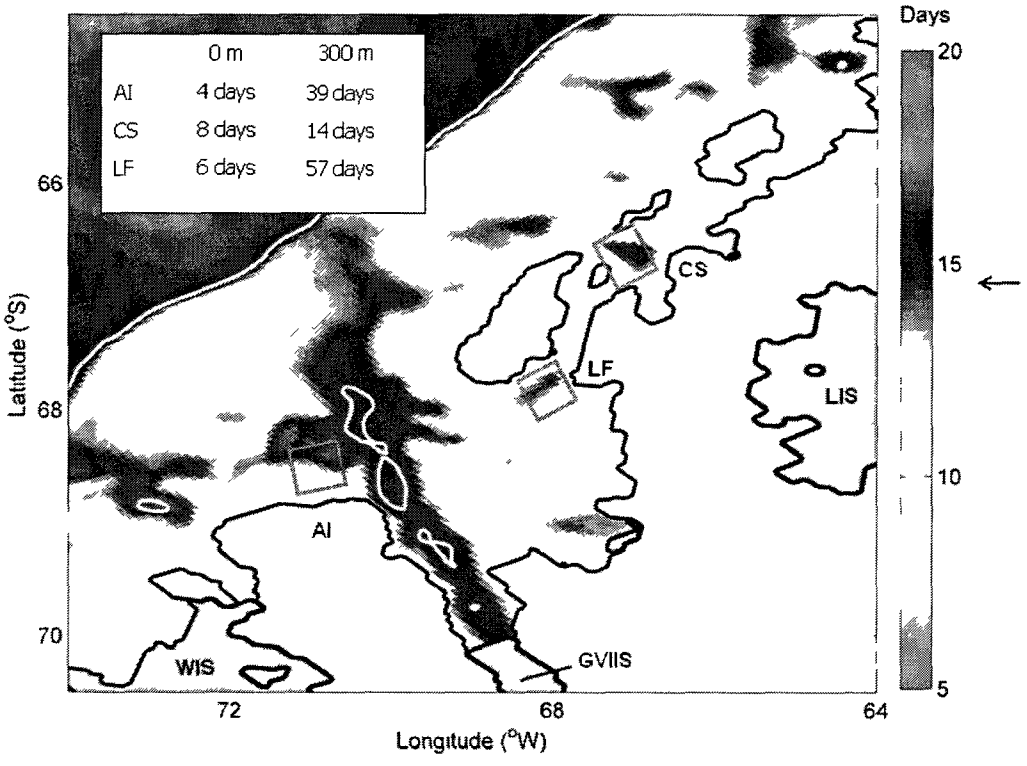

Fig. 30. Time (days) required for the simulated embryo-larvae particles to complete the descent-ascent cycle. The time required for development to the calyptopis I in the Alexander Island (AI), Crystal Sound (CS) and Laubeuf Fjord (LF) hot spot regions (red boxes) is indicated on the scale (black arrow). The table shows the residence times for particles at surface and 300 m that were obtained from the Lagrangian simulations presented in Chapter III (e.g. Table 6). The 800-m isobath (white line) shows the location of the shelf break and deep areas along the shelf.

Island regions are influenced by cold water coming from the Weddell Sea, and temperatures <-1°C delay development of the sinking embryo and increase hatching depths (Hofmann et al., 1992). Also larval mortality increases with exposure to temperatures of <-1°C for long periods during the calyptopis I stage (Ross et al., 1988). Throughout the mid-shelf of the wAP continental shelf are areas where the bottom

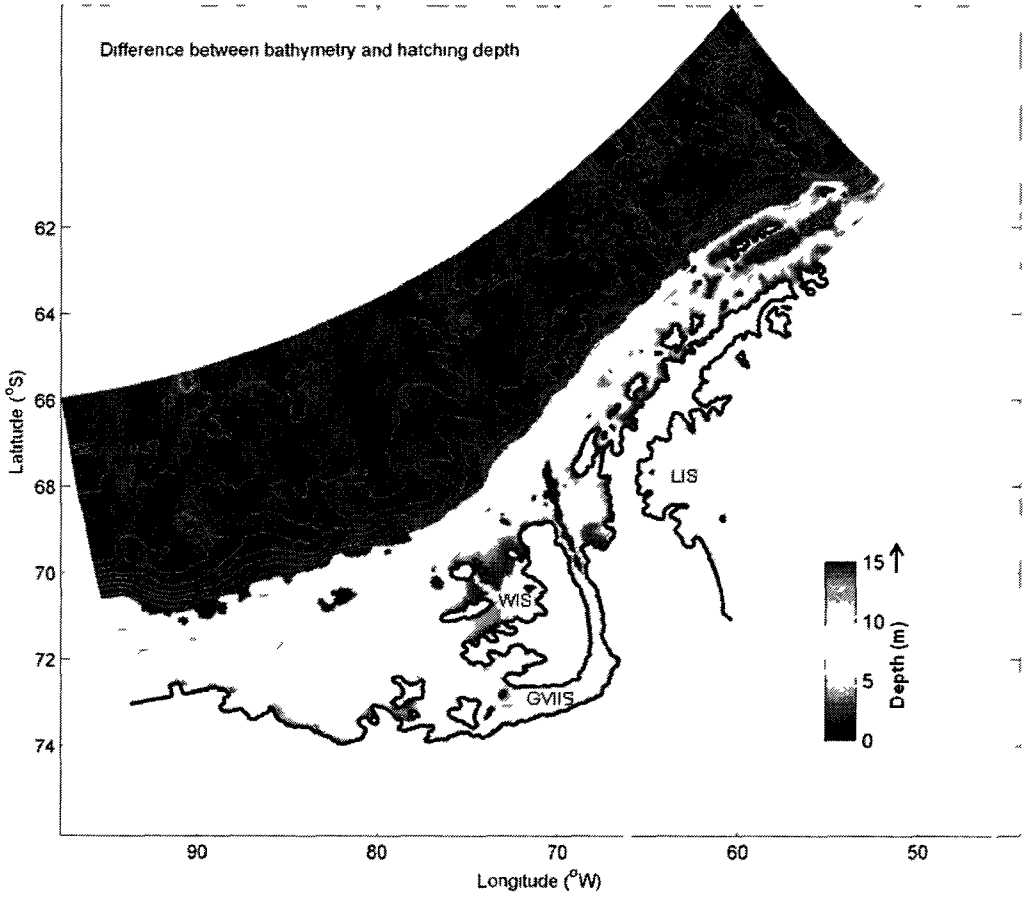

Fig. 31. Difference between the wAP continental shelf bathymetry and simulated embryo hatching depth Only differences of up to 15 m are indicated (dark red) because of the large differences in the deeper waters off the shelf. Bathymetry 500-m intervals (gray lines) and the Wilkins Ice Shelf (WIS), George VI Ice Shelf (GVIIS) and Larsen Ice Shelf (LIS) are shown.

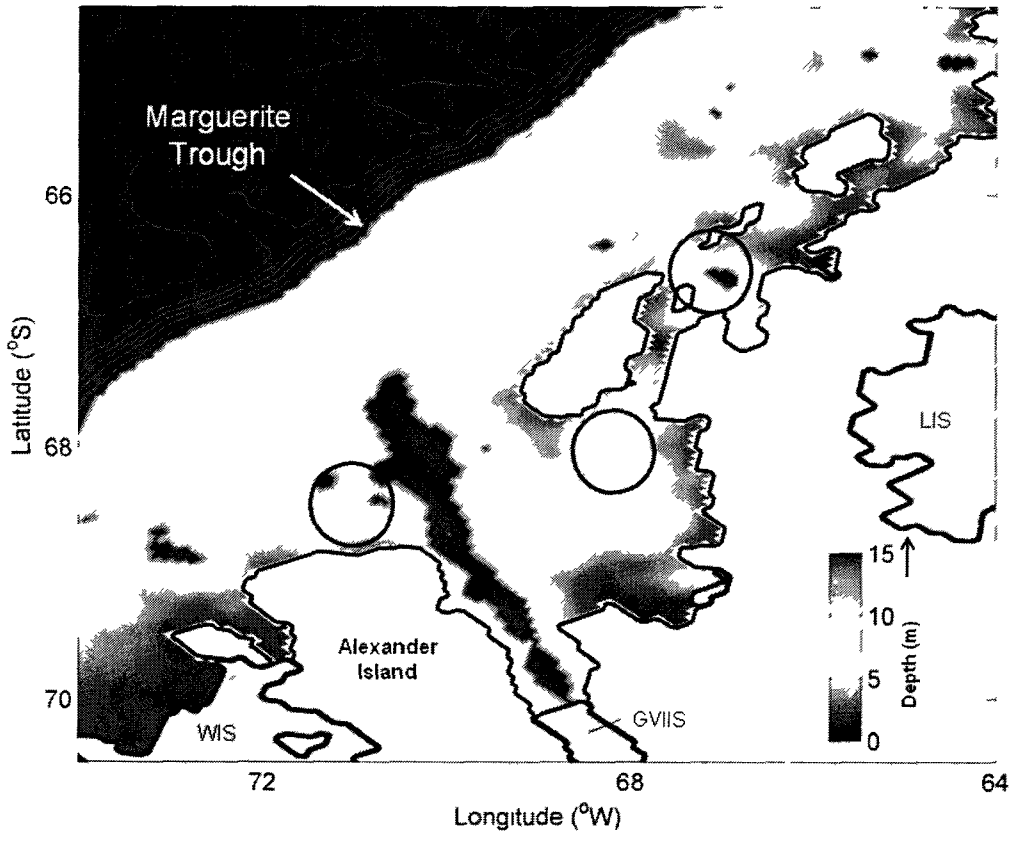

Fig. 32. Difference between Marguerite Bay bathymetry and simulated embryo hatching depth. Only differences of up to 15 m are indicated (dark red) because of the large differences in the deeper waters off the shelf. Location of biological hot spots (black circles) are shown. Bathymetry at 500-m intervals (gray lines), Marguerite Trough, and the Wilkins Ice Shelf (WIS) and George VI Ice Shelf (GVIIS) are shown.

depth exceeds hatching depth by 10-15 m. Along the inner shelf some regions where the difference is more than 10 m occur, but these are limited in extent (Fig 31).

Within the Marguerite Bay region, areas where the bottom depth exceeds the embryo hatching depth occur along Marguerite Trough and in the biological hot spots (Fig. 32). Smaller additional regions occur on mid-shelf off Alexander and Charcot Islands and off the northern end of Adelaide Island (Fig. 32). These additional areas

were also observed to have low export of simulated particles and limited connectivity with other shelf regions (see Table 14, Fig. 24). Residence times in both regions would support local development to calyptopis I.

5.3.3 Future environmental conditions scenarios

Potential perturbations to the descent-ascent cycle were tested using vertical distributions of temperature and density obtained from simulations with stronger winds and a stronger ACC transport (Dinniman et al., submitted). These modified conditions resulted in transport of more CDW onto the wAP continental shelf and more vertical mixing of the warmer water into the upper water column.

The difference in simulated embryo hatching time obtained for present and future conditions showed little change over most of the mid and outer regions of the wAP continental shelf (Fig. 33A). The only region where faster development (3-5 days) occurred was in the inner shelf to the south of Alexander Island. Two areas showed slight increases (2-3 days) in embryo development time (Fig. 33B). The largest was found around Anvers Island a smaller region occurred in the inner part of Marguerite Bay.

Similarly, hatching depth showed little change from present conditions (Fig. 34A, B). The largest differences occurred along Marguerite Trough and in the Crystal Sound hot spot regions where hatching depth shallowed by 10 to 20 m (Fig. 34B). Isolated regions of the wAP continental shelf showed increased hatching depths, but these were small relative to the overall shelf area (Fig. 34A, B).

Over the entirety of the wAP continental shelf the time required to complete the descent-ascent cycle differed only slightly between present and future conditions (Fig. 35A). Faster times occurred in the southern part of the wAP shelf near Alexander Island. Longer time occurred around Anvers Island (Fig. 35B).

The overall structure of the descent-ascent cycle is only slightly modified in limited

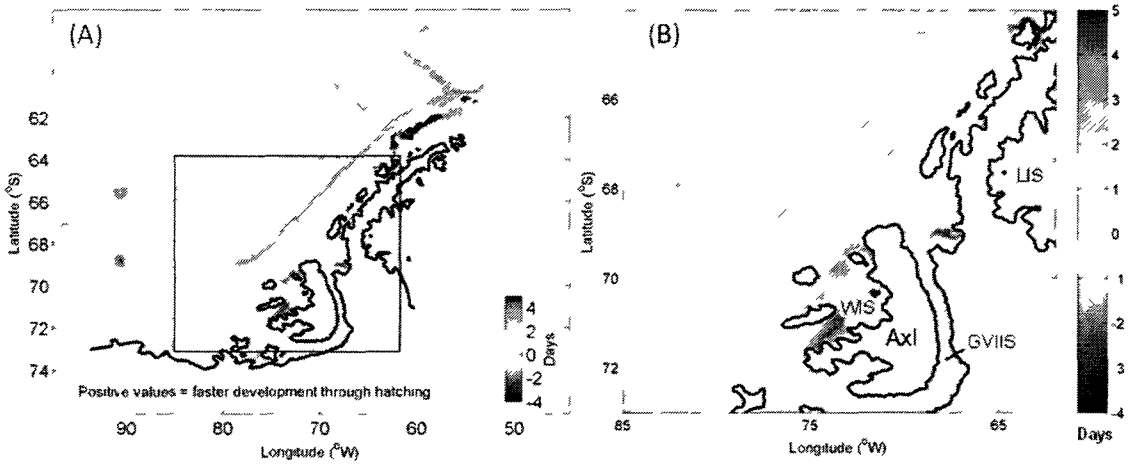

Fig. 33. Difference in simulated embryo hatching time calculated from simulations using temperature and density fields obtained for future (enhanced winds and ACC transport) and present environmental conditions for all of the (A) wAP model domain and (B) the Marguerite Bay region. Positive (negative) values indicate faster (slower) development of the embryo and less (more) time until hatching. Bathymetry at 500-m intervals (gray lines) and the Wilkins Ice Shelf (WIS), George VI Ice Shelf (GVIIS), Larsen Ice Shelf (LIS), and Alexander Island (AxI) are shown.

regions by the projected future changes in temperature and density structure on the wAP continental shelf. However, the possible important consequence of the projected future changes may be by modification of the biological hot spot regions on the wAP continental shelf. Thus, the flow fields from the future state simulations were used for Lagrangian particle tracking simulations. Inputs to the hot spot regions then were estimated from the particles that were transported to these regions (Fig. 36).

For the projected future circulation distributions, the regions of the mid and outer wAP continental shelf that contribute to the Crystal Sound hot spot differed from what was obtained for current conditions (Fig. 36A, D vs. 10A, D). Inputs still originate in the Bellingshausen Sea region and along the shelf break; however, a larger

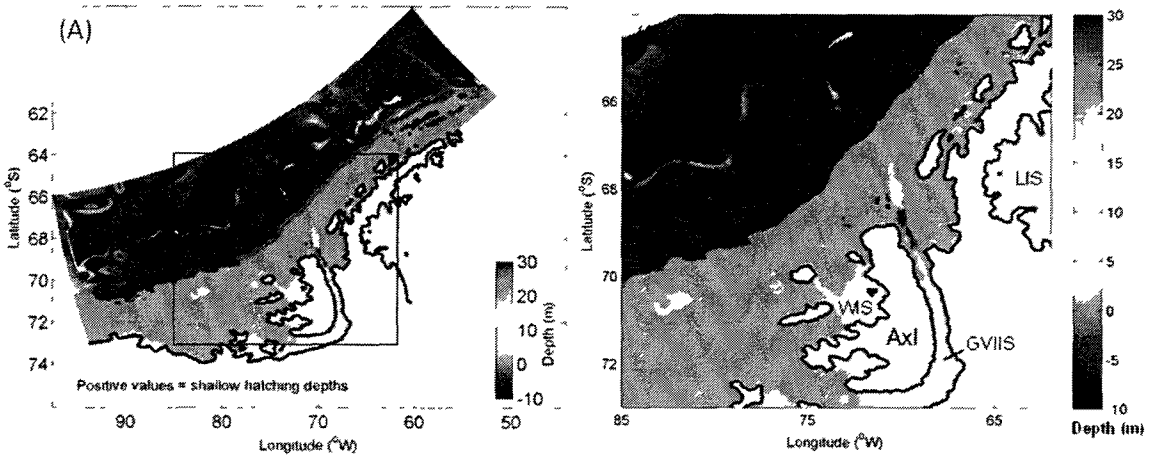

Fig. 34. Difference in simulated embryo hatching depth calculated from simulations using temperature and density fields obtained for future (enhanced winds and ACC transport) and present environmental conditions for all of the (A) wAP model domain and (B) the Marguerite Bay region. Positive (negative) values indicate shallower (deeper) embryo hatching depth. Bathymetry at 500-m intervals (gray lines) and the Wilkins Ice Shelf (WIS), George VI Ice Shelf (GVIIS), Larsen Ice Shelf (LIS), and Alexander Island (AxI) are shown.

percentage of particles were transported to this hot spot (40-80%) compared with the 20-60% that arrived for the present conditions simulation. The Alexander Island hot spot received inputs from the continental shelf area southwest of Marguerite Bay (Fig. 36B, E), similar to the inputs observed in the present conditions simulation. Additional inputs from regions along Marguerite Trough reached Alexander Island with the circulation produced by the future conditions. These new sources provide inputs (40-60%) from a common transport pathway that is cyclonic around Marguerite Bay (Fig. 36B, E). The Laubeuf Fjord region showed similar patterns of inputs for future and present environmental conditions (Fig. 10, Fig. 36C, F).

Sea ice distribution is an important factor affecting the reproductive success of

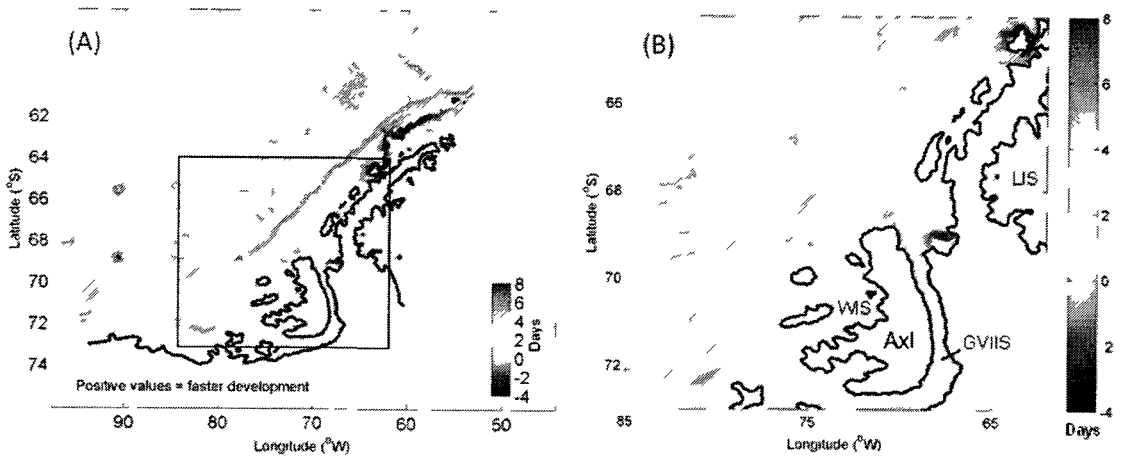

Fig. 35. Difference in time required to complete the descent-ascent cycle calculated from simulations using temperature and density fields obtained for future (enhanced winds and ACC transport) and present environmental conditions for all of the (A) wAP model domain and (B) the Marguerite Bay region. Positive (negative) values indicate faster (slower) cycle completion times. Bathymetry at 500-m intervals (gray lines) and the Wilkins Ice Shelf (WIS), George VI Ice Shelf (GVIIS), Larsen Ice Shelf (LIS), and Alexander Island (AxI) are shown.

Antarctic krill (Quetin and Ross, 2001). The simulated averaged winter sea ice distribution for present conditions showed 30%-50% coverage over much of the wAP continental shelf, with about 80% in Marguerite Bay and the area to the west towards the western Bellingshausen Sea (Fig. 37A). The simulation with the future environmental conditions resulted in reduced average winter sea ice coverage (Fig. 37B). Marguerite Bay was not completely covered by sea ice and in the western Bellingshausen Sea the 80% coverage boundary has moved onto the shelf (e.g. onshore from the 800-m isobath). The largest reduction in sea ice coverage was along the inner shelf north of Marguerite Bay and along the mid and outer shelf west of Alexander Island. The northern side of the wAP was more affected. Between Renaud

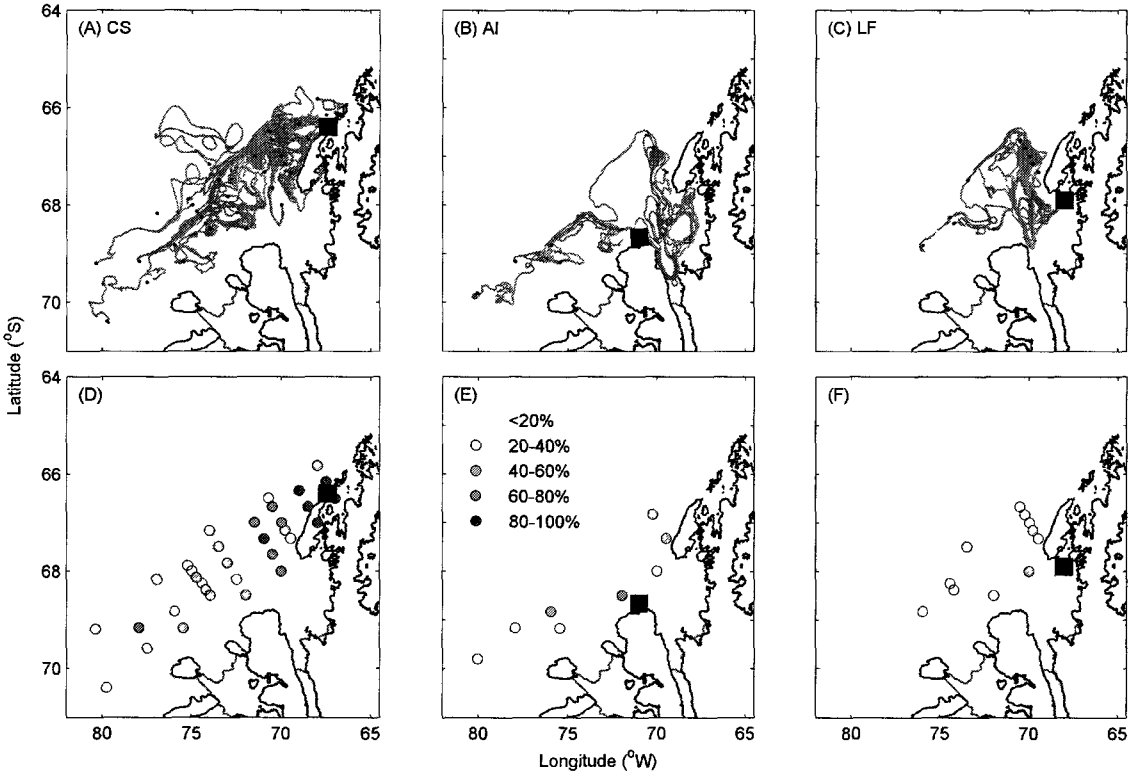

Fig. 36. Trajectories of simulated floats (gray lines) and the distribution of the source regions and associated percentage of particles that were provided to the (A, D) Crystal Sound (CS), (B, E) Alexander Island (AI), and (C, F) Laubeuf Fjord (LF) biological hot spot regions (indicated by filled square). Only the trajectories that originated in areas with contributions to the hot spots greater than 20% are shown. The simulated floats were released at 300 m (release point indicated by •) at 10-day intervals for 60 days in a grid of transects that extended across the continental shelf break (shown in Figure 2). The bottom bathymetry (m) is shown by the light gray lines.

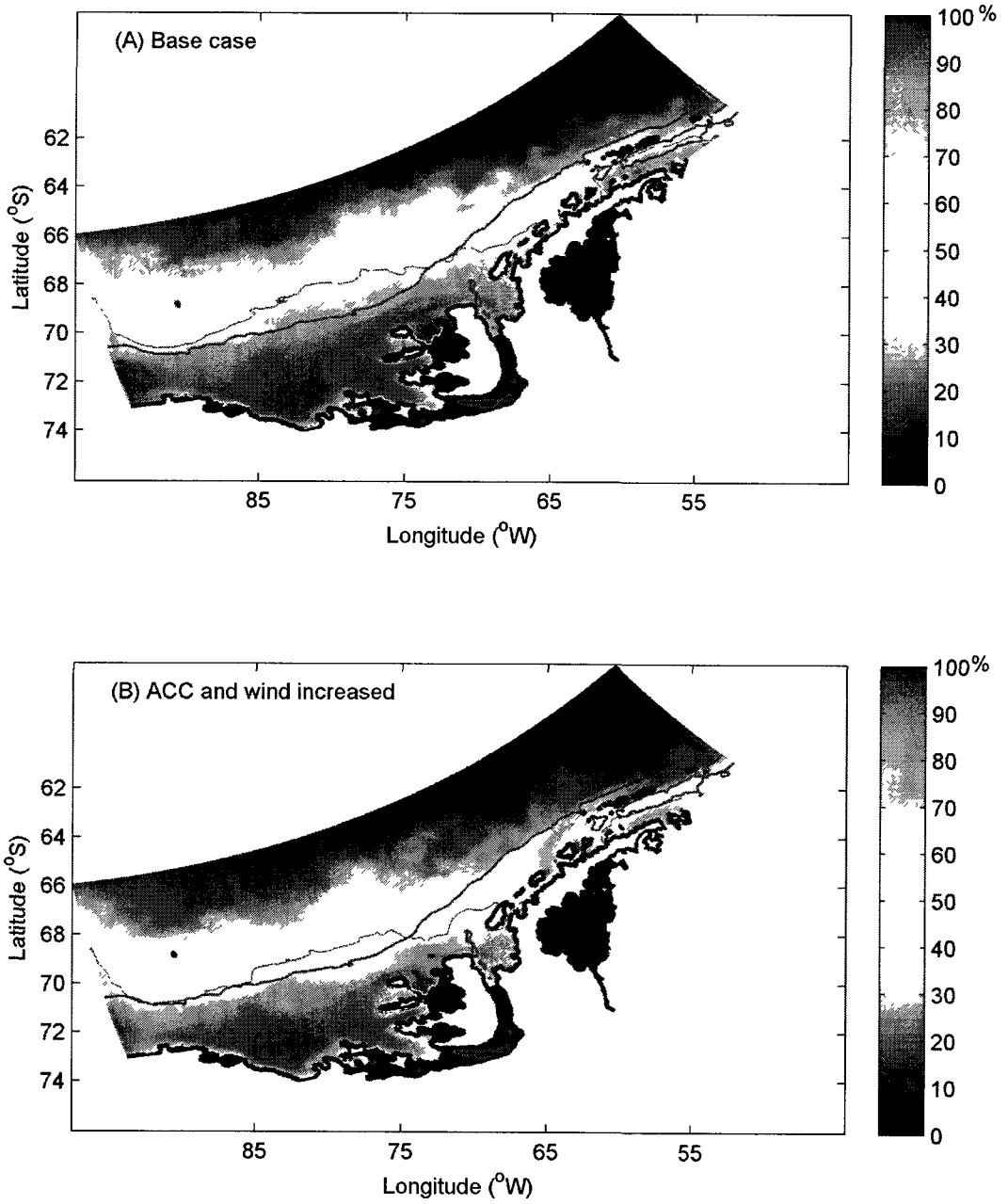

Fig. 37. Simulated average percent winter sea ice cover obtained for (A) present conditions and for (B) future conditions of increased winds and enhanced ACC transport. The 80% sea ice cover (black thin line) and 800-m isobath (black thick line) are shown.

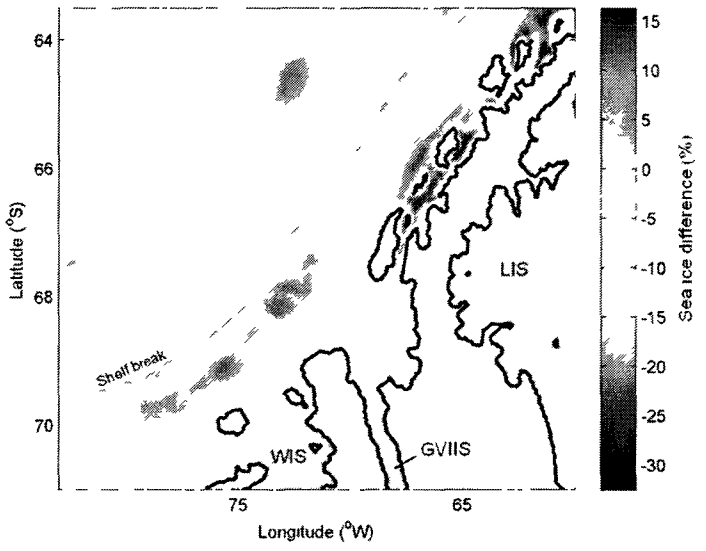

Fig. 38. Percent difference in the simulated winter sea ice coverage obtained for present conditions and future conditions of increased wind and enhanced ACC transport. Positive (negative) values indicate more (less) sea ice coverage for future environmental conditions. The Wilkins Ice Shelf (WIS), George VI Ice Shelf (GVIIS), Larsen Ice Shelf (LIS) and 800-m isobath (gray line) are shown.

Island and the Gerlache Strait the sea ice coverage decreased about 20%. Bransfield Strait also showed less sea ice cover, decreasing from 75% to 60%.

The difference in the mean winter sea ice coverage between future and present conditions around Marguerite Bay (Fig. 38) showed a 30% reduction in the Crystal Sound hot spot region. The Laubeuf Fjord hot spot region showed a reduction of approximately 15%. The Alexander Island hot spot and in general all the inner shelf north of Alexander Island showed a slight increase in sea ice cover (2-3%). The difference in the summer average distribution of sea ice between future and present conditions (Fig. 39) showed reduced sea ice south and west of the Marguerite Bay. A 20% reduction was observed along the north side of Alexander Island and at the

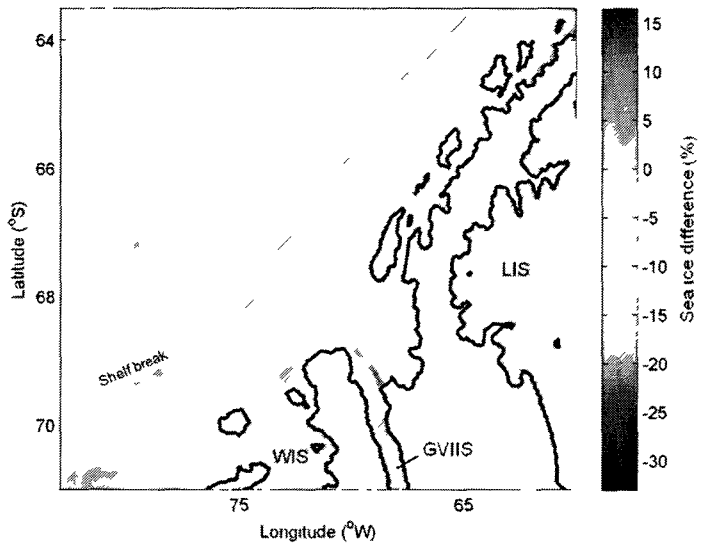

Fig. 39. Percent difference in the simulated summer sea ice coverage obtained for present conditions and future conditions of increased wind and enhanced ACC transport. Positive (negative) values indicate more (less) sea ice coverage for future environmental conditions. The Wilkins Ice Shelf (WIS), George VI Ice Shelf (GVIIS), Larsen Ice Shelf (LIS) and 800-m isobath (gray line) are shown.

entrance of George VI Sound.

The trajectories of the Lagrangian particles (e.g. Fig. 10, 11) showed that the areas with largest winter sea ice reductions are the same as those that provide particles to the biological hot spot regions (Fig. 40). The time scales of these particles are variable but are generally consistent with developmental times for krill larvae spawned along the mid and outer shelf, and towards the Bellingshausen Sea area (Fig. 41). The frequency distribution of the particles reaching the hot spots with times matching the developmental time scales for larvae and 1-year old Antarctic krill, showed that 17.6% of the particles reaching any of the hot spots corresponded to krill larvae from early stages (N1-C3) and 25.2% corresponded to larvae in the furcilia stage (Fig. 41).

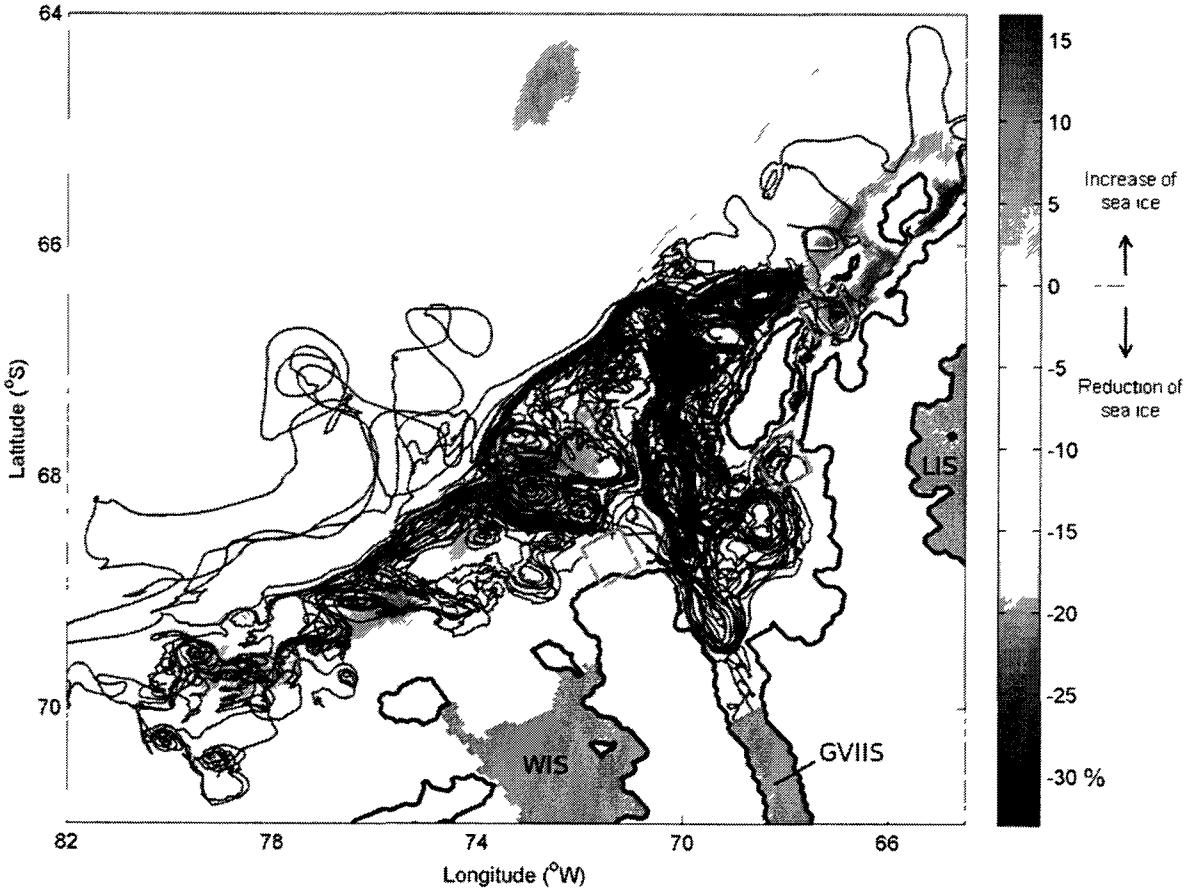

Fig. 40. Simulated trajectories (black lines) showing inputs to the biological hot spots regions overlaid on the percent difference in winter sea ice coverage obtained from the future and present environmental condition simulations. Positive (negative) values indicate more (less) sea ice under future environmental conditions of increased winds and enhanced ACC transport. The Wilkins Ice Shelf (WIS), George VI Ice Shelf (GVIIS), Larsen Ice Shelf (LIS) and 800-m isobath (gray line) are shown.

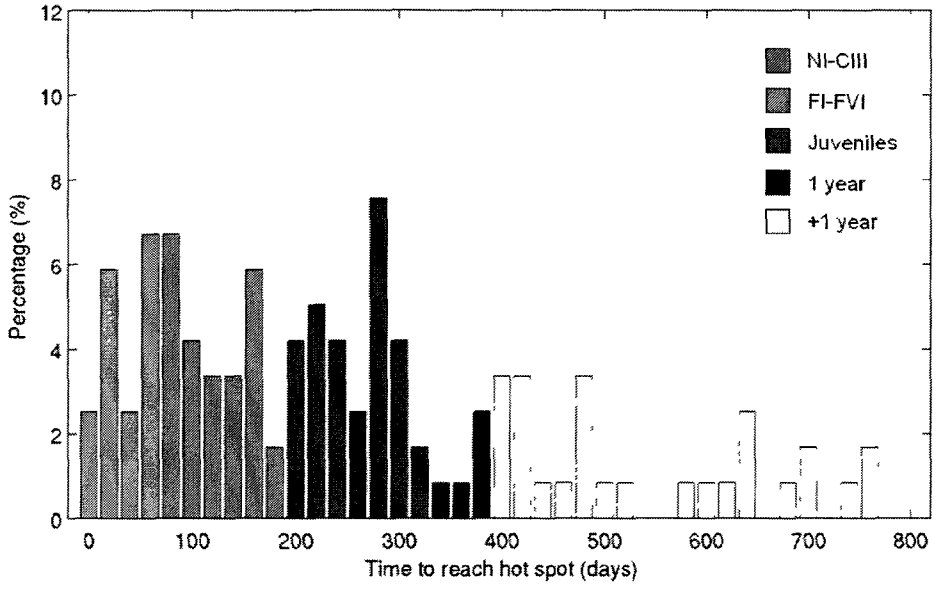

Fig. 41. Frequency distribution of the transport time for the simulated particles that provided inputs to the biological hot spots regions. The transport times were mapped into Antarctic krill life stages that correspond to Nauplius to Calyptopis (dark gray bars), Furcilia stages (green bars), 1 year old krill (black bars) and +1 year old krill (light gray bars) using the developmental times given in Table 10.

Juveniles (>191 days and <1 year old) correspond to 29.4% of the particles reaching the hot spots. This was the largest group reaching the hot spots after transport across the wAP shelf. These results imply that 72.2% of the progeny (larval and juvenile stages) resulting from summer reproduction along the wAP shelf would have to overwinter in areas where the highest reduction of sea ice was observed.

5.4 DISCUSSION

5.4.1 Controls by shelf bathymetry and sea ice

The descent-ascent cycle simulations showed that successful completion of this cycle is possible on the wAP continental shelf. Over most of the wAP shelf the first feeding stage of the larvae was able to return to the sea surface. The assumption that the embryo is nonviable or consumed if it hits the bottom prior to hatching places a constraint on the areas of the wAP shelf that will support successful completion of the descent-ascent cycle. In most simulations, hatching occurred between 400-600 m. Areas of the wAP shelf that are deeper than 500 m are limited to about 30% of the shelf area (Hofmann and Hüsrevoğlu, 2003), implying that only a small portion of this shelf may contribute to Antarctic krill populations.

On the wAP continental shelf the descent-ascent cycle takes about 15 days. The presence of CDW on the shelf (Klinck et al., 2004; Dinniman and Klinck, 2004) accelerates embryo and larvae development (Ross et al., 1988) and assures the successful completion of the cycle in the deeper regions. The shelf region north of Adelaide Island, which supported successful hatching of simulated embryos, is coincident with observed high abundances of Antarctic krill nauplii during the austral summer (Makarov et al., 1990). Eggs were also observed on the shelf, although not in high numbers (50 ind m^{-2}) (Makarov et al., 1990).

Average sea ice duration and extent have been identified as important contributors to krill reproduction and recruitment success (Loeb et al., 1997; Siegel and Loeb 1995; Ross et al., 1996; Quetin and Ross, 2003; Ducklow et al., 2007). The recruitment index of Antarctic krill is correlated with the timing of sea ice advance, with high recruitment occurring when sea ice advances earlier in the fall (Quetin et al., 1996; Quetin and Ross, 2003) and the duration and extent of winter sea ice affects recruitment success and reproduction (Quetin and Ross, 1991; Siegel and Loeb, 1995;

O'Brien et al., 2011). The simulated winter sea ice distributions obtained for future conditions showed a decrease in sea ice in the areas of wAP shelf that are coincident with the biological hot spots and the areas that provide inputs to these regions. Sea ice distribution and extent on the wAP sea ice is already changing with the advance occurring later in the fall and retreat occurring earlier in the spring (Smith and Stammerjohn, 2001; Parkinson, 2002). The results from this study suggest that recruitment success of krill populations on the wAP shelf will be affected by the projected future changes in winter sea ice distribution and extent.

5.4.2 Krill reproduction on the shelf

Observations of the abundance and distribution of Antarctic krill during the SO GLOBEC field studies suggested that Antarctic krill reproduction occurs in onshore and offshore areas of the wAP shelf (Ashjian et al., 2004; Daly, 2004; Lawson et al., 2004; Pakhomov et al., 2004; Wiebe et al. 2011). Simulations of the descent-ascent cycle suggested that successful reproduction can occur over the deeper regions of the wAP shelf (e.g. Fig. 28). The greatest abundance and biomass of larval krill were observed along the wAP mid shelf to the west of Adelaide Island during fall (Ashjian et al., 2004). This area is coincident with the area with older stages of krill larvae that originated from particles released in Marguerite Bay southwest of Adelaide Island (e.g. Fig. 24D). These deeper portions of the shelf were also where the descent-ascent cycle was successful.

Additional support for local reproduction of Antarctic krill on the wAP shelf comes from observed spatial distributions of zooplankton distribution and abundance (Marrari et al., 2011). Juvenile krill (one year old) were abundant (132 ind m^{-3}) on the inner shelf around Marguerite Bay, indicating successful recruitment from larvae produced the previous year (Daly, 2004). The depth distribution of Antarctic krill larvae during fall in Laubeuf Fjord (Daly, 2004) showed that late furcilia stages were

abundant in the upper 50 m. The Laubeuf Fjord region is a biological hot spot and also one that retained particles for over a year (e.g. Table 8). It is also one of the deeper regions of the innershelf where reproduction can successfully occur (e.g. Fig. 28). Moreover, net samples from the austral fall and winter showed that krill dominated the zooplankton biomass in the Laubeuf Fjord region between 50 and 100 m (Ashjian et al., 2004). This area also showed high backscattering returns (from acoustic surveys), which are related to zooplankton abundance (Lawson et al., 2004).

The vertical distribution and abundance of krill larvae obtained from net samples made in fall (Wiebe et al., 2011) showed high abundances of different life stages across the wAP shelf. Off Alexander Island, high abundances of calyptopis (756 ind m^{-2}) were observed. This region is also deep which allows completion of the descent-ascent cycle and therefore local reproduction. In this region the northeasterly flowing shelf currents along the outer part of Alexander Island turn across the wAP shelf along the southern flank of Marguerite Trough north of the hot spot off Alexander Island (e.g. Fig. 4). Thus, the simulated Lagrangian particle experiments showed that Alexander Island received inputs primarily from the adjacent shelf region from the same area where the highest number of calyptopis were observed. Analysis of Video Plankton Recorder measurements made during fall showed that larval krill were present across the entire shelf (Ashjian et al., 2008). Also, high larval abundances were found at depth along a transect that crossed Marguerite Bay, particularly along the portion that crossed Marguerite Trough (Ashjian et al., 2008). Observations from a deep water remotely operated vehicle made during the austral summer showed gravid females above the seabed in Marguerite Trough (Clarke and Tyler, 2008). These adult krill were actively feeding and exoskeletons resulting from molting that may have occurred as the result of spawning were observed. These observations support the conclusion from the simulations that this area of the wAP shelf can support local reproduction and subsequent retention of the early life stages of Antarctic krill.

5.4.3 Environmental change effect on lower and higher trophic levels

The habitat of the wAP continental shelf is structured by CDW and sea ice, which in turn have large effects on the ecosystem of the region (Hofmann and Murphy, 2004; Hofmann et al., 2008, 2011; Stammerjohn et al., 2008a). Changes in the wind speed are already documented for the Southern Ocean (Russell et al., 2006). Thus, perturbations to CDW and sea ice distribution and extent that may arise via global change could have significant effects on the biological production of this region. The simulation with increased winds showed that the volume of CDW introduced to the wAP increased as did the vertical mixing of this water into the upper water column (Dinniman et al., submitted). The consequences of this for sea ice were significant, resulting in reductions of summer and winter sea ice extent (Dinniman et al., submitted). However, the effect of this modified circulation had little effect on the descent-ascent cycle. Differences in hatching and developmental times between present and future conditions were small, with the effects confined to limited areas of the shelf. Thus, the ability for successful completion of the descent-ascent cycle on the wAP shelf will not be significantly altered for the projected future conditions used in this study. However, a reduction in winter sea ice has implications for the overwintering success of the larvae resulting from reproduction. This portion of the early life history of Antarctic krill is where the effect of the projected changes to the habitat may potentially have the largest effect.

The decreased simulated mean winter sea ice distribution was largest (relative of current conditions simulation) in the mid and inner shelf region of the wAP, which support the biological hot spots as well as successful reproduction. Thus, warming of the shelf waters may shorten the descent-ascent cycle time due to faster development. However, growth increments and daily growth rates for Antarctic krill across the Scotia Sea decreased with increasing krill length and decreased above a temperature optimum of 0.5°C. (Atkinson et al., 2006). This indicated that there is thermal

stress at the northern limit of Antarctic krill distribution. Increased volume of CDW transported onto the wAP shelf may support faster development of the embryo and larva and may contribute to increased reproduction in regions south of Marguerite Bay where depth does not constrain the descent-ascent cycle. Under current conditions, this region has lower temperatures which result in embryos hatching at greater depths. Thus, warming of the wAP shelf south of Marguerite Bay will support embryo hatching and thereby open new areas of the shelf where local krill reproduction can be successful. However, at the same time, warming of the shelf to the north of Marguerite Bay may result in temperatures above 0.5°C which may affect growth rates. Thus, a consequence of reduced sea ice, increased volume of CDW, and more open water on the wAP shelf may be shifting of the krill habitat boundaries to higher latitudes.

A reduction in sea ice extent and distribution will also affect higher trophic level predators. For example, simulations that linked climate variability and Adélie penguin chick growth and adult foraging showed that environmental changes that reduced prey density or increased adult foraging distance, as will occur with decreased sea ice, had negative impacts on chick success (Chapman et al., 2010). Also, reduced sea ice extent along the wAP may have already limited the distribution of Antarctic silverfish (Fuiman et al., 2002), which is an important prey item for Adélie penguins and their chicks (Chapman et al., 2010). Also, changes in the habitat are likely to alter the primary production, chlorophyll concentrations, and phytoplankton community composition in wAP shelf waters (Moline and Prézelin, 1996). These changes will affect the quality and quantity of food available to Antarctic krill and also to the higher trophic levels (Ross et al., 2000). Thus, regional warming and associated habitat changes may potentially alter the productivity and structure of the marine food web of the wAP continental shelf.

CHAPTER 6

SUMMARY

Numerical circulation models coupled with Lagrangian particle tracking studies have been used to investigate connectivity in many systems and to understand the relative role of the circulation in producing observed biological distributions (see review in de Young et al., 2010). These studies showed that the large scale flow is important in connecting regions for species that spawn in one region and recruit in another (Cowen et al., 2007) and that variability in the flow can result in variability in subsequent recruitment to these populations. The Antarctic krill populations along the wAP are at the extreme end of these studies in that the organism is long-lived, has a relatively long larval period, and is dependent on the structure of the habitat (depth and sea ice) for success of the early part of its life history. The results from this study provide insights into how Antarctic krill interacts with its habitat to ensure success of the descent-ascent cycle and maintenance of populations along the wAP continental shelf. A summary of the main findings for each of the research questions that underpin this study are given below.

Research question 1: What are the transport pathways, preferred sites for across-shelf exchange and residence time for localized areas of the wAP continental shelf?.

The simulated circulation distributions showed that the ACC influences the wAP shelf circulation. The Lagrangian particle tracking simulations showed that intrusions of CDW onto the shelf occur at specific sites that are associated with irregularities in the outer shelf bathymetry. Primary intrusion sites were the depression off Alexander Island and the outer Marguerite Trough at the shelf break. Across-shelf transports occurred over depths that coincided with the core of the CDW (300 - 500 m). The simulated residence times and transport pathways showed that the wAP shelf circulation produces areas where particles were retained. However, particle retention times

differed for the different biological hot spot regions. Crystal Sound and Laubeuf Fjord had retention times of over one year, while those for the Alexander Island hot spot were shorter. Inputs to hot spots regions occurred as a result of the advective circulation and originated in different regions of the Bellingshausen Sea and the adjacent wAP shelf. Alexander Island received inputs from the adjacent shelf region, while Crystal Sound received inputs from the Bellingshausen Sea as well as the adjacent shelf. Laubeuf Fjord received particles from Marguerite Bay and the local wAP shelf region.

Research question 2: What is the role of the circulation in developing and maintaining localized areas of enhanced production and in structuring the distributions of Antarctic krill larvae on the wAP continental shelf?.

The simulated particle distributions and transport pathways were strongly controlled by circulation over the wAP continental shelf. The circulation in the biological hot spot areas was controlled by bathymetry, outflow from the GVIIS, and wind patterns. These factors are persistent over time, resulting in a relatively stable circulation pattern throughout the year. The persistence of the circulation maintains conditions that may provide a dependable planktonic prey supply for the top predator populations associated with the hot spot regions. Thus, variability in the biological production in these regions may be controlled by the strength of the circulation and the particular source regions, which will affect the rate and type of inputs/prey, respectively.

Research Question 3: What is the contribution of local retention versus inputs from remote sources to maintenance of Antarctic krill populations on the wAP continental shelf?.

The Lagrangian tracking experiments showed that particles released in upstream regions of the Bellingshausen Sea were entrained in the north-northeasterly flowing ACC and transported along the outer shelf, reaching the wAP shelf in 120-150 days.

This transport time scale corresponds to the developmental times associated with early to late larval stages of Antarctic krill. Thus, the regions where onshelf movement of particles (related to krill larval stages) was observed were consistent with areas where persistent krill populations have been observed and with observed larval distributions, such us Crystal Sound and Laubeuf Fjord. Marguerite Trough is an important conduit for the transport of particles (and larvae) onto the shelf that originated in upstream regions of the Bellingshausen Sea. Two predominant transport pathways moved particles onto the shelf; the northern limb of Marguerite Trough which reaches Laubeuf Fjord, and the depression off Adelaide Island, which reaches Crystal Sound. The estimated residence times for inner shelf regions are long enough for the larvae originating in upstream regions to be retained and recruit to the shelf krill populations by fall when the seasonal pack ice closes. The Lagrangian experiments also showed that the area southwest of Alexander Island is a potential source of larval krill to the Marguerite Bay region, particle transport times were consistent with calyptopis 2 larvae and the estimated upstream spawning ground that would result in inputs of larvae to that portion of the wAP shelf that is from an area where high chlorophyll *a* concentrations have been observed.

The simulated dispersion of Antarctic krill larvae that originated along four regions of the inner shelf, showed distributions similar to observations obtained during SO GLOBEC field experiments. Numerical simulations suggested that if local reproduction occurs around Marguerite Bay, the late stage of furcilia larvae will be found on the mid-shelf north of Adelaide Island or within the fjords inside Marguerite Bay. The simulated dispersion and the residence times also suggested that embryos spawned on the shelf could develop into furcilia 3 larval stage before being exported or retained on the shelf and would provide the source of the furcilia 6 larvae observed later in the fall. Local reproduction does not imply local retention, which was the case for the simulated trajectories for particles released at the innershelf sites north

of the Marguerite Bay region. Specifically north of Renaud Island, where more than 50% of the individuals followed a downstream pathway, which may have implications for Antarctic krill populations on Bransfield Strait, Elephant Island and even South Georgia.

Research Question 4: How are Antarctic krill reproduction success and larval krill distribution modified by environmental conditions that may potentially occur as the result of global warming?.

The simulations of the descent-ascent cycle of Antarctic krill embryo-larvae suggested that reproduction is possible on the wAP continental shelf in areas where bottom depths exceed 500 m. However, these regions are limited and consist of less than 30% of the continental shelf. The presence of CDW on the wAP shelf enhances the development of the embryo-larvae and supports successful completion of the cycle at a depth that results in larvae remaining in good condition prior to reaching the first feeding stage. The simulated descent-ascent cycle was completed in 15-20 days in areas of the wAP shelf that were consistent with the biological hot spot regions. These time scales were less than the estimated residence times for inner shelf regions which provided additional support for the local circulation to enhance retention and favor reproduction.

Sea ice distribution is an important factor affecting timing and reproduction success of Antarctic krill. Future environmental conditions that may result from global warming resulted in significantly reduced simulated winter sea ice distributions. The largest reduction of sea ice distribution was observed from Marguerite Bay to the innershelf region north of Adelaide Island and along the mid and outer shelf west of Alexander Island. These regions coincide with the location of the biological hot spots. This result implies that krill larvae would have to overwinter in areas where the highest reduction of sea ice was observed.

The simulated Lagrangian particle trajectories showed that inputs to the areas

with the largest winter sea ice reductions came from the same areas over the shelf as was observed in the simulations assuming present conditions. The time scales for these inputs were variable but agreed with the development times of krill spawned in upstream source regions. The simulated trajectories under future environmental conditions suggested that the circulation would enhance advection of krill larvae to the shelf but that the recruitment and future reproduction will be altered by modifications to local conditions (reduction of sea ice, increase of water temperature, increase of fresh water from melting) that would impede survival of Antarctic krill that overwinter on the shelf.

This study provided insights into the role of ocean circulation in producing the observed biological distributions on the wAP shelf and the fate of krill distributions under present and future environmental conditions. However, some questions are still unanswered. The results obtained in this study have implications for the distributions of top predators on localized areas of the wAP shelf. Predator abundance and composition in the hot spot regions depend on the volume, type, and quality of the prey transported to these regions. Therefore, studies of food web structure and dominant trophic pathways are needed to understand the consequences of climate-induced changes for the resident predator assemblages on the wAP continental shelf. Additional modeling and observational studies are needed to extend the results of this study to understand the effect of modified sea ice, circulation and hydrographic properties of the wAP on the reproductive success, recruitment and retention of Antarctic krill. The importance of Antarctic krill in the wAP marine food web makes understanding the effects of rapid changes resulting from climate warming of critical.

REFERENCES

Abramowitz, M., Stegun, I. A., 1964. Handbook of mathematical functions with formulas, graphs, and mathematical tables. Tenth Printing AMS IA-National Bureau of Standards Applied Mathematics Series. Washington, DC, vol. 55, 1046 pp.

Ainley, D. G., DeMaster, D. P., 1990. Upper trophic levels in polar marine ecosystems. In: Polar Oceanography, Part B: Chemestry, Biology and Geology. Walker O. Jr. Smith (Ed.), San Diego, CA, pp. 599–630.

Ainley, D. G., Jacobs, S. S., 1981. Sea-bird affinities for ocean and ice boundaries in the Antarctic. Deep-Sea Research A 28, 1173–1185.

Ainley, D. G., Jacobs, S. S., Ribic, C. A., Gaffney, I., 1998. Seabird distribution and oceanic features of the Amundsen and southern Bellingshausen seas. Antarctic Science 10(2), 111–123.

Anderson, J. B., 1999. Antarctic marine geology. Cambridge University Press, Cambridge, London, 289 pp.

Arrigo, K. R., Worthen, D., Schnell, A., Lizotte, M. P., 1998. Primary production in Southern Ocean waters. Journal of Geophysical Research 103, 15587–15600.

Ashjian, C. J., Rosenwaks, G. A., Wiebe, P. H., Davis, C. S., Gallager, S. M., Copley, N. J., Lawson, G. L., Alatalo, P., 2004. Distribution of zooplankton on the continental shelf off Marguerite Bay, Antarctic Peninsula, during Austral Fall and Winter, 2001. Deep Sea Research II 51, 2073–2098.

Ashjian, C. J., Davis, C. S., Gallager, S. M., Wiebe, P. H., Lawson, G. L., 2008. Distribution of larval krill and zooplankton in association with hydrography in Marguerite Bay, Antarctic Peninsula, in austral fall and winter 2001 described using the Video Plankton Recorder. Deep-Sea Research II 55, 455–471.

Atkinson, A., Shreeve, R. S., Hirst, A. G., Rothery, P., Tarling, G. A., Pond, D. W., Korb, R. E., Murphy, E. J., Watkins, J. L., 2006. Natural growth rates in Antarctic krill (*Euphausia superba*): II. Predictive models based on food, temperature, body length, sex, and maturity stage. Limnology and Oceanography 51, 973–987.

Atkinson, A., Siegel, V., Pakhomov, E. A., Rothery, P., 2004. Long-term decline in krill stock and increase in salps within the Southern Ocean. Nature 432, 100–103.

Baker, A. d., 1954. The circumpolar continuity of Antarctic plankton species. Discovery Report 27, 201–218.

Batchelder, H. P., Edwards, C. A., Powell, T. M., 2002. Individual-based models of zooplankton populations in coastal upwelling regions: implications of diel vertical migration on demographic success and nearshore retention. Progress in Oceanography 53, 307–333.

Beardsley, R. C., Limeburner, R., Owens, W. B., 2004. Drifter measurements of surface currents near Marguerite Bay on the western Antarctic Peninsula shelf during austral summer and fall, 2001 and 2002. Deep-Sea Research Part II 51, 1947–1964.

Belèhradek, J., 1926. Influence of temperature on biological processes. Nature 118, 117–118.

Bodungen, B. V., Smetacek, V. S., Tilzer, M. M., Zeitzschel, B., 1986. Primary production and sedimentation during spring in the antarctic peninsula region. Deep-Sea Research A 33, 177–194.

Bolmer, S. T., 2008. A note on the development of the bathymetry of the continental margin west of the antarctic peninsula from 65° to 71°S and 65° to 78°W. Deep-Sea Research II 55, 271–276.

Box, G. E. P., Jenkins, G. M., Reinsel, G. C., 1994. Time Series Analysis-Forecasting and Control, 3rd Edition. Prentice-Hall, Englewood Cliffs, New Jersey.

Brierley, A. S., Watkins, J. L., 1996. Acoustic targets at South Georgia and the South Orkney Islands during a season of krill scarcity. Marine Ecology Progress Series 138, 51–61.

Brierley, A. S., Watkins, J. L., Murray, A. W. A., 1997. Interannual variability in krill abundance at South Georgia. Marine Ecology Progress Series 150 (1), 87–98.

Brierley, A. S., Demer, D. A., Watkins, J. L., Hewitt, R. P., 1999. Concordance of interannual fluctuations in acoustically estimated densities of Antarctic krill around South Georgia and Elephant Island: biological evidence of same-year teleconnections across the Scotia Sea. Marine Biology 134 (4), 675–681.

Brinton, E., 1991. Distribution and population structure of immature and adult *Euphausia superba* in the western Bransfield Strait region during the 198687 summer. Deep-Sea Research A 38, 1169–1193.

Bromwich, D. H., Stearns, C. R., 1993. Antarctic meteorology and climatology: studies based on automatic weather stations. In: Bromwich, D. H., Stearns, C. R.(Eds.), Antarctic Research Series, vol. 61. AGU, Washington, D.C. 207 pp.

Budgell, W. P., 2005. Numerical simulation of ice-ocean variability in the Barents Sea region. Ocean Dynamics 55, 370–387.

Burns, J. M., Costa, D. P., Fedak, M. A., Hindell, M. A., Bradshaw, C. J. A., Gales, N. J., McDonald, B., Trumble, S. J., Crocker, D. E., 2004. Winter habitat use and foraging behavior of crabeater seals along the western antarctic peninsula. Deep-Sea Research II 51, 2279–2303.

Burns, J. M., Hindell, M. A., Bradshaw, C. J., Costa, D. P., 2008. Fine-scale habitat selection of crabeater seals as determined by diving behavior. Deep-Sea Research II 55, 500–514.

Capella, J. E., Quetin, L. B., Hofmann, E. E., Ross, R. M., 1992. Models of the early life history of *Euphausia superba* - Part II. Lagrangian calculations. Deep-Sea Research A 39, 1201–1220.

Carlotti, F., Giske, J., Werner, F. E., 2000. Modeling zooplankton dynamics. In: Harris, R. P., Wiebe, P. H., Lenz, J., Skjoldal, H. R., Huntley, M. (Eds.), ICES Zooplankton Methodology Manual. Academic Press, Great Britain, pp. 571–667.

Carlotti, F., Wolf, U., 1998. A Lagrangian ensemble model of *Calanus finmarchicus* coupled with a 1-D ecosystem model. Fisheries Oceanography 7, 191–204.

Carton, J. A., Giese, B. A., 2008. A reanalysis of ocean climate using SODA. Monthly Weather Review 136, 2999–3017.

Chapman, E. W., Ribic, C. A., Fraser, W. R., 2004. The distribution of seabirds and pinnipeds in Marguerite Bay and their relationship to physical features during austral winter 2001. Deep-Sea Research II 51, 2261–2278.

Chapman, E. W., Hofmann, E. E., Patterson, D. L., Fraser, W. R., 2010. The effects of variability in Antarctic krill (*Euphausia superba*) spawning behavior and sex/maturity stage distribution on Adélie penguin (*Pygoscelis adeliae*) chick growth: A modeling study. Deep-Sea Research II 57, 543–558.

Chávez, F. P., Barber, R. T., 1987. An estimate of new production in the equatorial Pacific. Deep-Sea Research A 34, 1229–1243.

Clarke, A., Murphy, E. J., Meredith, M. P., King, J. C., Peck, L. S., Barnes, D. K. A., Smith, R. C., 2007. Climate change and the marine ecosystem of the western

Antarctic Peninsula. Philosophical Transactions of the Royal Society of London Series B 362, 149–166.

Clarke, A., Tyler, P. A., 2008. Adult Antarctic krill feeding at abyssal depths. Current Biology 18, 282–285.

Costa, D. P., 1991. Reproductive and foraging energetics of high latitude penguins albatrosses and pinnipeds implications for life history patterns. American Zoologist 31, 111–130.

Costa, D. P., Crocker, D. E., 1996. Marine mammals in the Southern Ocean. In: Foundations for Ecological Research West of the Antarctic Peninsula, 1996th Edition. Vol. 70 of American Geophysical Union, Antarctic Research Series. Washington, D.C., pp. 287–301.

Costa, D. P., Burns, J. M., Chapman, E. W., Hildebrand, J., Torres, J. J., Fraser, W., Friedlaender, A., Ribic, C. A., Halpin, P., 2007. US SO GLOBEC Predator Programme. GLOBEC International Newsletter 13, 62–66.

Costa, D. P., Klinck, J. M., Hofmann, E. E., Dinniman, M. S., Burns, J. M., 2008. Upper ocean variability in west Antarctic Peninsula continental shelf waters as measured using instrumented seals. Deep-Sea Research II 55, 323–337.

Cowen, R. K., Gawarliewicz, G., Pineda, J., Thorrold, S. R. ., Werner, F. E., 2007. Population connectivity in marine systems. An overview. Oceanography 20, 14–21.

Cuzin-Roudy, J., Jun. 1987a. Gonad history of the Antarctic krill *Euphausia superba* dana during its breeding season. Polar Biology 7 (4), 237–244.

Cuzin-Roudy, J., 1987b. Sexual differentiation in the Antarctic krill *Euphausia superba* dana (Crustacea: Euphausiacea). Journal of Crustacean Biology 7 (3), 518–524.

Daly, K. L., 1990. Overwintering development, growth, and feeding of larval *Euphausia superba* in the Antarctic marginal ice zone. Limnology and Oceanography 35 (7), 1564–1576.

Daly, K. L., 2004. Overwintering growth and development of larval Euphausia superba: an interannual comparison under varying environmental conditions west of the Antarctic Peninsula. Deep-Sea Research II 51, 2139–2168.

Daly, K. L., Macaulay, M. C., 1991. Influence of physical and biological mesoscale dynamics on the seasonal distribution and behaviour of *Euphausia superba* in the antarctic marginal ice zone. Marine Ecology Progress Series 79 (1), 37–66.

Deibel, D., Daly, K. L., 2007. Zooplankton processes. In: Polynyas: Windows into Polar Oceans. Vol. 74 of Elsevier Oceanography. Walker O. Jr. Smith and Dsome Barber (Eds.), pp. 271–321.

deYoung, B., Werner, F. E., Batchelder, H., Caroltti, F., Fiksen, O., Hofmann, E. E., Kim, S., Kishi, M. J., Yamazaki, H., 2010. Dynamics of marine ecosystems: integration to models of physical-biological interactions. In: Field, M. B. J. G., Harris, R. P., Hofmann, E. E., Perry, R. I., Werner, F. (Eds.), Marine Ecosystems and Global Change. Oxford University Press, pp. 89–128.

Dinniman, M. S., Klinck, J. M., 2004. A model study of circulation and cross-shelf exchange on the west Antarctic Peninsula continental shelf. Deep-Sea Research II 51, 2003–2022.

Dinniman, M. S., Klinck, J. M., Smith, W. O., 2003. Cross-shelf exchange in a model of the Ross Sea circulation and biogeochemistry. Deep-Sea Research II 50, 3103–3120.

Dinniman, M. S., Klinck, J. M., Smith, W. O., 2007. Influence of sea ice cover and

icebergs on circulation and water mass formation in a numerical circulation model of the Ross Sea, Antarctica. Journal of Geophysical Research 112 (C11013), 1–13.

Dinniman, M. S., Klinck, J. M., Smith, W. O., 2011. A model study of circumpolar deep water on the west antarctic peninsula and ross sea continental shelves. Deep-Sea Research II 58, 1508–1523.

Dinniman, M. S., Klinck, J. M., Hofmann, E. E., submitted. The influence of surface winds on Circumpolar Deep Water transport and ice shelf basal melt along the west Antarctic Peninsula. Journal of Climate.

Domack, E. W., Burnett, A., Leventer, A., 2003. Enviromental setting of the Antarctic Peninsula. In: Antarctic Peninsula climate variability: historical and paleoenvironmental perspectives. Vol. 79 of Antarctic Research Series. America Geophysical Union, pp. 1–13.

Donnelly, J., Torres, J. J., 2008. Pelagic fishes in the marguerite bay region of the west antarctic peninsula continental shelf. Deep-Sea Research II 55, 523–539.

Dorland, R. D., Zhou, M., 2008. Circulation and heat fluxes during the austral fall in George VI Sound, Antarctic Peninsula. Deep-Sea Research II 55, 294–308.

Ducklow, H. W., Baker, K., Martinson, D. G., Quetin, L. B., Ross, R. M., Smith, R. C., Stammerjohn, S. E., Vernet, M., Fraser, W., 2007. Marine pelagic ecosystems: the West Antarctic Peninsula. Philosophical Transactions of the Royal Society B 362, 67–94.

El-Sayed, S., 1977. Biological investigations of Marine Antarctic Systems and Stocks. Vol. I. Scott Polar Research Institute, Cambridge, England.

El-Sayed, S., 1987. Biological productivity of antarctic waters: present paradoxes and emerging paradigms. Vol. 71 of BIOMASS Science. pp. 1–22.

El-Sayed, S. Z., 1994. History, organization and accomplishments of the BIOMASS Programme. Sayed Z. El-Sayed (Ed.), Cambridge University Press, Cambridge, pp. 1–8.

Everson, I., Miller, D. G. M., 1994. Krill mesoscale distribution and abundance: results and implications of research during the BIOMASS Program. In: El-Sayed, S. Z. (Ed.), Southern Ocean ecology: the BIOMASS perspective. Cambridge University Press, Cambridge, pp. 129–143.

Fach, B. A., Hofmann, E. E., Murphy, E. J., 2002. Modeling studies of Antarctic krill *Euphausia superba* survival during transport across the Scotia Sea. Marine Ecology Progress Series (231), 187–203.

Fach, B. A., Hofmann, E. E., Murphy, E. J., 2006. Transport of Antarctic krill (*Euphausia superba*) across the Scotia Sea. Part II: Krill growth and survival. Deep-Sea Research I 53, 1011–1043.

Fach, B. A., Klinck, J. M., 2006. Transport of antarctic krill *(Euphausia superba)* across the Scotia Sea. Part I: Circulation and particle tracking simulations. Deep-Sea Research I 53, 987–1010.

Fairall, C. W., Bradley, E. F., Hare, J. E., Grachev, A. A., Edson, J. B., 2003. Bulk parameterization of airsea fluxes: updates and verification for the COARE algorithm. Journal of Climate 16, 571–591.

Fraser, F. G., 1936. On the development and distribution of the young stages of krill (*Euphausia superba*). Discovery Report 14, 1–192.

Fraser, W. R., Hofmann, E. E., 2003. A predators perspective on causal links between climate change, physical forcing and ecosystem response. Marine Ecology Progress Series 265, 1–15.

Fraser, W. R., Trivelpiece, W. Z., 1996. Factors controlling the distribution of seabirds: winter-summer heterogeneity in the distribution of Adélie penguin populations. In: Ross, R. M., Hofmann, E. E., Quetin, L. B. (Eds.), Foundations for Ecological Research West of the Antarctic Peninsula. Vol. 70 of Antarctic Research Series. American Geophysical Union, Washington, D.C., pp. 257–272.

Friedlaender, A. S., Halpin, P. N., Qian, S. S., Lawson, G. L., Wiebe, P. H., Thiele, D., Read, A. J., 2006. Whale distribution in relation to prey abundance and oceanographic processes in shelf waters of the western antarctic peninsula. Marine Ecology Progress Series 317, 297–310.

Fuiman, L. A., Davis, R. W., Williams, T. M., 2002. 2002. behavior of midwater fishes under the antarctic ice: observations by a predator. marine biology 140, 815822. Marine Biology 140, 815–822.

Guzmán, O., 1983. Distribution and abundance of Antarctic krill (*Euphausia superba*) in the Bransfield Strait. In: On the biology of krill, *Euphausia superba*. Vol. 4. Ber. Polarforsch, Sonderheft, pp. 169–190.

Haidvogel, D. B., Arango, H., Budgell, W. P., Cornuelle, B. D., Curchitser, E., Di Lorenzo, E., Fennel, K., Geyer, W. R., Hermann, A. J., Lanerolle, L., Levin, J., McWilliams, J. C., some J. Miller, A., Moore, A. M., Powell, T. M., Shchepetkin, A. F., Sherwood, C. R., Signell, R. P., Warner, J. C., Wilkin, J., 2008. Ocean forecasting in terrain-following coordinates: Formulation and skill assessment of the Regional Ocean Modeling System. Journal of Computational Physics 227, 3595–3624.

Häkkinen, S., Mellor, G. L., 1992. Modeling the seasonal variability of a coupled Arctic Ice-Ocean System. Journal of Geophysical Research 97, 20285–20304.

Hamming, R. W., 1973. Numerical methods for scientists and engineers, 2nd Edition. McGraw-Hill, New York 721 pp.

Hempel, I., Hempel, G., Baker, A. d., 1979. Early life history stages of krill (*Euphausia superba*) in Bransfield Strait and Weddell Sea. Meeresforschung 27, 267–281.

Hewitt, R. P., Demer, D. A., Emery, J. H., 2003. An 8-year cycle in krill biomass density inferred from acoustic surveys conducted in the vicinity of the South Shetland islands during the austral summers of 1991-1992 through 2001-2002. Aquatic Living Resources 16, 205–213.

Hofmann, E. E., Hüsrevoglu, Y. S., 2003. A circumpolar modeling study of habitat control of antarctic krill (*Euphausia superba*) reproductive success. Deep-Sea Research II 50, 3121–3142.

Hofmann, E. E., Klinck, J. M., 1998a. Hydrography and circulation of the Antarctic continental shelf: 150 °E eastward to the Greenwich Meridian. In: Robinson, A. R., Brink, K. H. (Eds.), The Sea. Vol. 11. Wiley, New York, pp. 997–1042.

Hofmann, E. E., Klinck, J. M., 1998b. Thermohaline variability of the waters overlying west Antarctic Peninsula continental shelf. In: Jacobs, S., Weiss, R. (Eds.), Ocean, Ice and Atmosphere: Interactions at the Antarctic Continental Margin. Vol. 75 of AGU Antarctic Research Series, pp. 67–81.

Hofmann, E. E., Lascara, C. M., 1998. Overview of interdisciplinary modeling for marine ecosystems. In: Robinson, A. R., Brink, K. H. (Eds.), The Sea. Vol. 10. Wiley, New York, pp. 507–540.

Hofmann, E. E., Lascara, C. M., 2000. Modeling the growth dynamics of Antarctic krill (*Euphausia superba*). Marine Ecology Progress Series 194, 219–231.

Hofmann, E. E., Murphy, E. J., 2004. Advection, krill, and Antarctic marine ecosystems. Antarctic Science 16, 487–499.

Hofmann, E. E., Capella, J. E., Ross, R. M., Quetin, L. B., Jul. 1992. Models of the early life history of *Euphausia superba*- Part I. Time and temperature dependence during the descent-ascent cycle. Deep-Sea Research I 39 (7-8), 1177–1200.

Hofmann, E. E., Lascara, C. M., Klinck, J. M., Smith, D. A., 1996. Palmer LTER: Interannual varibility in near-surface hydrography. Antarctic Journal of the United States 31, 174–176.

Hofmann, E. E., Klinck, J. M., Locarini, R. A., Fach, B. A., Murphy, E. J., 1998. Krill transport in the Scotia Sea and environs. Antarctic Science 10, 406–415.

Hofmann, E. E., Klinck, J. M., Costa, D. P., Daly, K. L., Torres, J. J., Fraser, W. R., 2002. US Southern Ocean Global Ocean Ecosystems Dynamics program. Oceanography 15 (2), 64–74.

Hofmann, E. E., Wiebe, P. H., Costa, D. P., Torres, J. J., 2004. An overview of the Southern Ocean Global Ocean Ecosystems Dynamics program. Deep-Sea Research II 51, 1921–1924.

Hofmann, E. E., Wiebe, P. H., Costa, D. P., Torres, J. J., 2008. Introduction to dynamics of plankton, krill, and predators in relation to environmental features of the western Antarctic Peninsula and related areas: SO GLOBEC Part II. Deep-Sea Research II 55, 269–270.

Hofmann, E. E., Costa, D. P., Daly, K. L., Dinniman, M. S., Klinck, J. M., Marrari, M., Padman, L., Piñones, A., 2009. Results from the US Southern Ocean GLOBEC synthesis studies. GLOBEC International Newsletter 15, 43–48.

Hofmann, E. E., Wiebe, P. H., Costa, D. P., Torres, J. J., 2011. Introduction to understanding the linkages between Antarctic food webs and the environment: A synthesis of Southern Ocean GLOBEC studies. Deep-Sea Research II 58, 1505–1507.

Holm-Hansen, O., Amos, A. F., Silva, S. N., ne, V. V., Helbling, E. W., 1994. In situ evidence for a nutrient limitation of phytoplankton growth in pelagic Antarctic waters. Antarctic Science 6 (3), 315–324.

Holt, R. S., Hewitt, R. P., Rosenberg, J. E., 1991. The US antarctic marine living resources (AMLR) program: 1990-91 field season activities. US Antarctic Journal 25 (5), 187–188.

Hosie, G. W., Ikeda, T., Stolp, M., 1988. Distribution, abundance and population structure of the antarctic krill (*Euphausia superba* dana) in the Prydz Bay region, Antarctica. Polar Biology 8, 213–224.

Howard, S. L., Hyatt, J., Padman, L., 2004. Mixing in the pycnocline over the western Antarctic Peninsula shelf during Southern Ocean GLOBEC. Deep-Sea Research II 51, 1965–1979.

Hunke, E. C., Jun. 2001. Viscous-Plastic Sea Ice Dynamics with the EVP Model: Linearization Issues. Journal of Computational Physics 170 (1), 18–38.

Hunke, E. C., Dukowicz, J. K., Sep. 1997. An ElasticViscousPlastic Model for Sea Ice Dynamics. Journal of Physical Oceanography 27 (9), 1849–1867.

Hunt, G. L. J., 1997. Physics, zooplankton, and the distribution of least auklets in the Bering Sea - a review. ICES Journal of Marine Science 34, 600–607.

Hunter, J. R., Craig, P. D., Phillips, H. E., 1993. On the use of random walk models

with spatially variable diffusivity. Journal of Computational Physics 106 (2), 366–376.

Huntley, M. E., Brinton, E., 1991. Mesoscale variation in growth and early development of *Euphausia superba* dana in the western Bransfield Strait region. Deep-Sea Research A 38, 1213–1240.

Huntley, M. E., Karl, D. M., Niiler, P. P., Holm-Hansen, O., 1987. Research on Antarctic Coastal Ecosystem Rates (RACER): an interdisciplinary field experiment. Deep-Sea Research I 38, 911–941.

Huntley, M. E., Karl, D. M., Niller, P., Holm-Hansen, O., 1991. Research on Antarctic Coastal Ecosystem Rates (RACER): an interdisciplinary field experiment. Deep-Sea Research A 38, 911–941.

Ichii, T., Katayama, K., Obitsu, N., Ishii, H., Naganobu, M., 1998. Occurrence of Antarctic krill (*Euphausia superba*) concentrations in the vicinity of the South Shetland islands: relationship to environmental parameters. Deep-Sea Research I 45, 1235–1262.

Ikeda, T., 1984. Development of the larvae of the Antarctic krill (*Euphausia superba* dana) observed in the laboratory. Journal of Experimental Marine Biology and Ecology 75 (2), 107–117.

Kanda, K., Takagi, K., Seki, Y., 1982. Movement of the larger swarms of antarctic krill *Euphausia superba* population off Enderby Land during 1976-1977 season. Journal of the Tokyo University of Fisheries 68, 25–42.

Kawaguchi, S., Satake, M., 1994. Relationship between recruitment of the Antarctic krill and the degree of ice cover near the South Shetland Islands. Fisheries Science 60, 123–124.

Kenney, R. D., Scott, G. P., Thompson, T. J., Winn, H. E., 1995. Estimates of prey consumption and trophic impacts of Cetaceans in the USA Northeast continental shelf ecosystem. Journal of Northwest Atlantic Fishery Science 22, 155–171.

Kils, U., 1982. Swimming behavior, swimming performance and energy balance of Antarctic krill *Euphausia superba*. BIOMASS Scientific Series 3, 1–122.

Klinck, J. M., 1998. Heat and salt changes on the continental shelf west of the Antarctic Peninsula between January 1993 and January 1994. Journal of Geophysical Research 103, 7617–7636.

Klinck, J. M., Hofmann, E. E., Beardsley, R. C., Salihoglu, B., Howard, S., 2004. Water-mass properties and circulation on the west Antarctic Peninsula Continental Shelf in Austral Fall and Winter 2001. Deep-Sea Research II 51, 1925–1946.

Large, W. G., van Loon, H., 1989. Large scale, low frequency variability of the 1979 FGGE surface buoy drifts and winds over the Southern Hemisphere. Journal of Physical Oceanography 19, 216–232.

Lascara, C. M., Hofmann, E. E., Ross, R. M., Quetin, L. B., 1999. Seasonal variability in the distribution of Antarctic krill, *Euphausia superba*, west of the Antarctic Peninsula. Deep-Sea Research I 46, 951–984.

Lawson, G. L., Wiebe, P. H., Ashjian, C. J., Gallager, S. M., Davis, C. S., Warren, J. D., 2004. Acoustically-inferred zooplankton distribution in relation to hydrography west of the Antarctic Peninsula. Deep-Sea Research II 51, 2041–2072.

Lawson, G. L., Wiebe, P. H., Stanton, T. K., Ashjian, C. J., 2008b. Euphausiid distribution along the Western Antarctic Peninsula - Part A: Development of robust multi-frequency acoustic techniques to identify euphausiid aggregations and quantify euphausiid size, abundance, and biomass. Deep-Sea Research II 55, 412–431.

Lawson, G. L., Wiebe, P. H., Ashjian, C. J., Stanton, T. K., 2008a. Euphausiid distribution along the Western Antarctic Peninsula - Part B: Distribution of euphausiid aggregations and biomass, and associations with environmental features. Deep-Sea Research II 55, 432–454.

Lennon, P. W., Loynes, J., Paren, J. G., Potter, J. R., 1982. Oceanographic observations from George VI Ice Shelf, Antarctic Peninsula. Annals of Glaciology 3, 178–183.

Loeb, V., Siegel, V., Holm-Hansen, O., Hewitt, R. P., Fraser, W., Trivelpiece, W. Z., Trivelpiece, S., 1997. Effects of sea-ice extent and krill or salp dominance on the Antarctic food web. Nature 387 (6636), 897–900.

Mackintosh, N. A., 1972. Life cycle of Antarctic krill in relation to ice and water conditions. Discovery Report 36, 1–94.

Mackintosh, N. A., 1973. Distribution of post-larval krill in the Antarctic. Discovery Report 36, 95–156.

Makarov, R., Enshenina, L. M., Spiridonov, V., 1990. Distributional ecology of euphausiid larvae in the Antarctic Peninsula region and adjacent waters. Proceedings of the NIPR Symposium on Polar Biology 3, 23–35.

Marr, J. W. S., 1962. The natural history and geography of the Antarctic krill *Euphausia superba* Dana. Discovery Report 32, 37–465.

Marrari, M., Daly, K. L., Hu, C., 2008. Spatial and temporal variability of SeaWiFS chlorophyll a distributions west of the Antarctic Peninsula: Implications for krill production. Deep-Sea Research II 55, 377–392.

Marrari, M., Daly, K. L., Timonin, A., Semenova, T., 2011. The zooplankton of Marguerite Bay, Western Antarctic Peninsula. Part I: abundance, distribution, and

population response to variability in environmental conditions. Deep-Sea Research II 58, 1599–1613.

Marschall, H. P., 1983. Sinking speed, density and size of euphausiid eggs. Meeresforschung 30, 1–9.

Marschall, H. P., 1988. The overwintering strategy of Antarctic krill under the pack-ice of the Weddell Sea. Polar Biology 9, 129–135.

Maslanyj, M. P., 1987. Seismic bedrock depth measurements and the origin of George VI Sound, Antarctic Peninsula. British Antarctic Survey Bulletin 75, 51–65.

Mellor, G. L., Kantha, L., 1989. An ice-ocean coupled model. Journal of Geophysical Research 94, 10937–10954.

Meredith, M. P., King, J. C., 2005. Rapid climate change in the ocean west of the Antarctic Peninsula during the second half of the 20th century. Geophysical Research Letters 32, L19604.

Miller, C. B., Lynch, D. R., Carlotti, F., Gentleman, W., Lewis, C. V. W., 1998. Coupling of an individual-based population dynamic model of *Calanus finmarchicus* to a circulation model for the Georges Bank region. Fisheries Oceanography 7, 219–234.

Moffat, C., Beardsley, R. C., Owens, B., van Lipzig, N., 2008. A first description of the Antarctic Peninsula Coastal Current. Deep-Sea Research II 55, 277–293.

Moffat, C., Owens, B., Beardsley, R. C., 2009. On the characteristics of Circumpolar Deep Water intrusions to the west Antarctic Peninsula Continental Shelf. Journal of Geophysical Research 114 (C05017), 1–16.

Moline, M. A., Prézelin, B. B., 1996. Long-term monitoring and analyses of physical factors regulating variability in coastal Antarctic phytoplankton biomass, in

situ productivity and taxonomic composition over subseasonal, seasonal and interannual time scales. Marine Ecology Progress Series 145, 143–160.

Murphy, E. J., Watkins, J. L., Reid, K., Trathan, P. N., Everson, I., Croxall, J. P., Priddle, J., Brandon, M. A., Brierley, A. S., Hofmann, E. E., 1998. Interannual variability of the South Georgia marine ecosystem: biological and physical sources of variation in the abundance of krill. Fisheries Oceanography 7, 381–390.

Murphy, E. J., Thorpe, S. E., Watkins, J. L., Hewitt, R., 2004. Modeling the krill transport pathways in the Scotia Sea: spatial and environmental connections generating the seasonal distribution of krill. Deep-Sea Research II 51, 1435–1456.

Murray, A. W., Watkins, J. L., Bone, D. G., 1995. A biological acoustic survey in the marginal ice-edge zone of the Bellingshausen Sea. Deep-Sea Research II 42, 1159–1175.

Nicol, S., 2003. Krill and currents-physical and biological interactions influencing the distribution of *Euphausia superba*. Ocean and Polar Research 24 (4), 633–644.

Nicol, S., 2006. Krill, currents, and sea ice: *Euphausia superba* and its changing environment. BioScience 56, 111–120.

Orsi, A. H., Whitworth, T., Nowlin, W. D., 1995. On the meridional extent and fronts of the Antarctic Circumpolar Current. Deep-Sea Research I 42, 641–673.

O'Brien, C., Virtue, P., Kawaguchi, S., Nichols, P. D., 2011. Aspects of krill growth and condition during late winter-early spring off East Antarctica (110 - 130°E). Deep-Sea Research II 58, 1211–1221.

Padman, L., Fricker, H. A., Coleman, R., Howard, S., Erofeeva, L., 2002. A new tide model for the Antarctic ice shelves and seas. Annals of Glaciology 34, 247–254.

Pakhomov, E. A., Atkinson, A., Meyer, B., Oettl, B., Bathmann, U., 2004. Daily rations and growth of larval krill *Euphausia superba* in the Eastern Bellingshausen Sea during austral autumn. Deep-Sea Research II 51, 2185–2198.

Parish, T. R., 1992. On the role of Antarctic katabatic winds in forcing large-scale tropospheric motions. Journal of the Atmospheric Sciences 49, 1374–1385.

Parish, T. R., Bromwich, D. H., 1987. The surface windfield over the Antarctic ice sheets. Nature 328, 51–54.

Parkinson, C. L., 2002. Trends in the length of the Southern Ocean sea ice season, 1979-1999. Annals of Glaciology 34, 435–440.

Piñones, A., Hofmann, E. E., Dinniman, M. S., Klinck, J. M., 2011. Lagrangian simulation of transport pathways and residence times along the western Antarctic Peninsula. Deep-Sea Research II 58, 1524–1539.

Potter, J. R., Paren, J. G., 1985. Interaction between ice shelf and ocean in George VI Sound, Antarctica. In: Jacobs, S. S. (Ed.), Oceanology ofthe Antarctica Continental Shelf. Antarctic Research Series, vol. 43. American Geophysical Union, Washington, DC, pp. 35–58.

Powers, J. G., Monaghan, A. J., Cayette, A. M., Bromwich, D. H., Kuo, Y., Manning, K. W., Nov. 2003. Real - Time mesoscale modeling over Antarctica: The Antarctic Mesoscale Prediction System. Bulletin of the American Meteorological Society 84 (11), 1533–1545.

Prézelin, B. B., Boucher, N. P., Smith, R. C., 1994. Marine primary production under the influence of the Antarctic ozone hole: Icecolors 90. In: Ultraviolet Radiation and Biological Research in Antarctica. Vol. 62 of American Geophysical Union. Weiler, S., Penhale, P. (Eds.), Washington, D.C., pp. 159–186.

Prézelin, B. B., Hofmann, E. E., Mengelt, C., Klinck, J. M., 2000. The linkage between Upper Circumpolar Deep Water (UCDW) and phytoplankton assemblages on the west Antarctic Peninsula continental shelf. Journal of Marine Research 58, 165–202.

Prézelin, B. B., Hofmann, E. E., Moline, M., Klinck, J. M., 2004. Physical forcing of phytoplankton community structure and primary production in continental shelf waters of the Western Antarctic Peninsula. Journal of Marine Research 62, 419–460.

Priddle, J., Croxall, J., Everson, I., Heywood, R. B., Murphy, E. J., Prince, P. A., Sear, C. B., 1988. Large scale fluctuations in distribution and abundance of krill - a discussion of possible causes. In: Sahrhage, D. (Ed.), Antarctic Ocean and resources variability. Springer Verlag, Berlin, pp. 169–182.

Quetin, L. B., Ross, R. M., 1984. Depth distribution of developing *Euphausia superba* embryos, predicted from sinking rates. Marine Biology 79, 47–53.

Quetin, L. B., Ross, R. M., 1991. Behavioral and physiological characteristics of the Antarctic krill, *Euphausia superba*. American Zoologist 31, 49–63.

Quetin, L. B., Ross, R. M., 2001. Enviromental variability and its impact on the reproductive cycle of Antarctic krill. American Zoologist 41, 74–89.

Quetin, L. B., Ross, R. M., 2003. Episodic recruitment in Antarctic krill *Euphausia superba* in the Palmer LTER study region. Marine Ecology Progress Series 259, 185–200.

Quetin, L. B., Ross, R. M., Clarke, A., 1994. Krill energetics: seasonal and environmental aspects of the physiology of *Euphausia superba*. In: El-Sayed, S. Z. (Ed.), Southern Ocean ecology. The BIOMASS perspective. Cambridge University Press, Cambridge, pp. 165–184.

Ribic, C. A., Chapman, E. W., Fraser, W. R., Lawson, G. L., Wiebe, P. H., 2008. Top predators in relation to bathymetry, ice and krill during austral winter in Marguerite Bay, Antarctica. Deep-Sea Research II 55, 485–499.

Ross, R. M., Quetin, L. B., 1983. Spawning frequency and fecundity of the Antarctic krill *Euphausia superba*. Marine Biology 77, 201–205.

Ross, R. M., Quetin, L. B., 1985. The effect of pressure on the sinking rates of the embryos of the Antarctic krill, *Euphausia superba*. Deep-Sea Research A 32, 799–807.

Ross, R. M., Quetin, L. B., 1986. How productive are Antarctic krill? Bioscience 36, 264–269.

Ross, R. M., Quetin, L. B., 1989. Energetic cost to develop to the first feeding stage of *Euphausia superba* Dana and the effect of delays in food availability. Journal Experimental Marine Biology and Ecology 133, 103–127.

Ross, R. M., Quetin, L. B., Amsler, M. O., Elias, M. C., 1987. Larval and adult Antarctic krill, *Euphausia superba*, 1986 winter observations at Palmer Station. Antarctic Journal of the United States 22, 205–206.

Ross, R. M., Quetin, L. B., Kirsch, E., 1988. Effect of temperature on developmental times and survival of early larval stages of *Euphausia superba* Dana. Journal Experimental Marine Biology and Ecology 121, 55–71.

Ross, R. M., Quetin, L. B., Lascara, C. M., 1996. Distribution of Antarctic krill and dominant zooplankton west of the Antarctic Peninsula. In: Ross, R. M., Hofmann, E. E., Quetin, L. B. (Eds.), Foundations for Ecological Research West of the Antarctic Peninsula. AGU Antarctic Research Series. America Geophysical Union, Washington, pp. 199–217.

Ross, R. M., Quetin, L. B., Baker, K. S., Vernet, M., Smith, R. C., 2000. Growth limitation in young *Euphausia superba* under field conditions. Limnology and Oceanography 45, 31–43.

Rossow, W. B., Schiffer, R. A., Nov. 1999. Advances in understanding clouds from ISCCP. Bulletin of the American Meteorological Society 80 (11), 2261–2287.

Russell, J. L., Dixon, K. W., Gnanadesikan, A., Stouffer, R. J., Toggweiler, J. R., 2006. The Southern Hemisphere westerlies in a warming world: propping open the door to the deep ocean. Journal of Climate 19, 6382–6390.

Savidge, D. K., Amft, J. A., 2009. Circulation on the West Antarctic Peninsula derived from 6 years of shipboard ADCP transects. Deep-Sea Research I 56 (10), 1633–1655.

Savidge, G., Harbour, D., Gilpin, L. C., Boyd, P. W., 1995. Phytoplankton distributions and production in the Bellingshausen Sea, Austral spring 1992. Deep-Sea Research II 42, 1201–1224.

Schnack-Schiel, S. B., Mujica, A., 1994. The zooplankton of the Antarctic Peninsula region. In: El-Sayed, S. Z. (Ed.), Southern Ocean ecology. The BIOMASS perspective. Cambridge University Press, Cambridge, pp. 79–92.

Serebrennikova, Y. M., Fanning, K. A., 2004. Nutrients in the Southern Ocean GLOBEC region: variations, water circulation, and cycling. Deep-Sea Research II 51, 1981–2002.

Shchepetkin, A. F., McWilliams, J. C., 2005. The regional oceanic modeling system (ROMS): a split-explicit, free-surface, topography-following-coordinate oceanic model. Ocean Modelling 9 (4), 347–404.

Siegel, V., 1985. The distribution pattern of krill, *Euphausia superba* west of the Antarctic Peninsula in February 1982. Meeresforschung 30, 292–305.

Siegel, V., 1986. Structure and composition of the Antarctic krill stock in the Bransfield Strait (Antarctic Peninsula) during the Second International BIOMASS Experiment (SIBEX). Archiv für Fischereiwissenschaft 37, 51–72.

Siegel, V., 1988. A concept of seasonal variation of krill (*Euphausia superba*) distribution and abundance est of the Antarctic Peninsula. In: El-Sayed, S. Z. (Ed.), Antarctic Ocean and Resources Variability. Springer-Verlag Berlin Heidelberg, Paris, pp. 219–230.

Siegel, V., 1989. Winter and spring distribution and status of the krill stock in Antarctic Peninsula waters. Archive für Fischereiwissenschaft 39 (1), 45–72.

Siegel, V., 1992. Assessment of the krill (*Euphausia superba*) spawning stock off the Antarctic Peninsula. Archive für Fischereiwissenschaft 41, 101–130.

Siegel, V., 2000. Krill demography and variability in abundance and distribution. Canadian Journal of Fisheries and Aquatic Sciences 57, 151–167.

Siegel, V., 2005. Distribution and population dynamics of *Euphausia superba*: summary of recent findings. Polar Biology 29, 1–22.

Siegel, V., Harm, U., 1996. The composition, abundance, biomass and diversity of the epipelagic zooplankton communities of the southern Bellingshausen Sea (Antarctic) with special reference to krill and salps. Archive of Fishery and Marine Research 44, 115–139.

Siegel, V., Kalinowski, J., 1994. Krill demography and small-scale processes: a review. In: El-Sayed, S. Z. (Ed.), Southern Ocean ecology. The BIOMASS perspective. Cambridge University Press, Cambridge, pp. 145–163.

Siegel, V., Loeb, V., 1994. Length and age at maturity of Antarctic krill. Antarctic Science 6, 479–482.

Siegel, V., Loeb, V., 1995. Recruitment of antarctic krill *Euphausia superba* and possible causes for its variability. Marine Ecology Progress Series 123, 45–56.

Siegel, V., Bergström, B., Strömberg, J. O., Schalk, P. H., 1990. Distribution, size frequencies and maturity stages of krill *Euphausia superba*, in relation to sea-ice in the northern Weddell Sea. Polar Biology 10, 549–557.

Siegel, V., de la Mare, W. K., Loeb, V., 1997. Long-term monitoring of krill recruitment and abundance indices in the Elephant Island area (Antarctic Peninsula). CCAMLR Science 4, 19–35.

Siegel, V., Loeb, V., Gröger, J., 1998. Krill (*Euphausia superba*) density, proportional and absolute recruitment and biomass in the Elephant Island region (Antarctic Penisnsula) during the period 1977 to 1997. Polar Biology 19, 393–398.

Sievers, H. A., Nowlin, J. W. D., 1984. The stratificationand water masses at Drake Passage. Journal of Geophysical Research 89, 10489–10514.

Smetacek, V., Scharek, R., Nothig, E. M., 1990. Seasonal and regional variation in the pelagial and its relationship to the life history cycle of krill. In: Kerry, K. R., Hempel, G. (Eds.), Antarctic ecosystems: ecological change and conservation. Springer-Verlag, Berlin, pp. 103–114.

Smith, D. A., Hofmann, E. E., Klinck, J. M., Lascara, C. M., 1999. Hydrography and circulation of the West Antarctic Peninsula Continental Shelf. Deep-Sea Research I 46, 925–949.

Smith, D. A., Klinck, J. M., 2002. Water properties on the west Antarctic Peninsula

continental shelf: a model study of effects of surface fluxes and sea ice. Deep-Sea Research II 49, 4863–4886.

Smith, R. C., Stammerjohn, S. E., 2001. Variations of surface air temperature and sea-ice extent in the western Antarctic Peninsula region. Annals of Glaciology 33, 493–500.

Smith, R. C., Baker, K. S., Fraser, W. R., Hofmann, E. E., Karl, D. M., Klinck, J. M., Quetin, L. B., Prézelin, B. B., Ross, R. M., Trivelpiece, W. Z., Vernet, M., 1995. The Palmer LTER: A long-term Ecological research program at Palmer Station, Antarctica. Oceanography 8 (3), 77–86.

Smith, R. C., Stammerjohn, S. E., Baker, K. S., 1996. Surface air temperature variations in the Western Antarctic Peninsula region. In: Ross, R. M., Hofmann, E. E., Quetin, L. B. (Eds.), Foundations for Ecological Research West of the Antarctic Peninsula. Vol. 70 of Antarctic Research Series. America Geophysical Union, pp. 105–121.

Smith, R. C., Baker, K. S., Byers, M. L., Stammerjohn, S. E., 1998. Primary productivity of the Palmer Long Term Ecological Research Area and the Southern Ocean. Journal of Marine System 17, 245–259.

Smith, W. O. J., Sakshaug, E., 1990. Polar phytoplankton. In: Smith, W. O. (Ed.), Polar Oceanography: Part B. Chemestry, Biology and Geology. Academic Press, San Diego.

Spiridonov, V. A., 1995. Spatial and temporal variability in reproductive timing of Antarctic krill (*Euphausia superba* dana). Polar Biology 15, 161–174.

Stammerjohn, S. E., Smith, R. C., 1996. Spatial and temporal variability of western Antarctic Peninsula sea ice coverage. In: Ross, R. M., Hofmann, E. E., Quetin,

L. B. (Eds.), Foundations for Ecological Research West of the Antarctic Peninsula. Vol. 70 of Antarctic Research Series. America Geophysical Union, Washington, DC, pp. 81–104.

Stammerjohn, S. E., Martinson, D. G., Smith, R. C., Iannuzzi, R. A., 2008a. Sea ice in the western Antarctic Peninsula region: Spatio-temporal variability from ecological and climate change perspectives. Deep-Sea Research II 55, 2041–2058.

Stammerjohn, S. E., Martinson, D. G., Smith, R. C., Yuan, X., Rind, D., 2008b. Trends in antarctic annual sea ice retreat and advance and their relation to El Niño - Southern Oscillation and Southern Annular Mode variability. Journal of Geophysical Research 113 (C03S90), 1–20.

Stein, M., 1981. Thermal structure of the weddel-scotia confluence during february 1981. Meeresforschung 29, 47–52.

Stein, M., 1983. The distribution of water masses in the South Shetland Islands area during FIBEX. Memoirs of National Institute of Polar Research Series, Special Issue 27, 16–23.

Stein, M., 1986. Variability of water masses and currents off Antarctic Peninsula during SIBEX. Archive für Fischereiwissenschaft 37 (1), 25–50.

Stein, M., 1988. Variation of geostrophic circulation off the Antarctic Peninsula and in the southwest Scotia Sea, 1975-1985. In: Sahrhage, D. (Ed.), Antarctic Ocean and Resources Variability. Springer-Verlag, pp. 81–91.

Stein, M., 1989. Seasonal variation of water masses in Bransfield Strait and adjacent waters. Archiv für Fischereiwissenschaft 39, 15–38.

Stein, M., 1992. Variability of local upwelling off the Antarctic Peninsula 1986–1990. Archiv für Fischereiwissenschaft 41, 131–158.

Sullivan, C. W., Ainley, D. G., 1987. Antarctic marine ecosystem research at the ice edge-zone. Antarctic Journal of the United States 22, 167–169.

Tarling, G. A., Cuzin-Roudy, J., Thorpe, S. E., Shreeve, R. S., Ward, P., Murphy, E. J., 2007. Recruitment of Antarctic krill *Euphausia superba* in the South Georgia region: adult fecundity and the fate of larvae. Marine Ecology Progress Series 331, 161–179.

Thiele, D., Chester, E. T., Moore, S. E., Sirovic, A., Hildebrand, J. A., Friedlaender, A. S., 2004. Seasonal variability in whale encounters in the Western Antarctic Peninsula. Deep-Sea Research II 51, 2311–2325.

Thompson, D. W. J., Solomon, S., 2002. Interpretation of recent Southern Hemisphere climate change. Science 296, 895–899.

Thorpe, S. E., Heywood, K. J., Stevens, D. P., Brandon, M. A., Jul. 2004. Tracking passive drifters in a high resolution ocean model: implications for interannual variability of larval krill transport to South Georgia. Deep-Sea Research I 51, 909–920.

Thorpe, S. E., Murphy, E., Watkins, J., May 2007. Circumpolar connections between Antarctic krill (*Euphausia superba* dana) populations: Investigating the roles of ocean and sea ice transport. Deep-Sea Research I 54, 792–810.

Toole, J. M., 1981. Sea ice, winter convection, and temperature minimum layer in the Southern Ocean. Journal of Geophysical Research 86, 8037–8047.

Trathan, P. N., Priddle, J., Watkins, J. L., Miller, D. G., Murray, A. W., 1993. Spatial variability of Antarctic krill in relation to mesoscale hydrography. Marine Ecology Progress Series 98, 61–71.

Trathan, P. N., Croxall, J. P., Murphy, E. J., May 1996. Dynamics of Antarctic

penguin populations in relation to inter-annual variability in sea ice distribution. Polar Biology 16 (5), 321–330.

Trenberth, K. E., 1991. Storm tracks in the Southern Hemisphere. Journal of Atmospheric Science 48, 2159–2178.

Trenberth, K. E., Large, W. G., Olson, J. G., 1990. The mean annual cycle in global ocean wind stress. Journal of Physical Oceanography 20, 1742–1760.

Širović, A., Hildebrand, J. A., Wiggins, S. M., McDonald, M. A., Moore, S. E., Thiele, D., 2004. Seasonality of blue and fin whale calls and the influence of sea ice in the Western Antarctic Peninsula. Deep-Sea Research II 51, 2327–2344.

van Franecker, J. A., 1992. Top predators as indicators for ecosystem events in the confluence zone and the marginal ice zone of the Weddell and Scotia Seas, Antarctica, November 1988 - January 1989. Polar Biology 12, 93–102.

Vaughan, D. G., Marshall, G. J., Connolley, W. M., Parkinson, C., Mulvaney, R., Hodgson, R., King, J. C., Pudsey, C. J., Turner, J., 2003. Recent rapid regional climate warming on the Antarctic Peninsula. Climate Change 60, 243–274.

Visser, A. W., 1997. Using random walk models to simulate the vertical distribution of particles in a turbulent water column. Marine Ecology Progress Series 158, 275–281.

Watkins, J. L., Murray, A. W. A., Daly, H. I., 1999. Variation in the distribution of Antarctic krill *Euphausia superba* around South Georgia. Marine Ecology Progress Series 188, 149–160.

Werner, F. E., Page, F. H., Lynch, D. R., Loder, J. W., Lough, R. G., Perry, R. I., Greenberg, D. A., Sinclair, M. M., 1993. Influences of mean advection and simple

behavior on the distribution of cod and haddock early life stages on Georges Bank. Fisheries Oceanography 2, 43–64.

Werner, F. E., Perry, R. I., Lough, R. G., Naimie, C. E., 1996. Trophodynamic and advective influences on Georges Bank larval cod and haddock. Deep-Sea Research II 43 (7-8), 1793–1822.

Whitehead, H., Brennan, S., Grover, D., 1992. Distribution and behavior of male sperm whales on the Scotian Shelf. Canadian Journal of Zoology 70, 912–918.

Wiebe, P. H., Ashjian, C. J., Lawson, G. L., nones, A. P., Copley, N. J., 2011. Horizontal and vertical distribution of euphausiid species on the Western Antarctic Peninsula U.S. GLOBEC Southern Ocean study site. Deep-Sea Research II 58, 1630–1651.

Wilkin, J., Hedström, K. S., 1998. Users manual for an orthogonal curvilinear grid-generation package. Technical, Institute of Marine and Coastal Sciences, Rutgers University.

Wishner, K. F., Schoenherr, J. R., Beardsley, R. C., Chen, C., 1995. Abundance, distribution and population structure of the copepod *Calanus finmarchicus* in a springtime right whale feeding area in the southwestern gulf of maine. Continental Shelf Research 15, 475–507.

Witek, Z., Koronkiewicz, A., Soszka, G. J., 1980. Certain aspects of the early life history of krill *Euphausia superba* dana (crustacea). Polish Polar Research 1, 97–115.

Zhou, M., Dorland, R. D., 2004. Aggregation and vertical migration behavior of *Euphausia superba*. Deep-Sea Research II 51, 2119–2137.

Zhou, M., Zhu, Y., Peterson, J. O., 2004. In situ growth and mortality of mesozooplankton during the austral fall and winter in Marguerite Bay and its vicinity. Deep-Sea Research II 51, 2099–2118.

Zwally, H. J., Comiso, J. C., Parkinson, C. L., Cavalieri, D. J., Gloersen, P., 2002. Variability of antarctic sea ice 1979-1998. Journal of Geophysical Research 107 (C5), 1–21.

VITA

Maria Andrea Piñones Valenzuela

Department of Ocean, Earth and Atmospheric Science

Old Dominion University

Norfolk, VA 23529

Education

B.S., Oceanography, 2003. Catholic University of Valparaiso, Valparaiso, Chile

M.S., Ocean and Earth Sciences, 2006. Old Dominion University, Norfolk, Virginia, USA

Ph.D., Oceanography, 2011. Old Dominion University, Norfolk, Virginia, USA

Publications

Piñones, A., Hofmann, E.E., Dinniman, M.S., Klinck, J.M., 2011. Lagrangian simulation of transport pathways and residence times along the Western Antarctic Peninsula. Deep-Sea Research II 58, 1524-1539.

Wiebe, P.H, Ashjian, C., Lawson, G.L., Piñones, A., Copley, N., 2011. Horizontal and vertical distribution of euphausiid species on the Western Antarctic Peninsula Southern Ocean GLOBEC study site. Deep-Sea Research II 58, 1630-1652.

Piñones, A., Castilla, J.C., Guiñez, R., Larger, J.L., 2007. Nearshore surface temperatures in Antofagasta Bay (Chile) and adjacent upwelling centers. Ciencias Marinas 33(1), 37-48.

Piñones, A., Valle-Levinson, A., Narváez, D.A., Vargas, C.A., Navarrete, S.A., Yuras, G., Castilla, J.C., 2005. Wind-induced variability in river plume motion. Estuarine, Coastal and Shelf Science 65, 513-525.

Typeset using LaTeX.